SURVEY ON VIBRATION TESTS ON MISSILE-LIKE STRUCTURES AND THE EFFECTS OF DAMPING

by   Dr. E. J. Rodgers
Dr. R. G. Sturm
J. D. Warrington

October 1967

RESEARCH LABORATORIES

BROWN ENGINEERING COMPANY, INC.

HUNTSVILLE, ALABAMA

TECHNICAL NOTE R-227

SURVEY ON VIBRATION TESTS ON MISSILE-LIKE STRUCTURES
AND THE EFFECTS OF DAMPING

OCTOBER 1967

Prepared For

STRUCTURES DIVISION
PROPULSION AND VEHICLE ENGINEERING LABORATORY
GEORGE C. MARSHALL SPACE FLIGHT CENTER

By

RESEARCH LABORATORIES
ADVANCED SYSTEMS AND TECHNOLOGIES GROUP
BROWN ENGINEERING COMPANY, INC.
HUNTSVILLE, ALABAMA
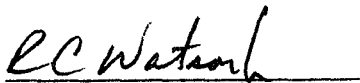
Contract No. NAS8-20073

Prepared By

Dr. E. J. Rodgers
Dr. R. G. Sturm
J. D. Warrington

ABSTRACT

This report examines developments in the field of vibrational testing of missile-like vehicles; particular attention is given to that information that sheds light on the effects of damping on the vibrational behavior. The results of the survey are used by the authors as a basis for the conclusions regarding damping information obtained from such tests and for making recommendations for obtaining damping information in future tests.

Approved:

R. C. Watson

R. C. Watson, Jr.
Vice President
Advanced Systems and Technologies Group

TABLE OF CONTENTS

LIST OF FIGURES

LIST OF FIGURES (Continued)

LIST OF FIGURES (Continued)

LIST OF FIGURES (Continued)

LIST OF TABLES

INTRODUCTION

This report is part of a study to determine the effect of damping on the vibrational behavior of missile-like structures. It is concerned with identifying and evaluating the experience existing in vibration testing of missile-like vehicles and in particular with the knowledge gained relating the damping effects to the vibrational behavior.

The purpose of this report is to identify and evaluate the knowledge that has been generated in vibration tests of missile-like structures and to see if this knowledge should have any effect on the design of future vibration tests in order to obtain information on the effects of damping of a structure on the vibrational behavior of the structure. In particular, this report examines developments in the field of vibrational testing of missile-like vehicles, how they have evolved, and what information has been obtained; particularly that information that sheds light on the effects of damping on the vibrational behavior. Attention is given to determining the various forms in which the raw data were obtained, the reduction methods that were used, and the methods of presenting the results. Pertinent observations of the various experimenters, particularly those observations regarding the effects of damping or the magnitudes of damping, in terms of conclusions reached and recommendations made are noted.

The results of the survey of past vibration tests serve as a basis for the authors to make conclusions and recommendations regarding vibration tests of missile-like structures and, in particular, the effects of damping on the vibrational behavior or the generation of data to determine these effects.

The test data surveyed in this report are limited to published data. The computerized literature search services of the Redstone Scientific Information Center were used to obtain an initial bibliography. This bibliography was reviewed and only those reports considered pertinent to the problem were obtained. These reports were then further reviewed to select those dealing with vibration tests to serve as the basis for the present survey. Reports dealing with analytical methods of prediction and calculated results are not included in this survey.

1

The following section deals with the survey of vibration tests on missile-like structures. It also includes the observations of the experimenters, including their conclusions and recommendations.

The third section concerns the evaluation of the vibration test data by the present authors including the accuracy of the test data, the comparisons between the test and analytical predictions, and any effects on damping.

The fourth section concludes the report and deals with the possible influence of this information on future tests. This section gives the author's recommendations as to what significant information to look for in future tests and recommendations for obtaining additional damping information from future tests.

An appendix giving a short summary of all of the reports reviewed is included as part of this report. References in the text of this report are those related to this appendix.

SURVEY OF VIBRATION TESTS ON
MISSILE-LIKE STRUCTURES

TYPES OF TESTS AND TECHNIQUES USED

Tests of missile-like structures in which the vibrational character-
istics were examined, either as the prime objective of the test program or
as a part of a larger test program, can be divided into three categories:

     1.   Flight tests

     2.   Prototype ground tests

     3.   Scale-model ground tests.

Flight Tests

Flight tests are at times designed to include a number of measurements
that would be useful in determining certain of the vibrational character-
istics of the vehicle. These data are only a small part of the test mission
of the vehicle. Many more important items regarding the performance of the
vehicle are normally being sought. Crystal accelerometers and barium titanate
accelerometers have been used on some flight tests. These accelerometers
were located in a limited number of positions on the vehicle [A1]*, in some
cases on an instrument package or on an engine as indicated in Figure 1.
The output data of the accelerometers were telemetered to the ground stations.

Prototype Ground Tests

More extensive information is obtained using a full-scale prototype
which has been instrumented extensively for tests dealing primarily in deter-
mining the vibrational characteristics of the vehicle. These vehicles are
supported either vertically or horizontally by cable-springs arrangement.
The smaller vehicles have been suspended horizontally, e.g., the Thor Delta [B7].
The most common practice on the larger vehicles of the Saturn-type has been
to suspend these vertically using a multi-cable spring arrangement as indi-
cated in Figure 2.

---

*Superscripts refer to references included in an appendix to this report.
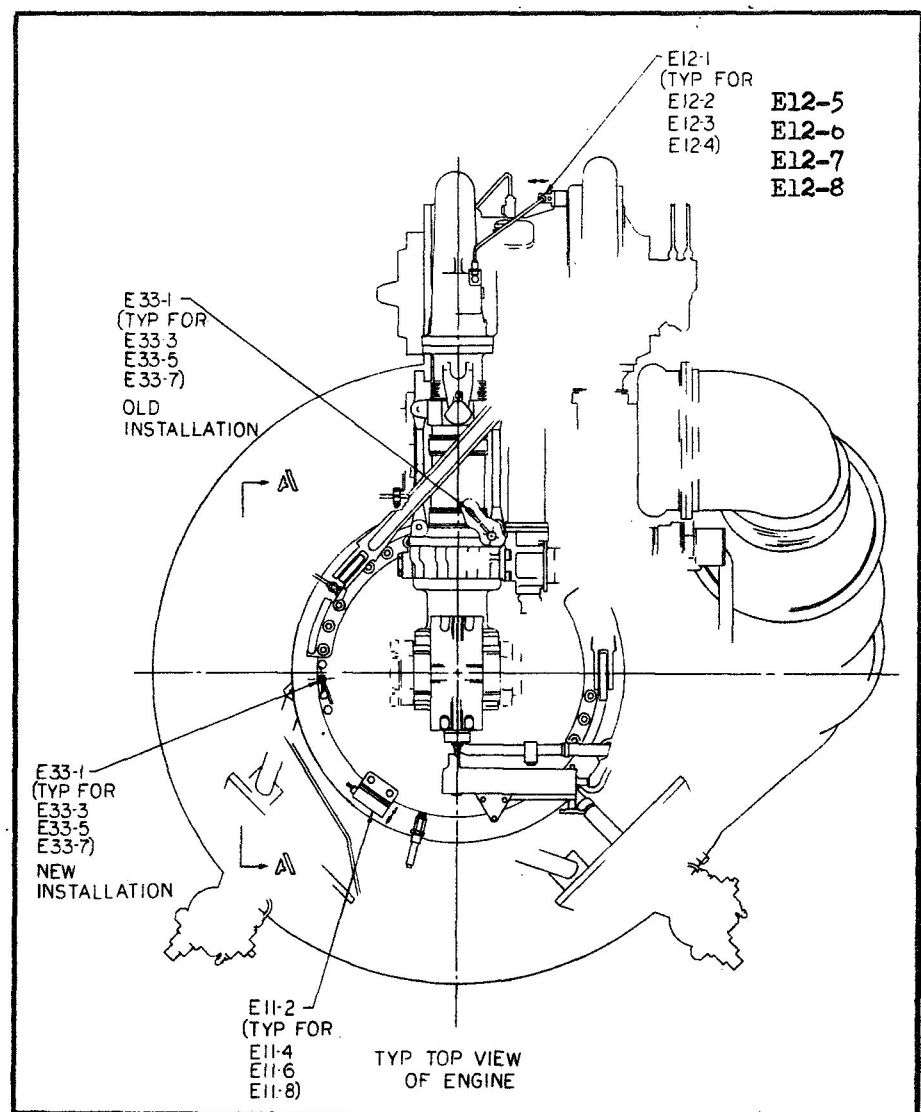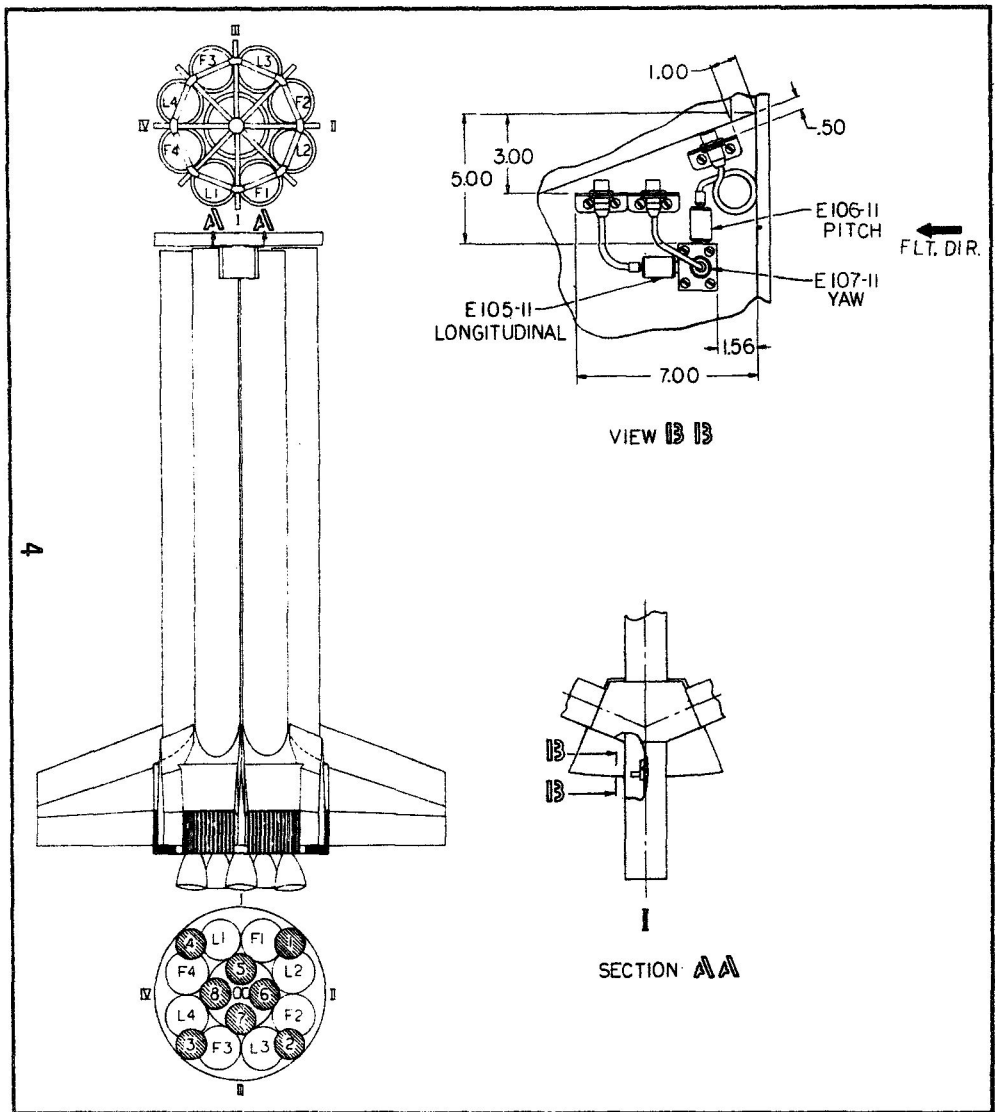
Figure 1. Illustrative Locations of Accelerometers (from Ref. A1)
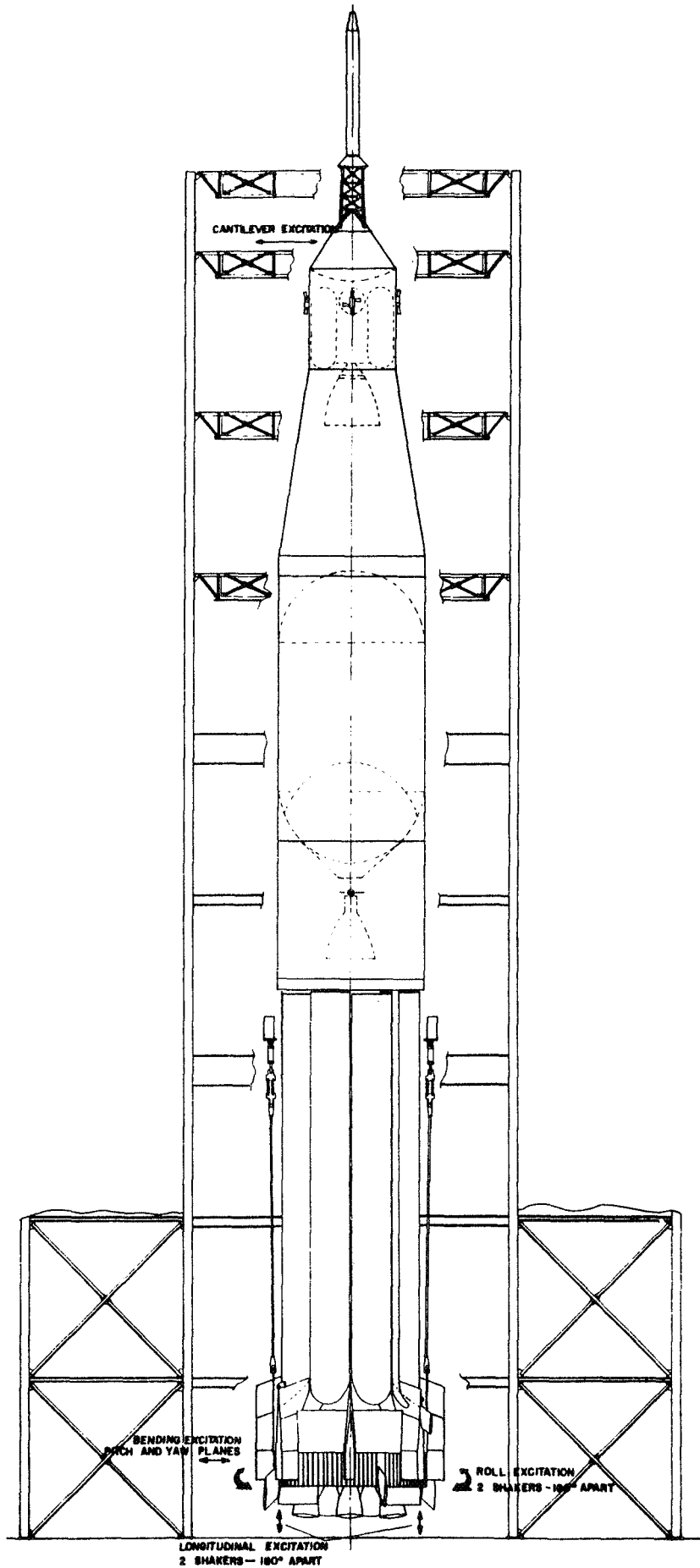
Figure 2.   Saturn Vehicle Suspended in a Free-Free Condition
            (from Ref. B3)

5

Extensive instrumentation, both on the vehicle as well as readout equipment on the ground has been used to obtain detailed information regarding the vibrational characteristics. Ground tests on the Saturn IB, for example, used about 75 accelerometers located at 15 different stations as well as accelerometers located on the fins and cables[B3]. In addition, the tests also incorporated 15 rate gyros and 4 control accelerometers. The model was excited in the pitch, yaw, and torsion planes using electro-magnetic shakers. The vehicle could be excited in its various modes, and the mode shape as well as natural frequency determined. In some cases, the data were such that the damping factor for the vehicle could be obtained; in others, the design of the test did not allow for the determination of the damping factor. Some tests, however, were primarily aimed at determining the damping factor of the vehicle.

Large-Scale Model Ground Tests

Large-scale models of vehicles have been used to determine the vibrational characteristics of the full-scale vehicle[C2]. These scale models were geometrically similar to the full-scale vehicle with the inertial and elastic properties scaled according to similarity conditions. Attempts were also made in these models to simulate the sloshing of fuels. The models were supported by spring-cable systems similar to those used in the vibrational tests of the full-scale prototype. Tests of the scale models were also made to determine the effect of the suspension systems from that of two cables to the eight-cable suspension system used in the full-scale prototype tests of the Saturn vehicles[C3]. The models were extensively instrumented using unbonded strain gage type accelerometers. In addition, certain tests used an accelerometer with a vacuum attachment as a portable pickup to determine the direction of motion of the outer booster tank of the Saturn SA-1 scale model test. Not only can extensive instrumentation be used on the vehicle, but supporting readout and analysis equipment can be used on the ground.

In most cases, the model was excited by an electromagnetic shaker acting in one plane[C3]. However, in some cases, up to eight electromagnetic shaker arrangements have been used to excite the model in various modes of motion[C1]. As in the full-scale prototype test, the model can be excited by the magnetic shakers in pitch, yaw, and torsion.

6

PERTINENT INFORMATION OBTAINED FROM TESTS

Only those data dealing with the vibration characteristics and damping of the vehicle are covered in this section. The tests may have been designed to obtain additional information or may have been aimed primarily at obtaining information other than the vibrational or damping performance.

Flight Tests

The vibrational performance of the vehicle is only a small part of usual flight test programs. The exciting forces are not controllable and usually are those arising from the environment or from the propulsion system of the vehicle. Accelerations sensed at limited locations are normally telemetered to the ground. A spectral analysis of these acceleration readings is conducted using data for small periods of time with the signal repetitiously reproduced.

For the case of flight tests of the Javelin vehicle[A2], signals from seven accelerometers mounted in an instrumentation package were used. A spectral analysis of the acceleration data for certain phases of the flight was conducted using 1.5 to 2 seconds of signals repetitiously reproduced. The reduced data were presented as frequency as a function of time, average acceleration as a function of time, and acceleration spectral density as a function of frequency at different times for the different acceleration gauges. The frequencies of vibration are higher than those of interest for the first, second and third modes.

Flight tests of the NASA Scout ST-1[A3] vehicle included instrumentation for vibration measurement. A limited number of crystal accelerometers were installed on the vehicle to sense the normal and transverse accelerations. Rate-gyro readings were also used to check the accelerations and deflections. These rate-gyros were located in the payload section. Although this instrumentation was primarily intended to obtain the environmental vibration measurements during the third and fourth stage motor burning, they also supplied information which was useful in obtaining the bending and damping characteristics. The data obtained from the tests were subjected to a spectral analysis using a Davis-Wave Analyzer and two-second tape loops for a frequency range of 0 to 4000 hertz, with a filter nominal bandwidth of 20 hertz and the average linear mode of operation. More refined analyses were

7

conducted as well. Figures 3, 4, and 5 show plots of the frequencies of the first, second and third modes as a function of flight time for the first, second and third stages of the vehicle. The damping ratio for the second and third stage of the vehicle is also shown as a function of flight time. The assumed value of 0.01 is indicated for comparison. The measured values are as much as three times the assumed value. The method of determining the damping ratio from the experimental data was not discussed in the report. It was probably determined from the bandwidth of the various modes determined from the spectral analysis.

Prototype Ground Tests

Vibration tests of the Thor-Delta missile[B7] were conducted to improve the analytical model used to predict the vibrational characteristics. Figure 6 shows the modal shapes and frequencies as predicted by a preliminary mathematical model, as obtained from the tests and as predicted by the modified mathematical model. The tests were also used to evaluate the operation of the control system in a vibrational environment where bending dynamics, as well as localized vibration effects, could be observed.

A full scale test vehicle made up of a Lance for the first stage, a Lance for the second stage, a Recruit for the third stage, and a T-55 for the fourth stage was vibration-tested by NASA/Langley Research Center[B8]. The calculated and experimental modal shapes for the first three modes compared quite favorably as shown in Figure 7.

Although the structure was supposedly geometrically symmetrical about the longitudinal axis, a small but consistent difference in the vibration characteristics of the first three modes for tests conducted for longitudinal planes ninety degrees with respect to each other showed some variation in the frequencies, Figure 8. These differences were believed to be due to tolerances and fabrication effects which could also produce unpredictable variations and frequencies of several percent in vehicles which are supposedly similar.

The effects of joint looseness between the joints of the stages of the vehicle were also investigated. Figure 9 shows the variation of natural frequency of the first mode with joint looseness and amplitude of oscillation. The tests showed that reductions in the natural frequency of the first mode of up to 20 percent could exist during unwinding of the screw joints between
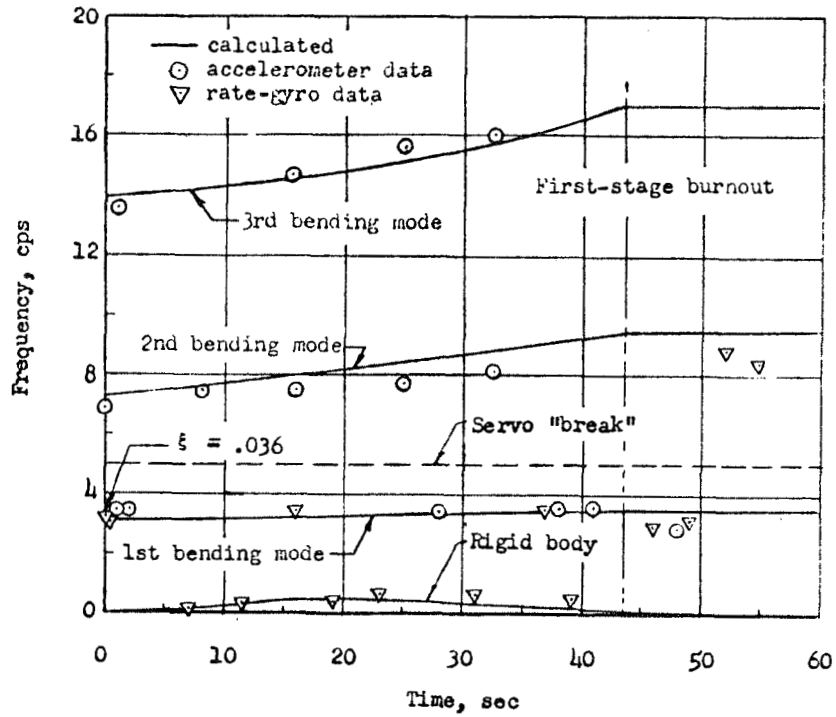
Figure 3.   In-Flight Measured and Calculated Data, First
Stage (from Ref. A3)

9
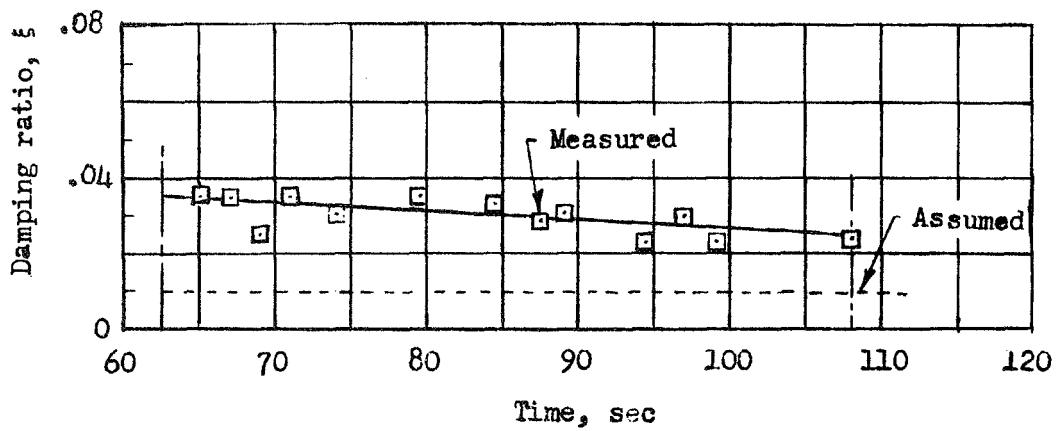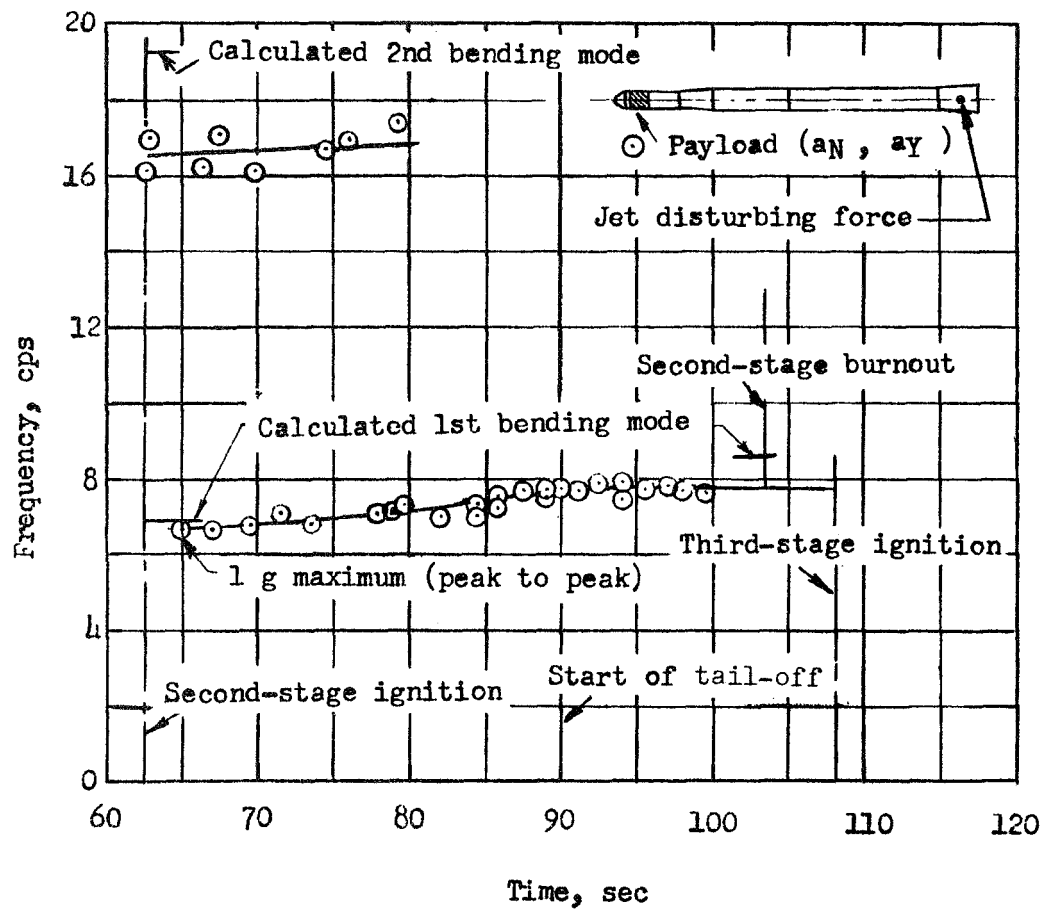
Figure 4. In-Flight Measured and Calculated Data, Second Stage (from Ref. A3)
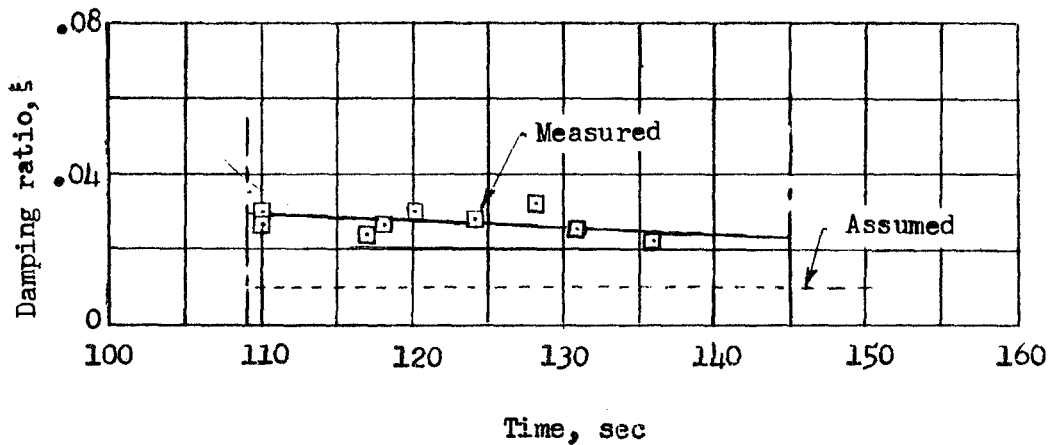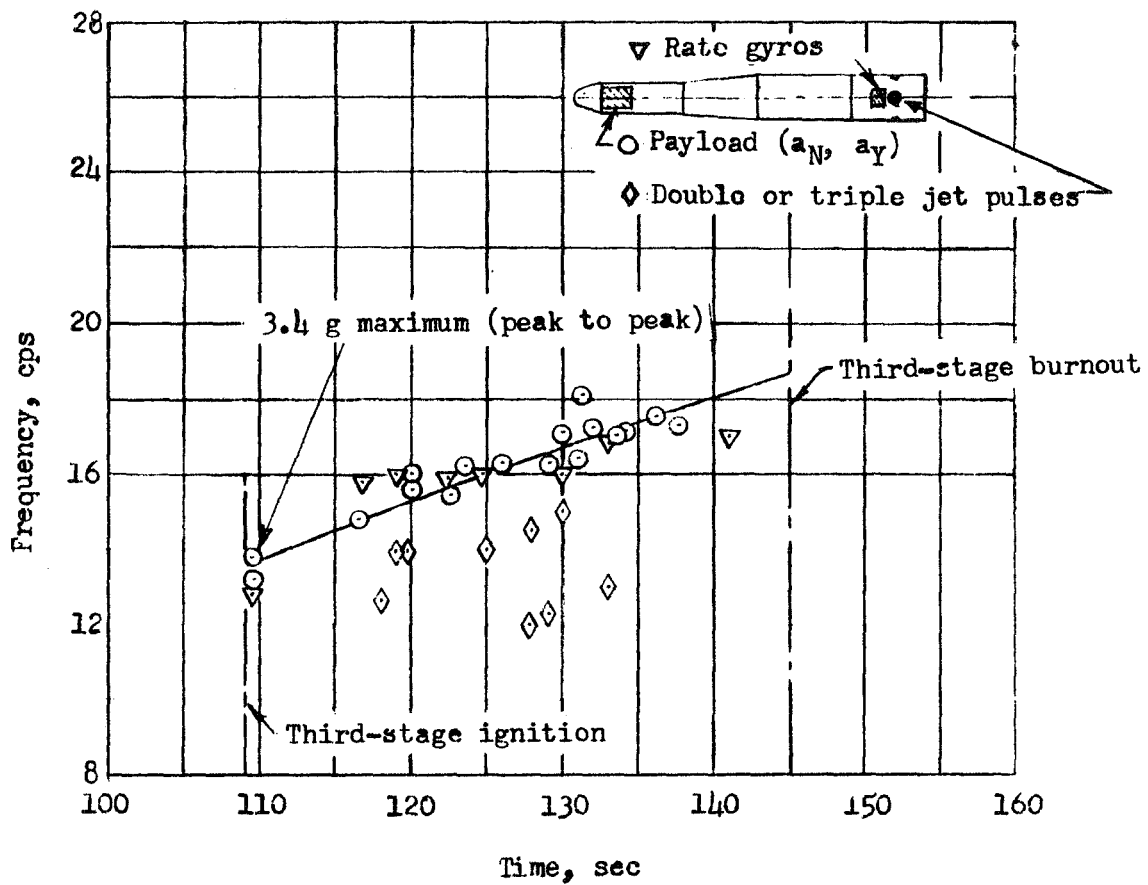
Figure 5. In-Flight Measured and Calculated Data, Third Stage
(from Ref. A3)

11

THIRD BODY BENDING MODE

3RD MODE FREQUENCY

PRELIM. COMP. MODE   26.1 cps
TEST MODE   19.3 cps
FINAL COMP. MODE   23.0 cps

RELATIVE DEFLECTION

SECOND BODY BENDING MODE

2ND MODE FREQUENCY

PRELIM. COMP. MODE   17.9 cps
TEST MODE   14.5 cps
FINAL COMP. MODE   14.7 cps

RELATIVE DEFLECTION

FIRST BODY BENDING MODE

1ST MODE FREQUENCY

PRELIM. COMP. MODE   4.9 cps
TEST MODE   4.5 cps
FINAL COMP. MODE   4.7 cps

RELATIVE DEFLECTION

Figure 6.   Measured and Computed Modal Shapes for Thor Delta
(Ground Test) (from Ref. B7)

FIRST MODE

SECOND MODE

NORMALIZED
DEFLECTIONS

THIRD MODE

—— CALCULATED
o   EXPERIMENT

Z/L
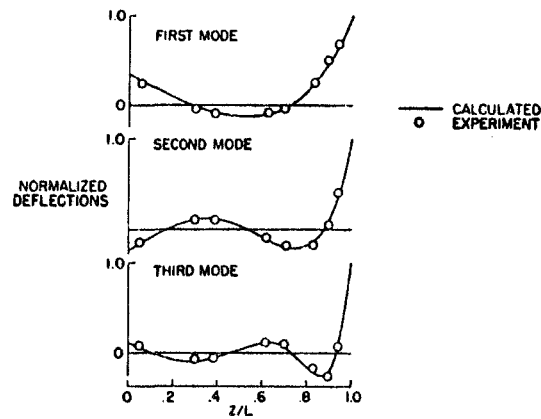
Figure 7.   Comparison of Experimental and Natural Mode Shapes for
Lance Recruit Assembly (from Ref. B8)

12

MODE	CALCULATED FREQUENCIES	TEST 1	TEST 2	TEST 3
		EXPERIMENTAL FREQUENCIES		
1	5.46	5.41	5.45	5.36
2	11.45	10.54	10.62	10.33
3	19.82	17.22	16.24	15.88

(ALL FREQUENCIES GIVEN IN CYCLES PER SECOND)
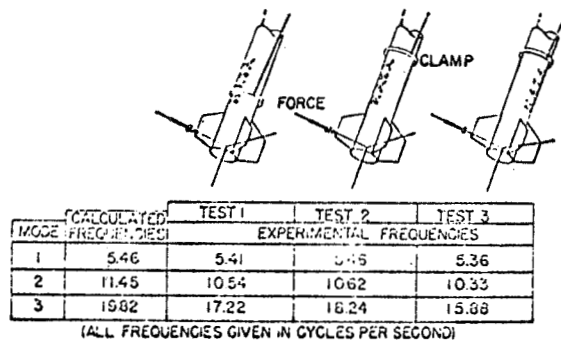
Figure 8. Comparison of Experimental and Calculated Natural
Frequencies for Three Test Conditions for Lance
Recruit Assembly (from Ref. B8)
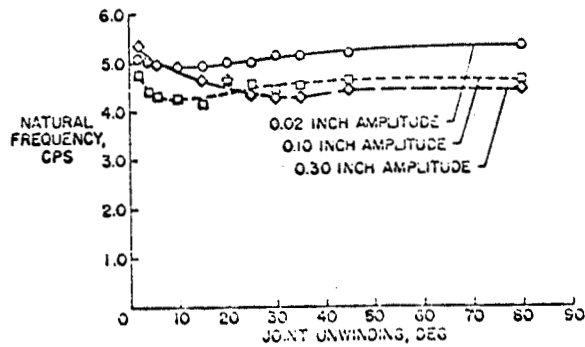
Figure 9. Variation of Natural Frequency of First Mode with
Joint Looseness and Amplitude of Oscillation for
Lance Recruit Assembly (from Ref. B8)

13

the second and third stages. (The authors of the report stated that observations with many rocket vehicles show that significant local contributions to flexure frequently originate at joints and that these joint effects must be included in the analyses involving flexure. The problem has been treated empirically at NASA/Langley Research Center with satisfactory results in the determination of the natural vibration characteristics and in aeroelastic problems. The report shows some experimental results for various types of joints in terms of joint rotation constants for various degrees of tightness of the joint.)

The most extensive dynamic tests to determine the vibrational characteristics of full-scale vehicles have been performed on the Saturn family of vehicles[B2]. These tests were carried out for various loading conditions of the vehicle to determine the flight characteristics for different portions of the flight path. The data from these tests are extensively documented. The accelerometer measurements are presented in different ways, e.g., as plots of displacement per unit force as a function of frequency (Figure 10); displacement at numerous stations along the structure at various resonant frequencies (Figure 11); resonant frequency as a function of simulated time after firing (Figure 12); or amplitude as a function of time for natural decay (Figure 13). Damping information is obtained from these data assuming a single degree-of-freedom formulation with viscous damping. A typical set of data for damping is shown in Table 1.

Full-scale tests of the Atlas/Agena configuration were conducted primarily to establish the damping of the vehicle[B6]. The peak-to-peak amplitude of position transducers, at each cycle of the transient decay, was measured and plotted as a function of the number of cycles of decay. A typical plot is shown in Figure 14. The damping ratio was related to the slope of the line tangent to the curve (related to a single degree-of-freedom viscous damping model). Results of this test indicated that in all but two cases the damping ratio reduced with amplitude. The reason for this behavior was explained as being due to a decrease in friction between the buildup section. This decrease in friction becomes negligible with a decrease in the amplitude of motion. Two cases were observed which did not follow this behavior. No explanation could be offered for these two unusual cases.
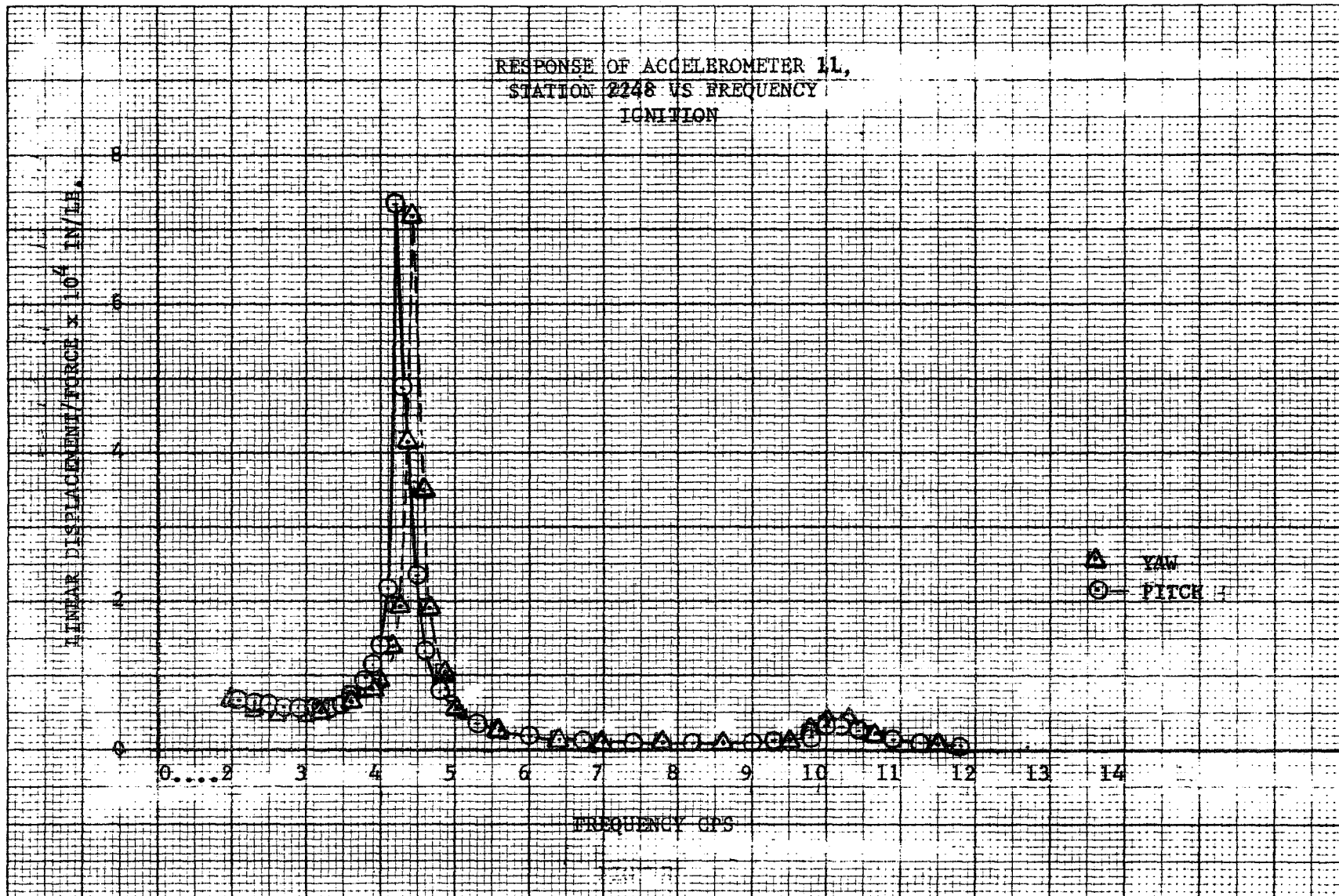
Figure 10. Response as a Function of Frequency of Pitch and Yaw for Saturn
Vehicle (from Ref. B2)
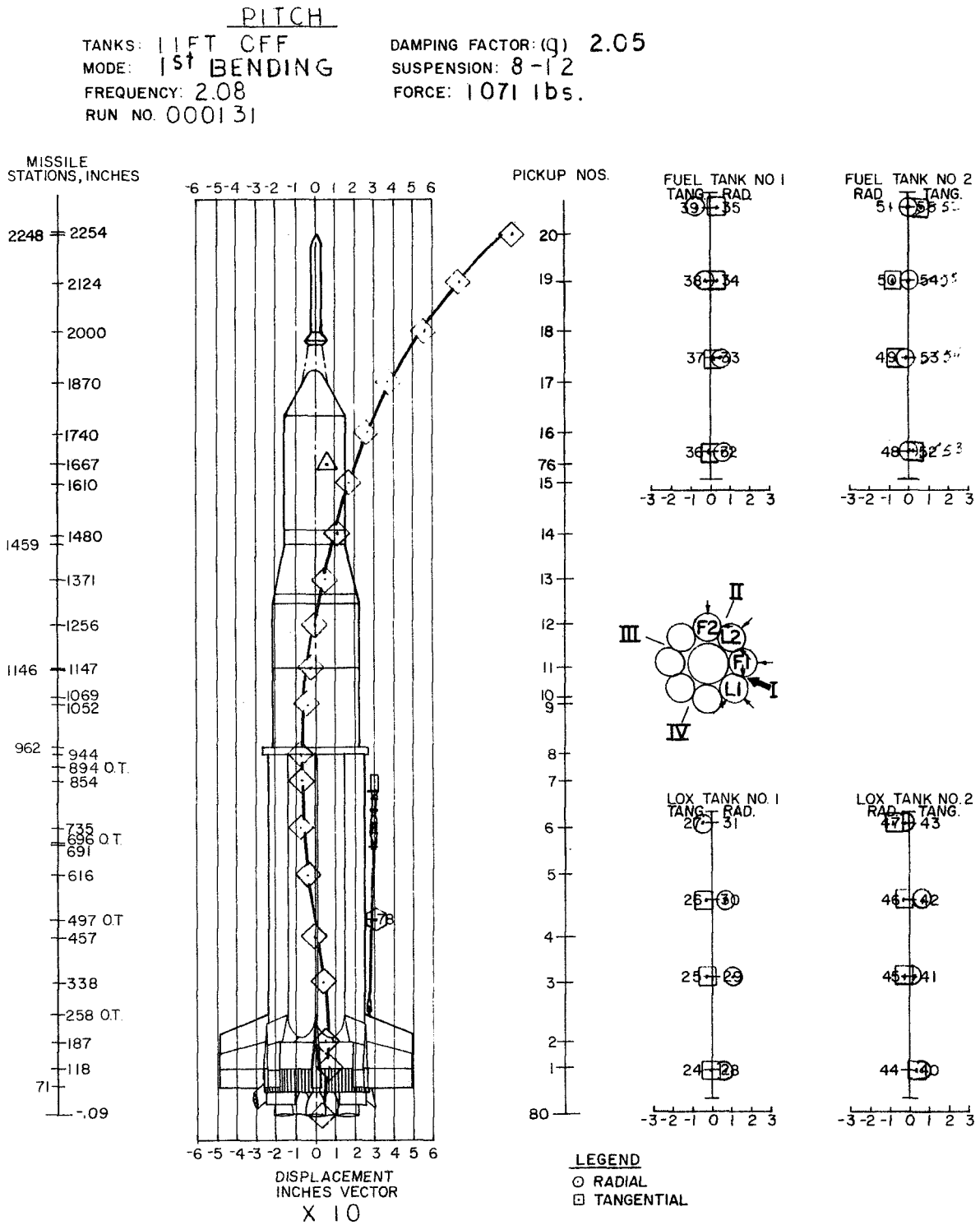
Figure 11. First Bending Mode (Pitch) for Saturn Vehicle (from Ref. B2)
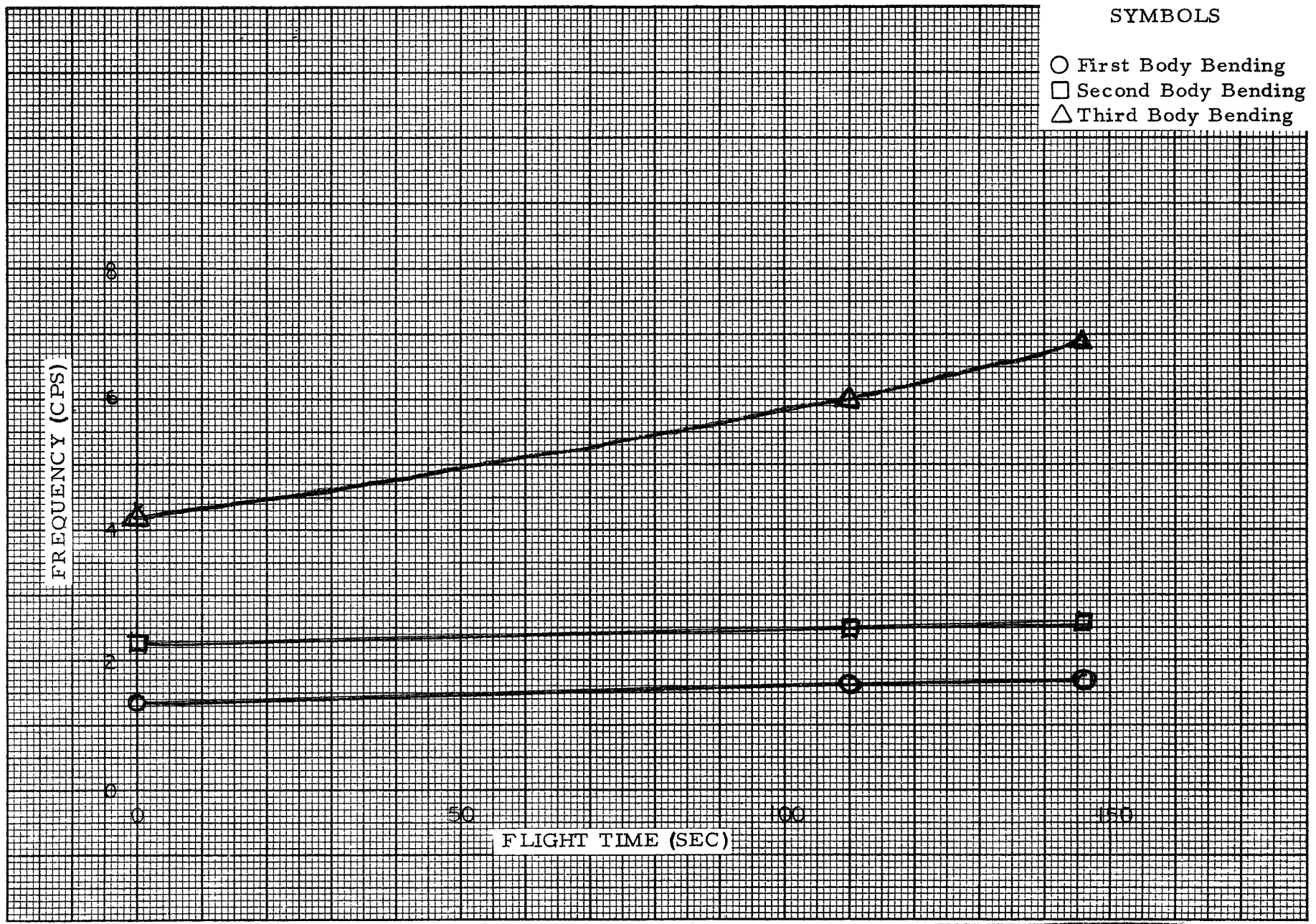
Figure 12. Pitch, Bending Frequency Variation with Simulated Flight Time for SA-202 (from Ref. B3)
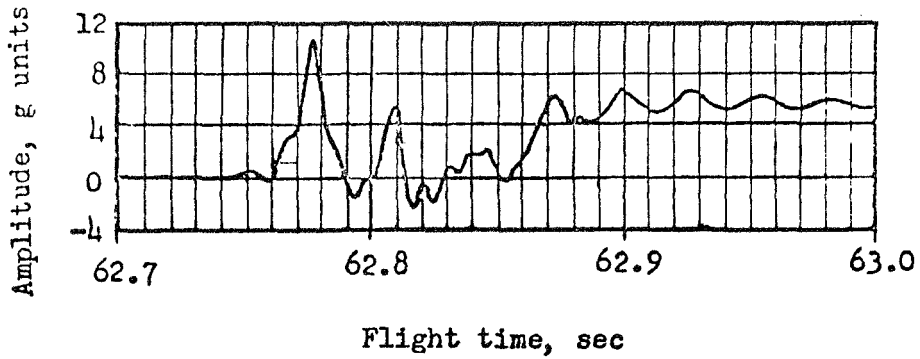
Time history of the amplitude of payload longitudinal linear acceleration at second-stage ignition.
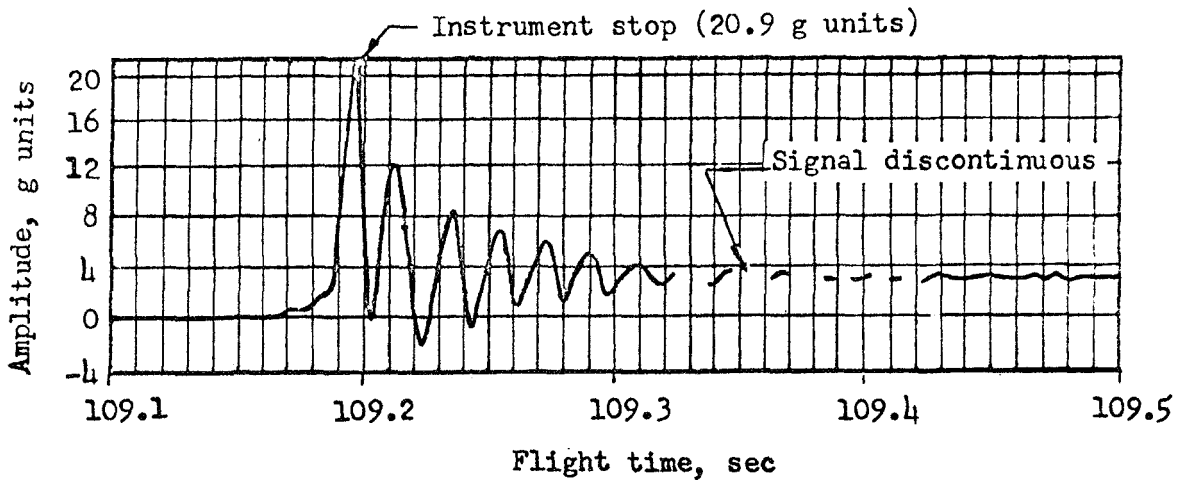
Time history of the amplitude of payload longitudinal linear acceleration at third-stage ignition.

Figure 13. Amplitude as a Function of Time for Natural Decay of Vibration for Scout Vehicle (from Ref. A3)

18
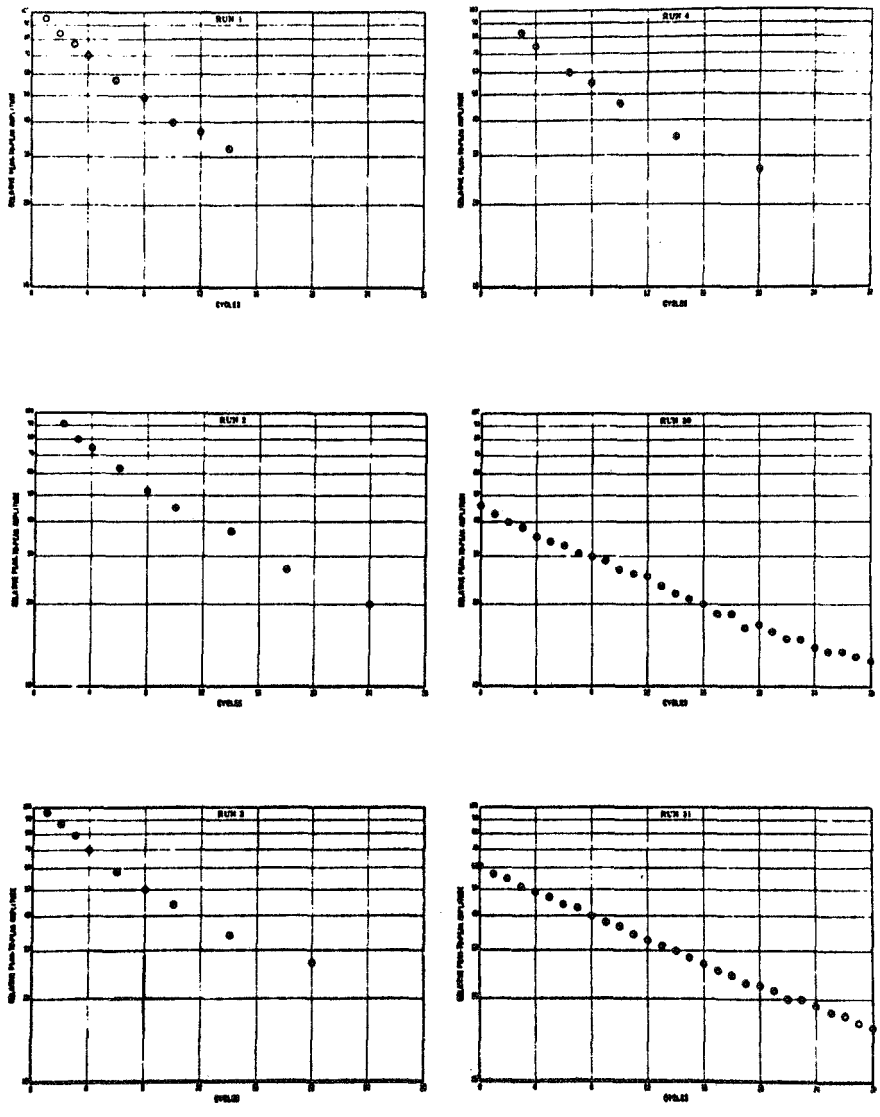
Figure 14. Typical Plots of Data for Determination of Damping
Factors for Atlas-Agena Assembly (from Ref. B6)

TABLE 1

TYPICAL RESONANT FREQUENCIES AND STRUCTURAL DAMPING FACTORS (from Ref. B2)

Run Number	Mode	Frequency (Hz)	Damping (g)
Longitudinal, Liftoff, 8-8 Suspension			
030001	Bouncing	01.550	--
030005	R_2	04.900	--
030007	R_3	05.780	--
030011	R_4	06.510	1.82
030014	R_5	07.540	2.58
030016	First Longitudinal Mode	10.170	3.34
030020	Engine and Thrust Structure	13.700	2.05
030022	Fuel Tank	16.410	2.58
030024	R_9	18.640	6.09
030026	R_{10}	20.770	--
030031	R_{11}	24.830	2.28
Longitudinal, 146 sec, 4-E4 Suspension			
230001	Bouncing	01.830	1.96
230003	First Longitudinal Mode	11.410	5.08
230005	Outer Tanks	14.220	5.17
230010	S-IV Engine and Outer Tanks	20.530	5.17
230012	S-IV Bulkhead	25.850	4.41
230014	S-IV Bulkhead and Outer Tanks	28.120	3.56
230016	Outer Tanks	35.870	--
Torsion, Liftoff, 8-8 Suspension			
020003	Outer Tanks Tangent	02.356	2.01
020006	Tower Lateral	03.592	3.38
020007	First Torsion	03.687	4.32
020012	Tower Lateral	04.036	3.07
020014	Cluster	05.660	2.10
020016	Second Outer Tanks Tangent	06.594	3.60
020020	R_7	10.040	--
020023	R_8	10.560	--

Scale Model Ground Tests

The Martin Company used a one-fifth scale Titan III vehicle as a dynamic test model to verify the analytical model used for vibration analysis of the Titan III vehicle[C1]. In the cited reference, the authors list some of the advantages of large-scale model testing. These include cost items as well as the large amount of data that can be obtained from model tests. Figure 15 shows the first three pitch modes as predicted by the analytical model and as obtained experimentally using the one-fifth scale model. One problem pointed out by the authors is that of structural damping simulation. They stated that structural damping may not be simulated accurately due to deviations in local nonstructural details such as lack of insulation. Structural damping data obtained in the Titan III scale model vibration tests are shown in Figure 16; full-scale data derived indirectly indicated higher values. Based on these and other tests, the authors concluded that to provide high fidelity scaling, the length of a model should be somewhere on the order of 25 to 40 feet and that this length is more important than the scale factor used. Smaller lengths would require skin thickness scaling which would be prohibitive as well as difficulties in achieving scaling in tolerances.

A one-fifth scale dynamic model of the Saturn SA-1 vehicle was tested at Langley Research Center in order to determine the feasibility of using dynamically scaled models to obtain vibration data[C4]. Figures 17, 18 and Table 2 show a comparison of the resonant frequencies, mode shapes and damping from the model with the ground vibration surveys of a full-scale Saturn vehicle. The first bending mode frequency parameters agreed within 6 percent, provided the rigid body suspension system rocking frequency parameters were in agreement. The frequency parameters of the cluster modes were about 10 percent below the full scale frequency parameters. The damping was of the same order of magnitude as the full scale vehicle for most of the modes, and agreement was found between the lower mode shapes. Significant differences were found between the model and full-scale higher mode shapes. These were believed to be caused by structural simplifications made in the second stage structure of the model. Nonlinear effects were observed both in the model and full-scale vehicle for the first bending mode response. These effects were characterized by a decrease of resonant frequency with increase of vibration amplitude.

21
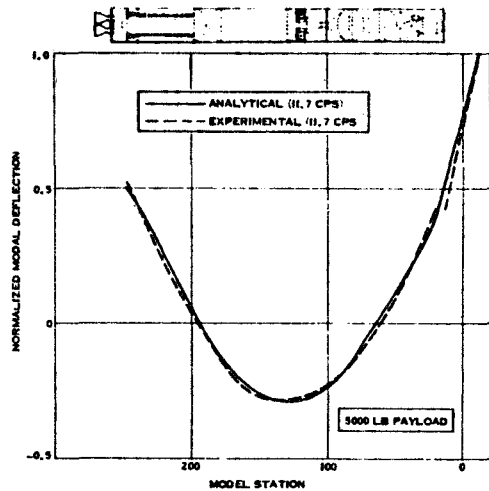
Figure 15a. First Pitch Mode - Lift-Off - Configuration 3-A
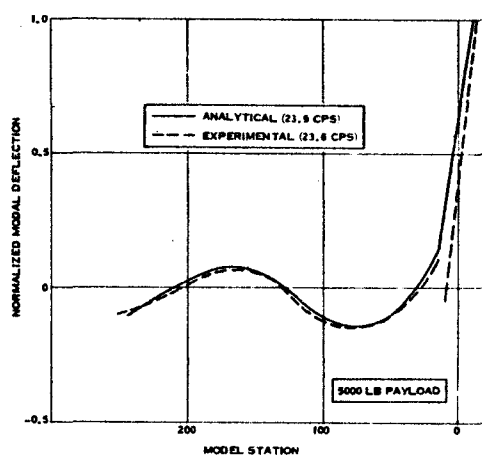
Figure 15b. Second Pitch Mode - Lift-Off - Configuration 3-A
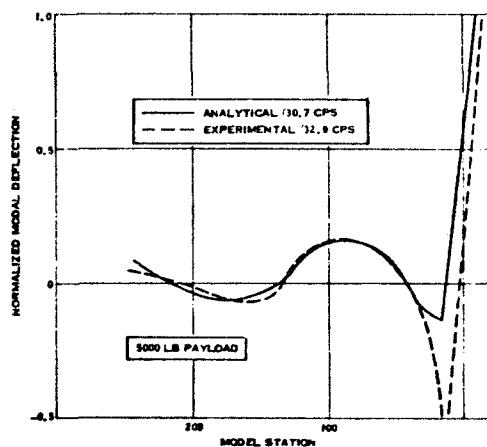
Figure 15c. Third Pitch Mode - Lift-Off - Configuration 3-A

Figure 15. Measured and Computed Lateral Mode Shapes for Titan III
Full Size (from Ref. C1)
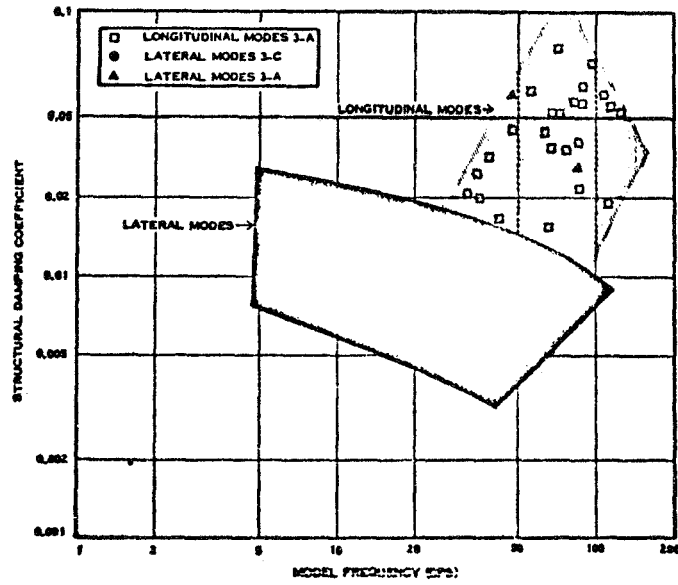
Figure 16. Summary of Modal Damping Data - Titan III, 1/5 Scale Model (from Ref. C1)
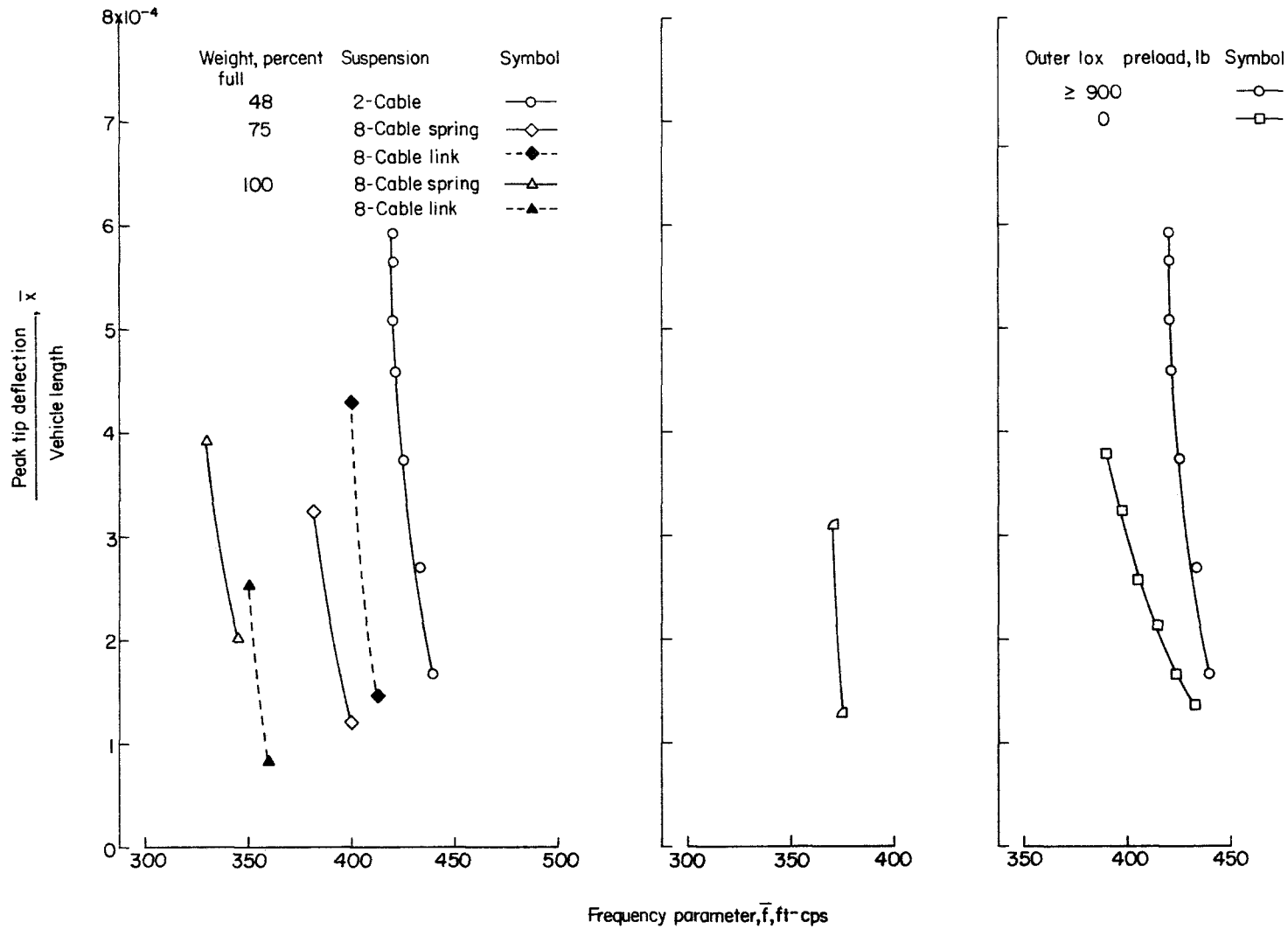
(a) Effect of suspension and weight variations. 1/5-scale model; outer lox preload ≈ 900 lb.

(b) Full-scale vibration test vehicle. Block II(SAD-5). Lift-off weight.

(c) Effect of outer lox tank preload. 1/5-scale model; two-cable suspension; weight at maximum dynamic pressure.

Figure 17. Variation of Resonant Frequency of Saturn First Bending Mode with Vibration Amplitude (from Ref. C4)
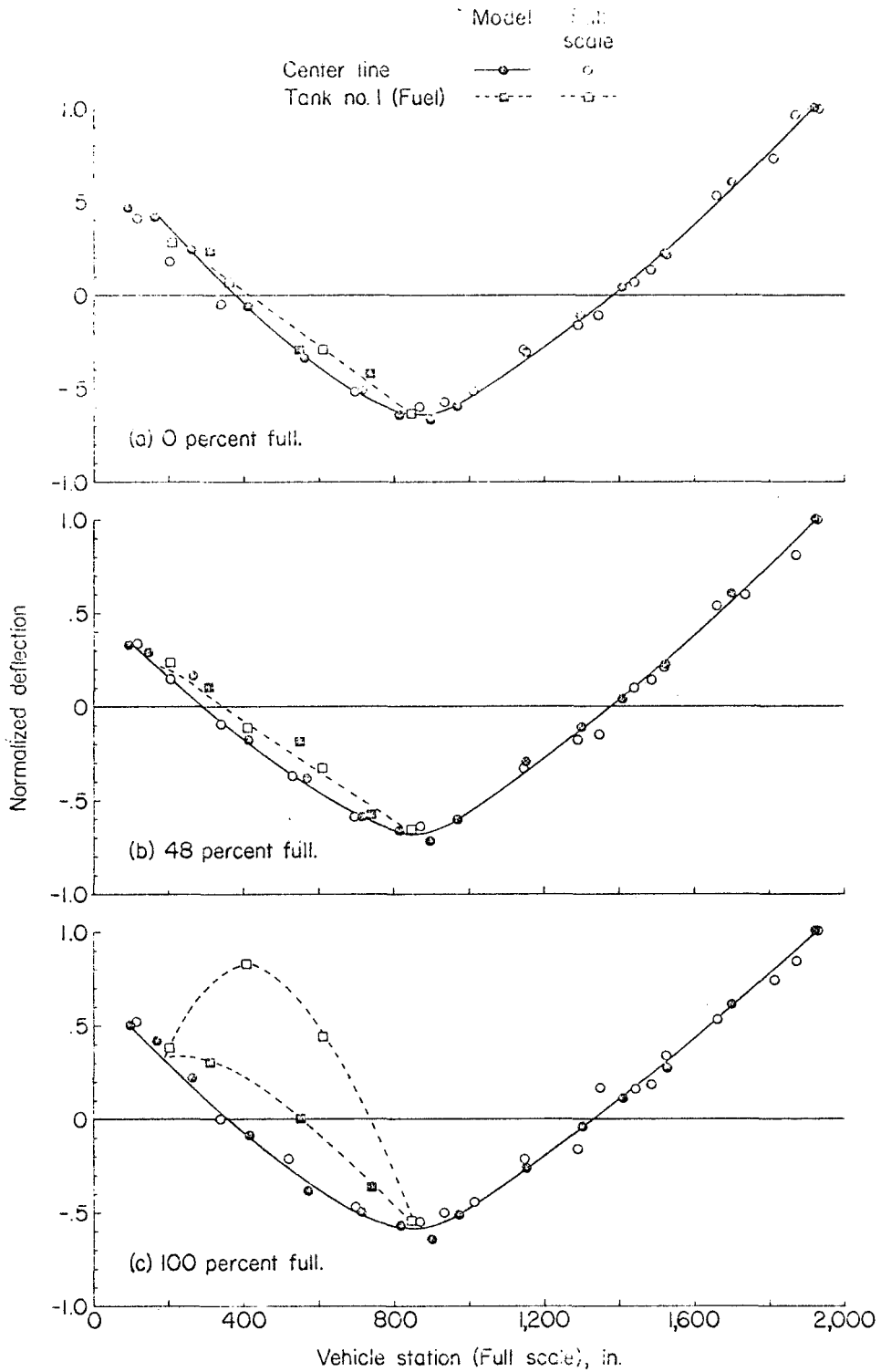
Figure 18. Comparison of Model with Full-Scale First Bending Modes of Saturn (from Ref. C4)

EVALUATION OF VIBRATION TEST METHODS AND DATA

GENERAL

Three methods of obtaining the vibrational characteristics of missile-like configurations have been used. Damping information has been obtained for each of these methods. These three methods are

- Free-flight testing

- Full-scale captive or ground tests

- Large-scale model captive tests.

Free-flight vibration testing is probably the most expensive and offers the most limited and least accurate information regarding the vibrational performance and damping information. The variables of the experiment are not controllable. The instrumentation is limited and the telemetry system for transmitting the basic data to the ground is rather complicated. Free-flight testing should be used primarily for limited verification of other test data obtained by controlled ground tests. Flight testing is not the best method for generating basic data regarding the vibrational characteristics of the vehicle or the effects of damping on such vibrational characteristics.

Full-scale captive tests[B2], though expensive, allow for extensive instrumentation and control of the variables of the experiments. Large amounts of data have been obtained primarily during the Saturn program. Support systems have been designed and used that very closely simulate the free-free flight conditions. Time schedules as well as other demands on the vehicle essentially preclude the evaluation of design modifications based on previous tests.

Large-scale model captive-tests allow extensive instrumentation and control of the variables of the tests. The effects of design modifications based on previous tests are more likely to be evaluated since the demands on the models will not be as great as those on the full-scale vehicles. The models can also be used to generate much more information due to their availability.

In any overall program all three methods of testing should be used. During the design process of the vehicle, large-scale model captive-tests should be used to verify the design as well as to generate information on which design changes can be based. After the design has been frozen and a prototype built, full-scale captive tests should be conducted to determine any scaling effects that are unpredictable. Certain of the flights should then incorporate a limited amount of instrumentation to spot-check the data of the full-scale captive tests.

ACCURACIES

Very little documentation regarding the accuracies of vibrational testing is available. In some cases qualitative information is given. In general, the flight test method seems to be subject to the largest errors. Errors can be introduced by environmental effects on the instrumentation, such as changes in temperature, by the lack of understanding of the externally and randomly applied forcing functions, and by errors in the telemetering process. In one case mentioned, fictitious peaks in the accelerometer data were introduced due to loss of telemetering data at various flight times.

The accuracy of full-scale ground test results have, in general, been considered good. Instrumentation errors were minimized by proper calibration of equipment and the control and understanding of the environment, e.g., variations of accelerometer readings with temperature due to viscous damping (oil) used in the accelerometers. The suspension systems used can also introduce errors; however, care was taken in the design of the suspension system to minimize these errors. In certain tests the accuracy and reliability of the test data was questioned due to lack of understanding and due to lack of instrumentation. In general, however, the experimental errors seem to be small. Documentation of the errors of the instrumentation would be of great help to those reading and interpreting the test data.

The accuracies and experimental errors involved in large-scale ground testing are generally the same as those for full-scale captive ground tests. A possible source of error in extrapolating the data of large-scale ground tests to that for the full-scale vehicle is that due to deviations in local nonstructural details such as lack of insulation, giving structural damping values which may be different from that of the full-scale vehicle. Another

28

possible source of error is that due to the differences in the suspension systems used to simulate the free-free conditions. Again, the documentation of the experimental errors of the tests would be valuable to those using or interpreting the test data.

COMPARISON WITH ANALYTICAL PREDICTIONS

The limited amount of instrumentation used in flight tests does not give sufficient data for the determination of the mode shapes. The frequencies of the first three bending modes for various flight times have compared favorably with analytical predictions (Figure 3). Indications from the reports surveyed are that 1 percent damping ratio was used in the analytical predictions. The in-flight damping data gives a variation of the second and third stages of the configuration decreasing from about 3 percent to about 2 percent during the flight history (Figure 4). The damping is probably that assumed for a viscous single degree-of-freedom system.

The extensive instrumentation used on full-scale ground tests permits an accurate determination of the modal shapes and frequencies for about the first three modes. These mode shapes and frequencies compare quite well with analytical predictions (Figures 6, 7, and 8). Coupling effects between various components and motion appear to be higher than expected[C1]. Deviations between the predicted and experimental frequencies and modal shapes can usually be explained by the factors in the test not accounted for in the analytical models such as engine resonances. In general, the damping has been found to be quite small, usually on the order of 2 to 3 percent. The damping in torsion is usually higher than that in the lateral direction.

The same remarks regarding large-scale ground tests can be made as those above for the full-scale ground tests (Figure 15). Local vibrational effects in the large-scale model differing from those in the full-scale ground tests may exist. These local vibration effects could be important. In one case[A3], a control box was rendered inoperative because of vibration chatter.

DAMPING

The test data from either of the methods of testing is often used to obtain a value of damping ratio, assuming a viscous type of damping and a

29

single degree-of-freedom model. The damping ratio is normally expressed in terms of the percent of critical damping.

From flight test data a value of damping ratio of about 3 to 3.5 percent, decreasing with an increase of frequency to about 2.5 percent, was found to exist (Figure 4). This was based on a limited amount of data at limited locations of the body.

Full-scale captive tests have indicated damping ratios as high as 7 percent (Figure 17). Most of the data, however, shows damping between 5 percent and 1 percent of critical (Figure 14). The damping data is quite scattered; in general, the damping seems to increase with increased frequencies corresponding to higher modes. Trends are not quite clear for a given mode, e.g., in the lateral modes some data for the Titan III[C1] showed a considerable scatter and a slight decrease with increasing frequencies. The data for the other mode of this reference is too scattered to allow determination of any trend in the damping with increases of frequencies. The modal frequencies vary with time due to variations of fuel in the vehicle. The damping on the full-scale vehicles also seems to be dependent somewhat on the suspension system used. This effect can be minimized with proper design of the suspension system.

Full-scale damping tests on the Atlas vehicles have indicated that in all but two cases shown the damping ratio decreased with a decrease in amplitude[B6]. The differing of the two cases was not explained. Explanation of the decrease in damping with the decrease in amplitude is based on the relative motion at the joints resulting in lower damping for smaller motion at the joint.

Damping data from large-scale model captive tests show that longitudinal damping varies from as high as 8 percent to slightly greater than 1 percent[B6]. No significant effect of frequencies is seen for these longitudinal modes. Damping of the lateral modes from about 3 percent down to about 0.3 percent has been observed. The trend seems to be such that the damping decreases with increasing frequencies. Model tests also show that the damping decreases as the vibration amplitude decreases. These data are based on determining the damping early in the decrement and after a considerable decrease in amplitude.

SUMMARY, CONCLUSIONS, AND RECOMMENDATIONS

Test methods for determining the vibrational characteristics of missile-like configurations are well developed and give results which are quite good. These tests have not only been used to study the vibrational characteristics of the vehicle up to the first three modes but have also been used to verify and/or modify the equations of motion of the system, primarily the mass terms in the equations. Results from the tests show that the first three modal shapes and associated frequencies are predicted fairly accurately using a lumped mass parameter technique for writing the equations of motion. The damping of the structures is evidently small since the frequencies and modal shapes as given by the equations ignoring damping (or assuming a damping value of about 1 percent) compare very favorably with the experimental modal shapes and frequencies.

Essentially three general categories of vibration tests have been used. These are

●Flight tests

●Full-scale captive tests, and

●Model captive tests.

Only very limited information can be obtained from flight tests. Since this type of test is extremely expensive and affords very limited data, the flight test approach should only be used to verify results from other types of tests and not to generate original information. Information for design and research purposes should be generated on models. The model type of testing is probably the least expensive in the long run and allows the generation of more useful information to aid in the design process. Experience with model vibration testing shows that large-scale models should be used in order to be able to apply the model data to a full-scale vehicle. Vibration testing of the full-scale vehicle should also be employed in order to verify the design as well as to check on local effects such as local vibrations that may result in undesired behavior of the full-scale vehicle, e.g., the vibrational effects on components of a control system.

All of the three methods of vibration testing have been used to some
extent to try to determine the damping of the configuration as well as the
effects of damping on the vibrational characteristics of the vehicle. The
damping values determined from the vibration tests have been based on a
single degree-of-freedom viscous damped model and therefore have very limited
value. The tests have shown the damping, as based on this model, to be small
but do not allow for the determination of the effects of local changes in
damping on the vibrational behavior. The damping coefficient based on this
single degree-of-freedom viscous model not only incorporates the actual
damping occurring in the vehicle and at the joints but also includes the
elastic and mass properties of the vehicle. If one of these is changed, e.g.,
the mass, the decay of any motions would differ although the actual damping
at various locations in the vehicle could remain the same. To illustrate
this point, consider the simple two degree-of-freedom mass spring viscous
damper system shown on the sketch below[D1].
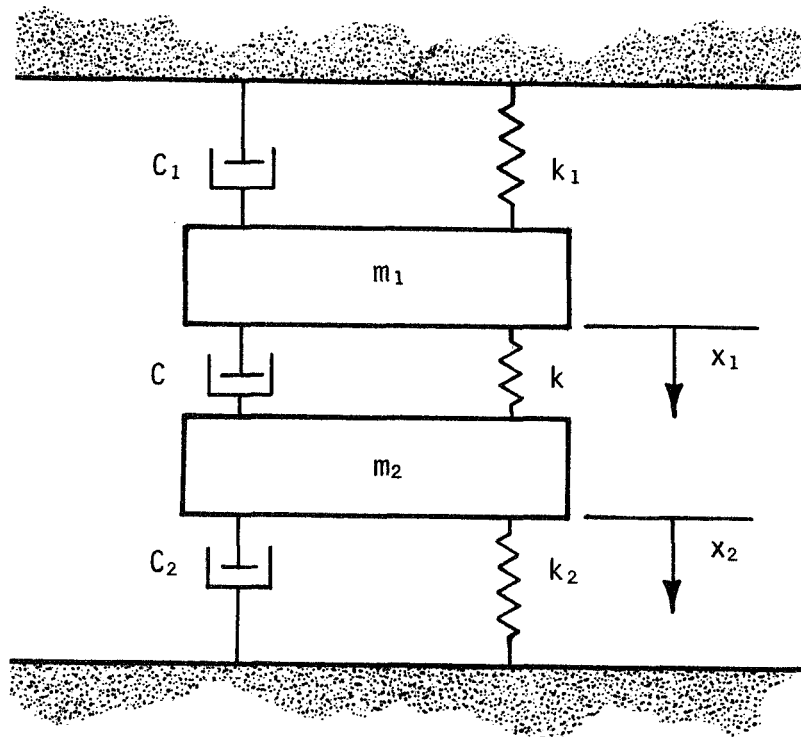
The characteristic equation for the system is the fourth-degree equation

$$S^4 + \left(\frac{C_1 + C}{m_1} + \frac{C_2 + C}{m_2}\right)S^3 + \left(\frac{k_1 + k}{m_1} + \frac{k_2 + k}{m_2} - \frac{C^2}{m_1\,m_2}\right)S^2$$

$$+ \left[\frac{C_1\,(k_2 + k) + C_2\,(k_1 + k) + C\,(k_1 + k_2)}{m_1\,m_2}\right]S + \frac{k_1\,k_2 + k\,(k_1 + k_2)}{m_1\,m_2} = 0 \ .$$

Consider the case where the damping coefficients C, C_1, and C_2 are small and with mass and spring characteristics such that one of the modes is associated with a very low frequency. For the system postulated, the characteristic equation for the low frequency mode could be approximated by the last three terms of the equation as

$$S^2 + \left[\frac{C_1\,(k_2 + k) + C_2\,(k_1 + k) + C\,(k_1 + k_2)}{m_1\,(k_2 + k) + m_2\,(k_1 + k) - C^2}\right]S + \frac{k_1\,k_2 + k\,(k_1 + k_2)}{m_1\,(k_2 + k) + m_2\,(k_1 + k) - C^2} = 0$$

or

$$S^2 + 2\zeta\omega_n\,S + \omega_n^2 = 0$$

where ω_n^2 is the equivalent undamped natural frequency and ζ is the equivalent damping ratio.

Examination of this reduced equation shows that the effective damping value for the assumed mode is dependent on the mass and elastic properties of the systems as well as the damping coefficients C, C_1, and C_2. Thus a change in the mass distribution could result in a change in frequency and effective damping. This illustration indicates that the effective damping value is quite complicated and that it is difficult, if not impossible, to interpret the physical origin of the effective damping from experimental data for a complicated vehicle assuming single degree-of-freedom equations for data reduction. The observed behavior of the "effective" damping with frequency and amplitude when mass changes have also occurred needs further clarification.

The basic mechanism associated with damping of various components of the structure, especially of joints, is not well understood. In order to understand this mechanism so as to incorporate any advantages of joint design in the design of the structure (controlling the modal shapes and frequencies), studies of much simpler systems have to be undertaken. Further investigations aimed primarily at a better understanding of the joint damping phenomena are essential for advances in the design of more optimum missile-like structures.

More useful information regarding the damping of the vehicle can probably be obtained from the vibration test methods presently being employed. The instrumentation involved would be essentially the same; however, the test procedure may be somewhat different. A study is presently underway in the Research Laboratories of Brown Engineering Company to obtain better damping information. Equations of motion for the system incoporating damping as an unknown quantity are being written. Using these equations, the test conditions and test procedure necessary to obtain the damping terms are being investigated. As shown in some of the references of this report[B1,B5,D1], the mass parameters of the system have been determined using such equations. The determination of the distributed damping over the vehicle, if obtainable from vibration tests, should be of greater use to the designer than the effective damping value presently obtained.

TABLE 2

COMPARISON OF DAMPING FACTORS OBTAINED FROM FULL-SCALE AND 1/5-SCALE MODEL OF SATURN SA-1
(from Ref. C4)

$$\left(g = \frac{1}{2\pi n} \log_e \frac{x_n}{x_0} \right)$$

Configuration	Damping Factors for -						
	Booster Tank Empty (Burnout)		48 Percent Full (Maximum Dynamic Pressure)		75 Percent Full (35 sec)	100 Percent Full (Lift-Off)	
	Soft Suspension	Stiff Suspension	Soft Suspension	Stiff Suspension	Soft Suspension	Soft Suspension	Stiff Suspension
First Bending Mode							
Full-Scale Saturn	0.024	--	0.023		0.116	0.026	--
1/5-Scale Model - 2 Cable	0.030, 0.017		0.032, 0.017		0.020	0.033, 0.025	
1/5-Scale Model - 8 Cable	0.032, 0.015	0.03	0.030, 0.013	0.033, 0.012	0.037, 0.015	0.030	0.01
First Cluster Mode							
Full-Scale Saturn	--	--	0.024		0.028	0.026	--
1/5-Scale Model - 2 Cable	--	--	0.023, 0.011		0.025, 0.015	0.017	
1/5-Scale Model - 8 Cable	--	--	--	0.030, 0.013	--	--	--
Second Cluster Mode							
Full-Scale Saturn	--	--	--	--	0.021	0.022	--
1/5-Scale Model - 2 Cable	--	--	--		0.022, 0.016	0.014	
1/5-Scale Model - 8 Cable	--	--	--	--	0.012	0.015	0.018
Second Bending Mode							
Full-Scale Saturn	0.018	--	--	--	0.010	0.010	--
1/5-Scale Model - 2 Cable	0.046, 0.032	--	--	--	0.039, 0.019	0.010	
1/5-Scale Model - 8 Cable	--	--	--	--	0.017	--	--

REFERENCES

FULL SCALE FLIGHT TESTS

A1. "Vibration and Acoustic Analysis, Saturn SA-10 Flight", by Measuring and Evaluation Section, George C. Marshall Space Flight Center, NASA TMX-53366, December 8, 1965

A2. Oleson, M. W., "Report on Acceleration and Vibration Data from Javelin (8.02) Vehicle", Naval Research Laboratory, Memo-Report-1074, July 1960

A3. Mayhue, Robert J., "NASA Scout ST-1, Flight-Test Results and Analysis, Launch Operations, and Test Vehicle Description", Langley Research Center, NASA-TN-D-1240, June 1962

FULL SCALE GROUND TESTS

B1. Papadopoulos, James G., "Dynamic Test Results of SAD-5", MSFC-NASA, MSFC-MTP-AERO-63-46, June 1963

B2. "Saturn I Dynamic Test", "Ground Vibration Survey SAD 8 and 9", by Dynamic Test Branch, Structures and Mechanics Engineering Department, Chrysler Corporation, HSM-R102, February 23, 1965

B3. "Saturn I-B Dynamic Test", "Final Report, Total Vehicle Testing of Saturn I-B, Dynamic Test Vehicles, SA200-D in SA202, SA203, SA206 and SA207 Configurations", Chrysler Corporation, HSM-R856, January 31, 1966

B4. Walker, J. H. and R. A. Winje, "An Investigation of Low Frequency Longitudinal Vibration of the Titan II Missile During Stage I Flight", TRW Space Technology Laboratory, BSD-TR-65-165, June 1965

B5. Watson, Charles E. and Kay W. Slayden, "Experimental Vibration Program on a Full Scale Saturn Space Vehicle", George C. Marshall Space Flight Center, NASA-MTP-P&VE-S-62-3, April 26, 1962

B6. "Space Launch Vehicle Full Scale Damping Tests", by General Dynamics Astronautics, A Division of General Dynamics Corporation, G.D.A.-63-0376, Contract AF-04/694/185, June 1963

B7. Abrams, S. S. and R. F. Teuber, "Thor Delta Vibration Test", Environmental Quarterly, Douglas Aircraft Company, Inc., September 1963

B8. Alley, V. L., Jr. and S. A. Leadbetter, "Prediction and Measurement of Natural Vibrations of Multistage Launch Vehicles", AIAA Journal, 1, No. 2, April 1962

MODEL GROUND TESTS

C1. Jaszlics, I. J. and George Moroson, "Dynamic Testing of a 20% Scale Model of the Titan III", Paper in AIAA Symposium, September 1965

C2. Mixon, J. S., J. J. Catherin and Ali Arman, "Investigation of the Lateral Vibration Characteristics of a 1/5 Scale Model of Saturn SA-1", NASA TN-D-1593, January 1963

C3. Mixon, J. S. and J. J. Catherine, "Experimental Lateral Vibration Characteristics of a 1/5 Scale Model of Saturn SA-1 with an Eight Calbe Suspension System", NASA TN-D-2214, November 1964

C4. Mixon, J. S. and J. J. Catherine, "Comparison of Experimental Vibration Characteristics Obtained from a 1/5 Scale Model and from a Full-Scale Saturn SA-1", NASA TN-D-2215, November 1964

D1. Tse, F. S., I. E. Morse and R. T. Hinkle, Mechanical Vibrations, Ally and Bacon, Inc., Boston, Massachusetts, 1963

APPENDIX A - FULL SCALE FLIGHT TEST
SUMMARY DATA SHEETS

A1. *"Vibration and Acoustic Analysis, Saturn SA-10 Flight", by Measuring and Evaluation Section, George C. Marshall Space Flight Center, NASA TMX-53366, December 8, 1965*

Purpose and Scope

The SA-10 flight was tested to determine abnormalities in vibration characteristics, if any, and to provide a comparison with previous flights of SA-8 and SA-9. Of particular significance was the vibration of the instrument unit during the S-IV powered flight.

Test Setup and Procedure

The SA-10 vehicle comprised the S-I stage, the S-IV stage, instrument unit, a boilerplate model of the Apollo spacecraft and the Pegasus satellite. Accelerometer mounting locations on the S-1 section are shown schematically in Figure A-1, and accelerometer mountings on the instrument unit are shown in Figure A-2.

Fifty-four vibration transducers (accelerometers) and three acoustic transducers were mounted on the SA-10 vehicle.

SS/FM telemetry systems were mounted in the vehicle. The multiplexed signals were transmitted from the vehicle over UHF radio channel and were received by ground receiving stations.

The receiver output was fed through a demultiplexer and each channel transposed from its assigned position in the spectrum to its original frequency.

Equipment

The data acquisition system for the vibration and acoustic data for each point of observation consisted of a transducer, an emitter follower, an amplifier, a multiplexer, a transmitter, a receiver, a demultiplexer, and a recorder.

The records thus obtained were processed with the random vibration analyzer (RAVAN). This equipment was developed by the MSFC computer Laboratory for use in conjunction with the IBM 7094.

Readings Obtained

Readings on the mean value, standard deviation, skewness and kurtosis are obtained for the data for each tape.

A vibration power spectrum in terms of g^2/Hz and the sound pressure spectrum level in terms of dB/Hz were obtained and are presented in this report. Spectral plots are presented in Appendix B of the report. A typical set of data as recorded is shown in Figure A-3.
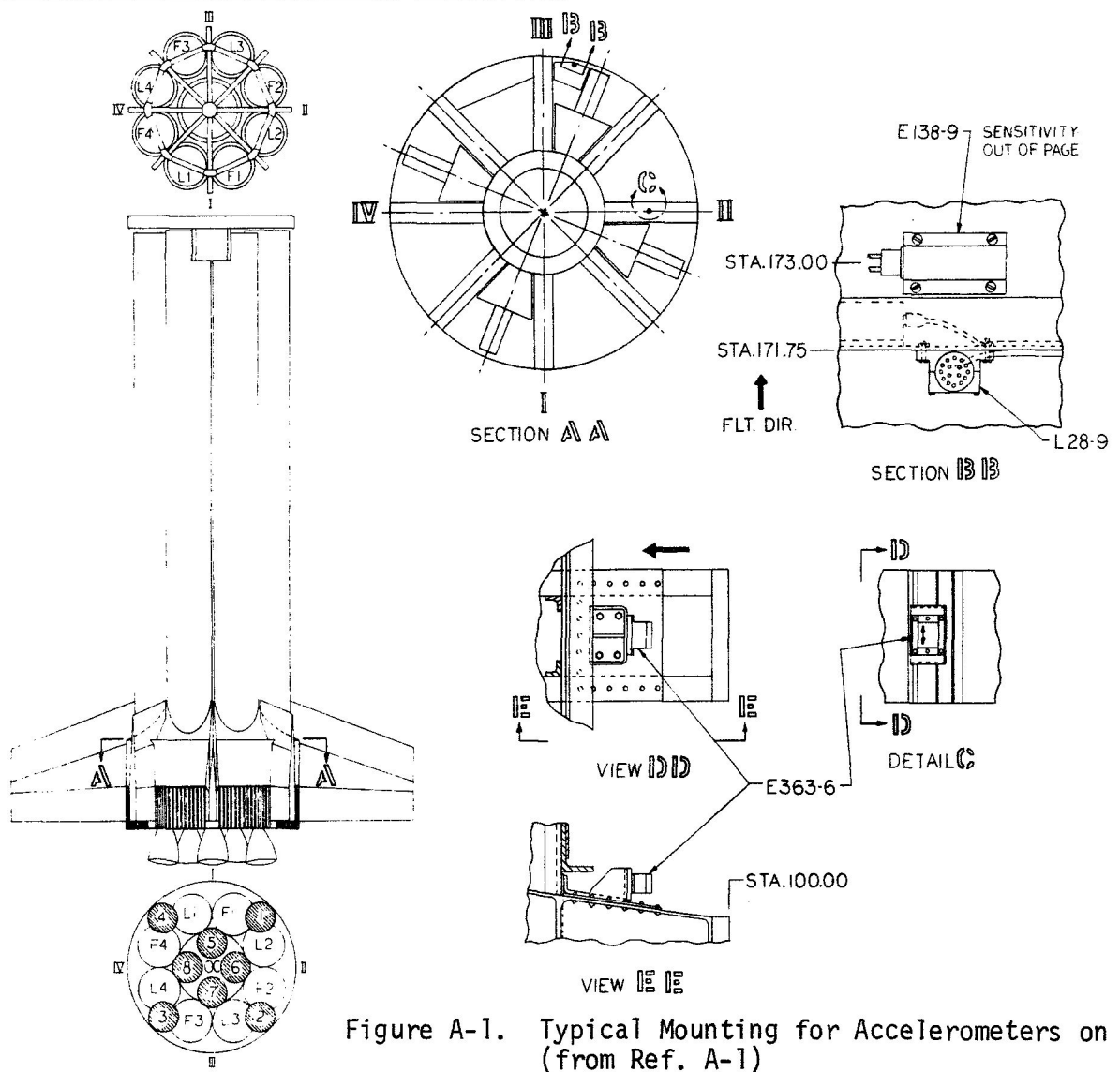
SATURN I - BLOCK II EFFECTIVITY						
MEAS	SA 5	SA 6	SA 7	SA 8	SA 9	SA 10
E 138-9	X	X	X	X	X	
E 363-6	X	X	X	X	X	
L 28-9	X	X		X	X	X

E 138-9 — SENSITIVITY OUT OF PAGE

SECTION A A

FLT. DIR.

STA. 173.00

STA. 171.75

L 28-9

SECTION B B

VIEW D D

DETAIL C

E 363-6

STA. 100.00

VIEW E E

MEASUREMENT LOCATIONS S-1 STAGE

CHECKED BY

ORIGINATED BY

DATE 9-4-64   SHEET 4 of 17

Figure A-1. Typical Mounting for Accelerometers on S1-Stage (from Ref. A-1)

COMMAND RECEIVER

GUIDANCE COMPUTER

STA. 1459.284

GUIDANCE DECODER

VIEW A A

MOUNT

PANEL

E349-802

L.O.O

E348-802

SKIN

SECTION B B

STA. 1493.284

STA. 1459.284

Figure A-2. Typical Mounting for Accelerometers on the Instrument Unit
(from Ref. A-1)

MEASUREMENT
LOCATIONS
IU

CHECKED BY

ORIGINATED BY

DATE
2-8-65

SHEET 10 OF 17
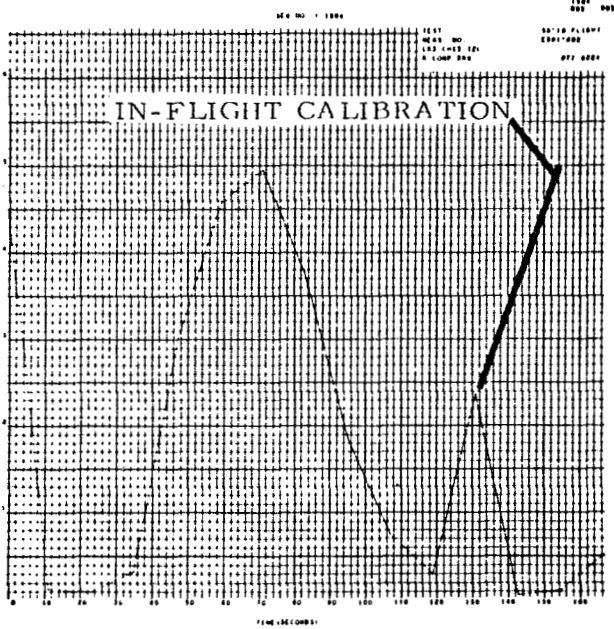
TIME HISTORY

Meas. No. ___E381-802___

Description ___Lower Instrument Unit___

___Mounting Ring___

Sensitivity ___Longitudinal___

Location: Page ___27___

Calibration ___± 10 G___

Remarks ___In-flight calibration at___

___130.7 seconds.___
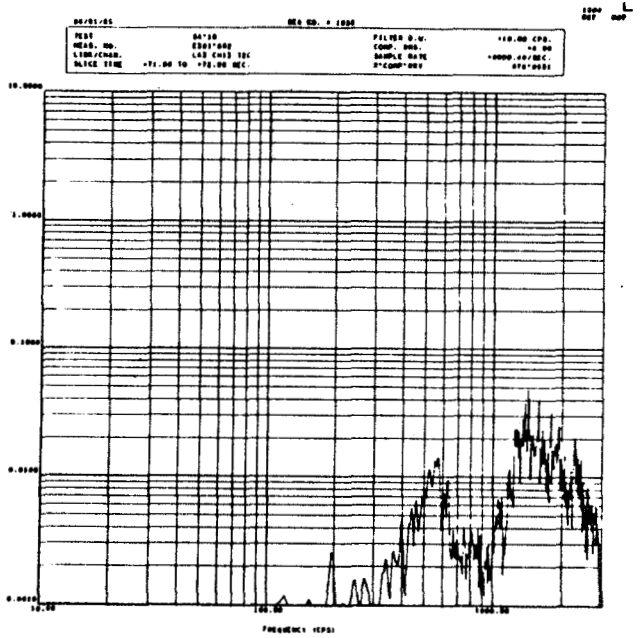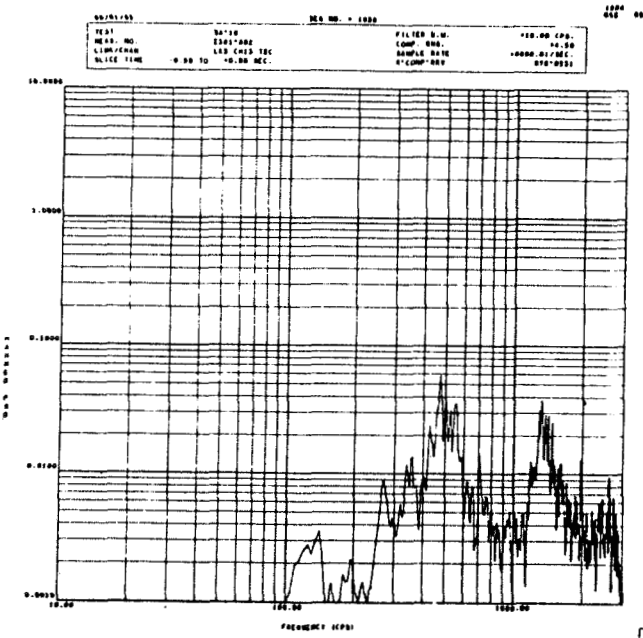
FREQUENCY SPECTRUM

FREQUENCY SPECTRUM

Figure A-3. Typical Form of Data Records Obtained (from Ref. A1)

Vibration Characteristics Noted

The vibrational excitation for the Saturn vehicle in flight is classed in three categories:

  1) Acoustic - from turbulence of exhaust gases

  2) Mechanical - from engines

  3) Aerodynamic - from turbulent boundary layer.

● The general level of response of the S-1 stage did not exceed expected levels.

● An attempt was made to correlate engine impulses with lateral buckling of shear beams or shear panels, but the data from the combustion chamber domes is questionable.

● Vibration of the spider beams and upper structure was greatest (9.94 grams) at 590 hertz as was the case for the SA-8.

● Vibration of the S-1 engine indicated a normal powered flight but the measurements on the combustion chamber dome were not considered valid.

● Vibration of the thrust chamber dome was also considered invalid and further studies are being made to define the problem.

● Vibration of the turbine gear box for each engine was found to be small and consistent with previous measurements of Block II vehicles.

● Vibration of the S-1 fuel tank skirt was comparable in magnitude to that previously measured but at a much lower frequency.

● Vibration of the I.U. (Instrument Unit) also agreed with previous results on the SA-8 and SA-9. No malfunction resulted from the vibration.

● Components of the I.U. vibrated considerably as they did in previous tests but were not considered detrimental to the proper functioning of the unit.

● Vibrations of the Pegasus (Apollo) capsule in general were considered to be negligible.

● Vibration, at low frequencies, of parts of Pegasus was somewhat greater than for SA-9 flight but the validity of the measurements is questioned.

● The acoustic vibrations of the I.U. and Apollo were in good agreement with those of SA-8.

● Acoustic response measurements of the S-I stage are considered invalid.

● Vibration of the Apollo Adapter persisted through the flight whereas in SA-8 they did not.

Comparisons Made

Comparisons with former tests have been covered in "Vibration Characteristics Noted".

Damping Value Obtained

There was no specific attempt to determine damping factors. Amplitudes of vibration, however, were no higher than observed for previous tests or for ground tests.

Conclusions Drawn

The SA-10 vehicle flight test indicated that the vibration environment recorded agreed closely with that recorded for SA-8 and SA-9.

Vibration of the Pegasus satellite during the S-IV powered flight were extremely low.

In general the acoustic data obtained from the S-I stage were questioned because condensation from the thrust area caused a malfunction in the data acqusition system.

A2. *Oleson, M. W., "Report on Acceleration and Vibration Data from Javelin (8.02) Vehicle", Naval Research Laboratory, Memo-Report-1074, July 1960*

Purpose and Scope

The primary objective of this flight was to obtain data defining the environmental vibration induced in a payload by operation of the fourth stage X-248 A-6 rocket motor.

It was also an object to evaluate vehicle performance, particularly with reference to vibration and to thrust acceleration, and to measure galactic radio noise.

This report presents the results of the measurements of vehicle thrust acceleration during flight of the Javelin (8.02) Vehicle and an analysis of significant differences between this flight and an earlier flight of Javelin (8.01).

Test Setup and Procedure

The payload structure, instrumentation, and data analysis techniques employed for Javelin (8.02) were substantially the same as for Javelin (8.01), "Preliminary Report on Acceleration and Vibration Data from Javelin (8.01) Vehicle" by M. W. Oleson, NRL Memo-Report 1024.

Equipment

Table A-1 is a summary of the telemeter and instrumentation allocation for Javelin (8.02).

Readings Obtained

Data results presented in the form of tables and charts were based on analysis of telemetered signals as recorded from the primary receiving station located at the Wallops Island launching site. Figure A-4 shows typical data curves analyzed.

Vibration Characteristics Noted

Sustained vibration levels were highest on the payload baseplate during burning of the fourth stage. The vibration signals during the first three stages were below 1 g.

The maximum acoustic level reached was 114 dB in the payload.

The maximum peak-to-peak amplitudes of vehicle were as follows:

First Stage	-	6.0 g
Second Stage	-	5.5 g
Third Stage	-	14.0 g
Fourth Stage	-	4.5 g

Comparisons Made

Substantial differences exist between data measured on Javelin (8.02) and on the earlier Javelin (8.01) flight. The random vibration and acoustic levels of the (8.02) were lower in amplitude and had a different time profile than did the (8.01). The thrust accelerations for (8.02) were consistently lower than for (8.01). Random vibration levels reached 1 g to 3 g for (8.01) but only 0.2 g to 0.7 g for (8.02).

Damping Values Obtained

No discussion of damping and no indication of damping values are given in the report.

Conclusions Drawn

Comparison with the earlier Javelin (8.01) flight indicates substantial difference in the vibration data reflecting changes in the flight performances. These differences are attributed to variations in the flight performances.

| | | TRANSDUCERS | | | | | |
| Telemeter FM/FM | | (Through Powered Phase) | | | (During Coast Phase) | | |
Subcarrier Frequency (KCPS)	Nominal Signal Bandwidth (CPS)	Location Number (See Sketch)	Type and Model	Maximum Signal Capability (Overall Peak g)	Location Number (See Sketch)	Type and Model	Maximum Signal Capability (Overall Peak g)
Direct	50 4500	7	Endevco 2213	68	M O N I T O R		
70	DC 5000	5	Endevco 2213	71	5	Endevco 2213	71
40	DC 3800	6	Endevco 2213	80	G A L A C T I C N O I S E Experiment		
22	DC 3000	4* 2 3 10	Endevco 2213 Altec 610A	68 28 59 127db	9	Schaevitz VG 5	3.7
14.5	DC 1500	1	Endevco	20	G A L A C T I C N O I S E Experiment		
10.5		8	Schaevitz VG-30	36	8	Schaevitz VG-30	36

* Transducers 4,3,2 and 10 are telemetered sequentially at two
second intervals.
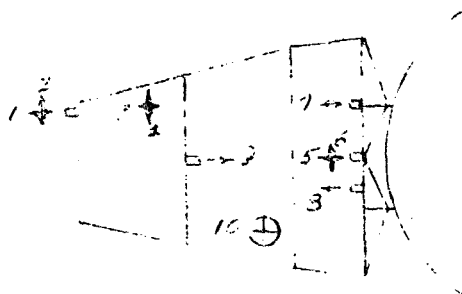
Javelin Payload
Showing
Transducer Locations

46
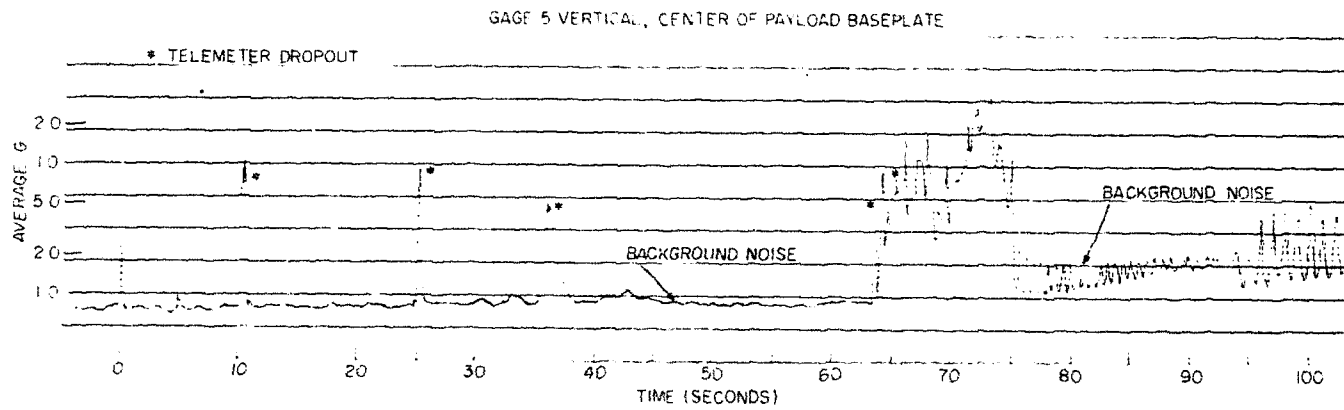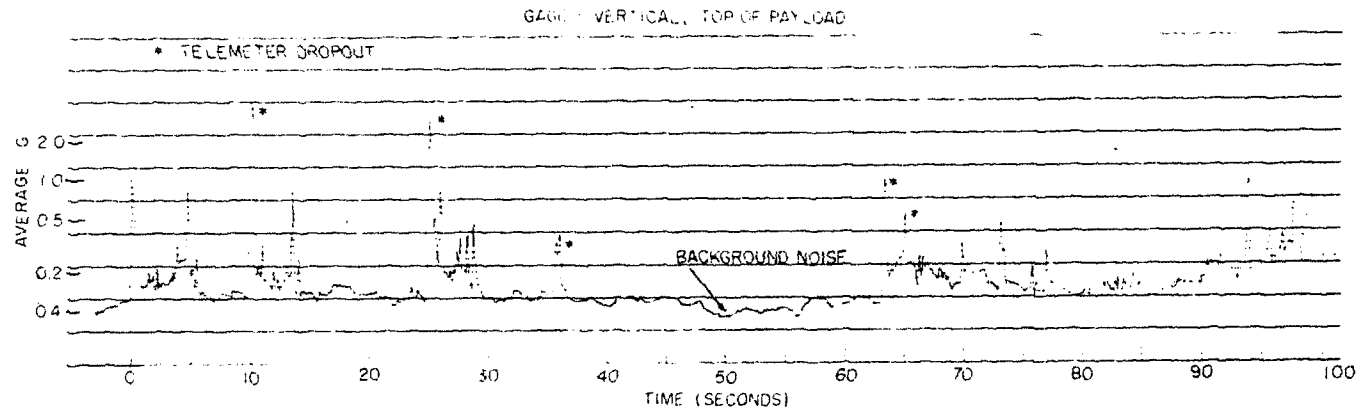
Figure A-4.   Average Vibration Acceleration Level During Flight
               (from Ref. A-2)

47

A3. *Mayhue, Robert J., "NASA Scout ST-1, Flight-Test Results and Analysis, Launch Operations, and Test Vehicle Description", Langley Research Center, NASA-TN-D-1240, June 1962*

Purpose and Scope

The Langley Research Center conducted a series of flight tests to determine the performance of the Scout vehicle (Scout ST-1) and performance for the purpose of:

- To corroborate design concepts of the system by performing a high-altitude probe mission

- To obtain measurements of flight environmental conditions and vehicle performance characteristics, and

- To gain operational experience with vehicle and support equipment.

The tests utilized proven telemeter systems using FM/AM transmission of skin temperatures, compartment temperatures, local linear vibration accelerations, pressure, overall accelerations, radiation level and fin position.

The vehicle was launched from NASA's Wallops Station. Its apogee was planned for 2,020 miles, a short range of 4,400 nautical miles. Its maximum velocity was expected to be about 22,000 ft/sec.

Test Setup and Procedure

The vehicle shown in Figure A-5 was instrumented with standard instrument systems for using FM/AM transmission. The telemetered returns were received by ground systems previously checked out. It was tracked on its flight with tracking radars, telemetry and tracking cameras.

A command destruct system was incorporated in the first and second stage for emergency use.

Preflight checkout and calibration was performed on all equipment and vehicle mass properties.

Equipment

The tracking radars used included the RCA AN/FPS-16, the Reeves Mod III SCR-584. Additional tracking data were supplied by the Millstone Hill experimental radar of the MIT Lincoln Laboratory.

Velocity data were supplied by a Model 10A Doppler Velocimeter.

Wallops Station telemeter receivers were used to record telemetered data.

A quick-look system in a Goddard Space Flight Center telemeter trailer was employed.

48
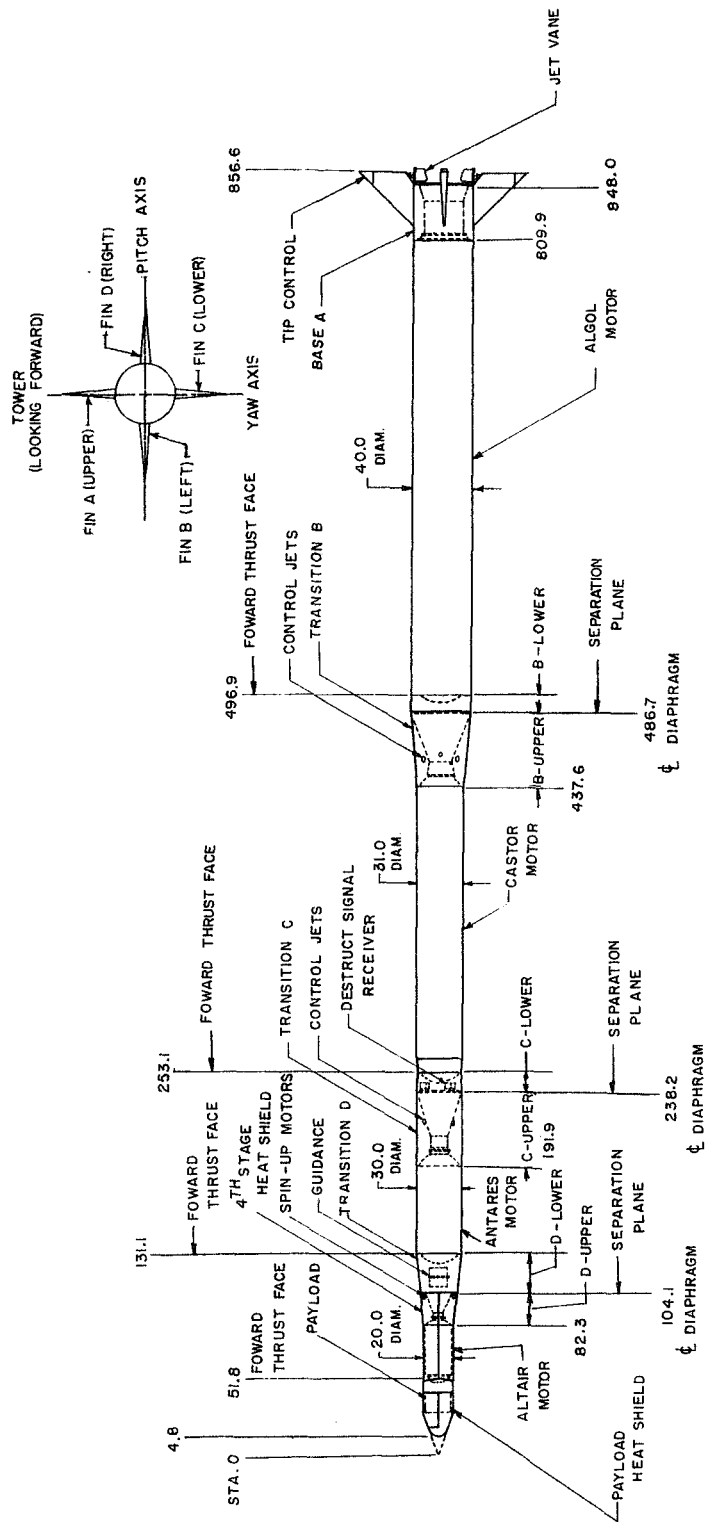
Figure A-5. General Arrangement and Major Assemblies of ST-1 Test Vehicle (from Ref. A3)

49

All equipment was checked out and found to be within factory specifications.

Readings Obtained

Telemeter tape recordings of all performance characteristics during flight were analyzed by automatic filters. Of significance here is the vibrational data which was processed through frequency filter analog analyzers. Along with behavior characteristics in general the vibrational characteristics were carefully recorded.

Vibration Characteristics Noted

The first stage vibration showed no sustained vibration. Figures A-6a and A-6b show the times, amplitudes and frequencies of the sporadic vibration in the first stage. Figures A-7a and A-7b show the time amplitude histories for the second and third stages, respectively.

A typical wave analyzer output is shown in Figure A-8. It is from such data that structural damping factors were obtained.

Comparisons Made

Tables A-2, A-3, A-4, and A-5 show comparisons between measured and computed quantities. In general the agreement between predicted and measured values (where both were obtained) were very good.

While no predictions were made the vibration histories of the guidance package show large amplitudes, causing the control system to chatter. Figure A-9 shows maximum "g" value amplitudes of 70 whereas the noise level was not more than ±6 g.

Damping Values Obtained

No values of damping are given. There was, however, the high amplitude of vibration of the guidance package which suggests low damping values.

Conclusions Drawn

"Overall results obtained from the flight have shown that the design concepts of the system are sound. In addition, this flight test has led to the discovery and solution of problem areas associated with the early development phases of the vehicle and components."

Large vibrations of the control package caused a switch to chatter and resulted in a constant switching in and out of the high and low reaction-jet controls during the third stage burning.
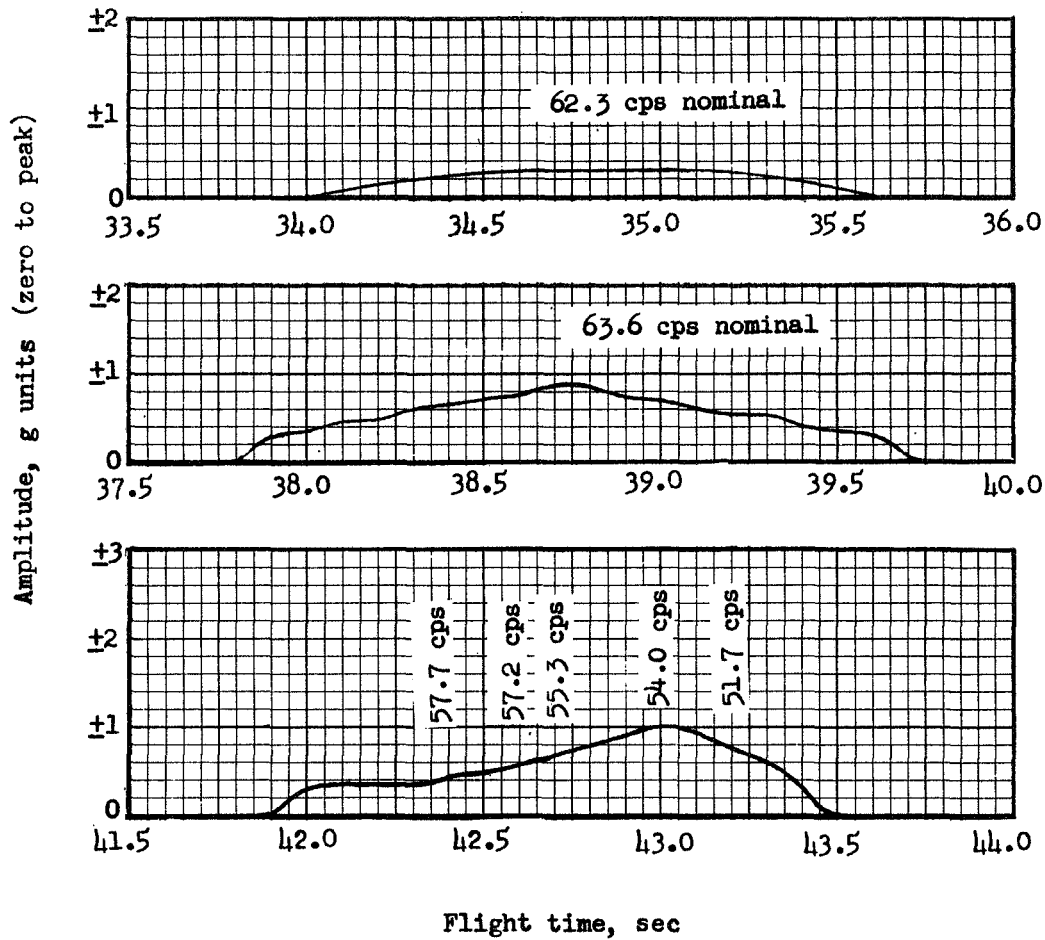
Figure A-6a. Time Histories of Amplitudes of Payload Longitudinal
Linear Accelerations During First-Stage Burnout
(from Ref. A3)
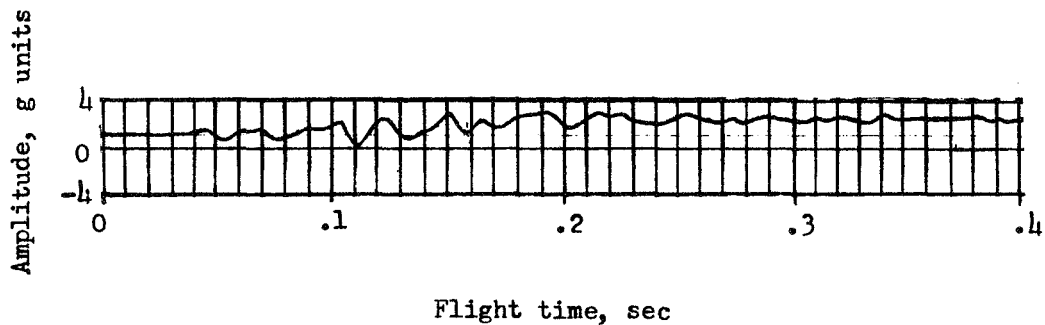
Figure A-6b. Time History of the Amplitude of Payload Longitudinal
Linear Acceleration at First-Stage Ignition (from Ref. A3)
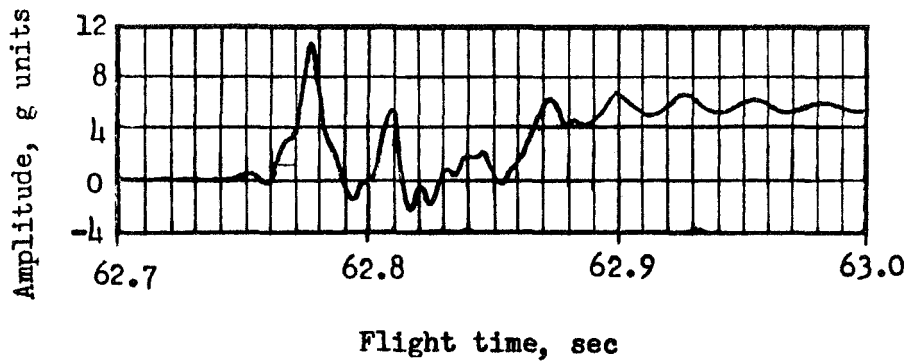
Figure A-7a. Time History of the Amplitude of Payload Longitudinal Linear Acceleration at Second-Stage Ignition (from Ref. A3)
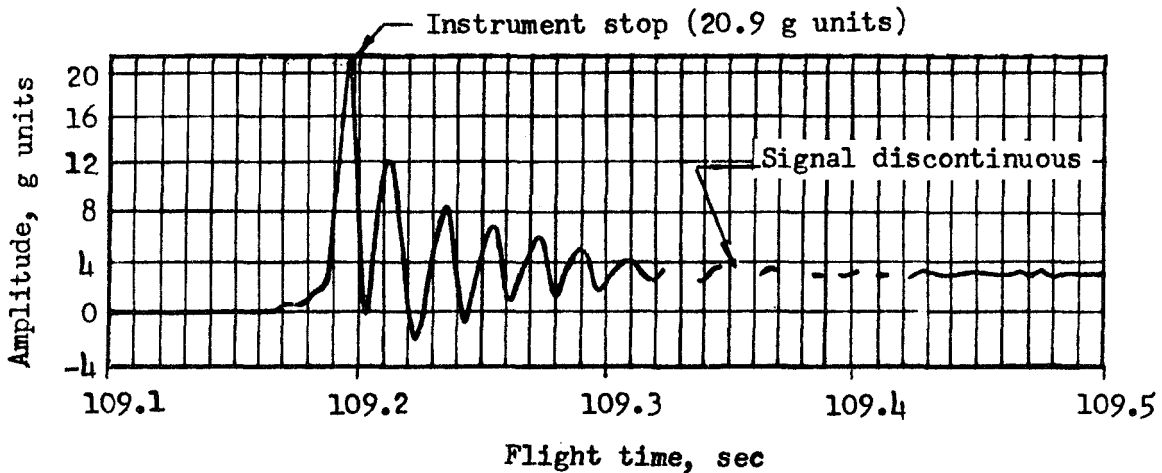
Figure A-7b. Time History of the Amplitude of Payload Longitudinal Linear Acceleration at Third-Stage Ignition (from Ref. A3)
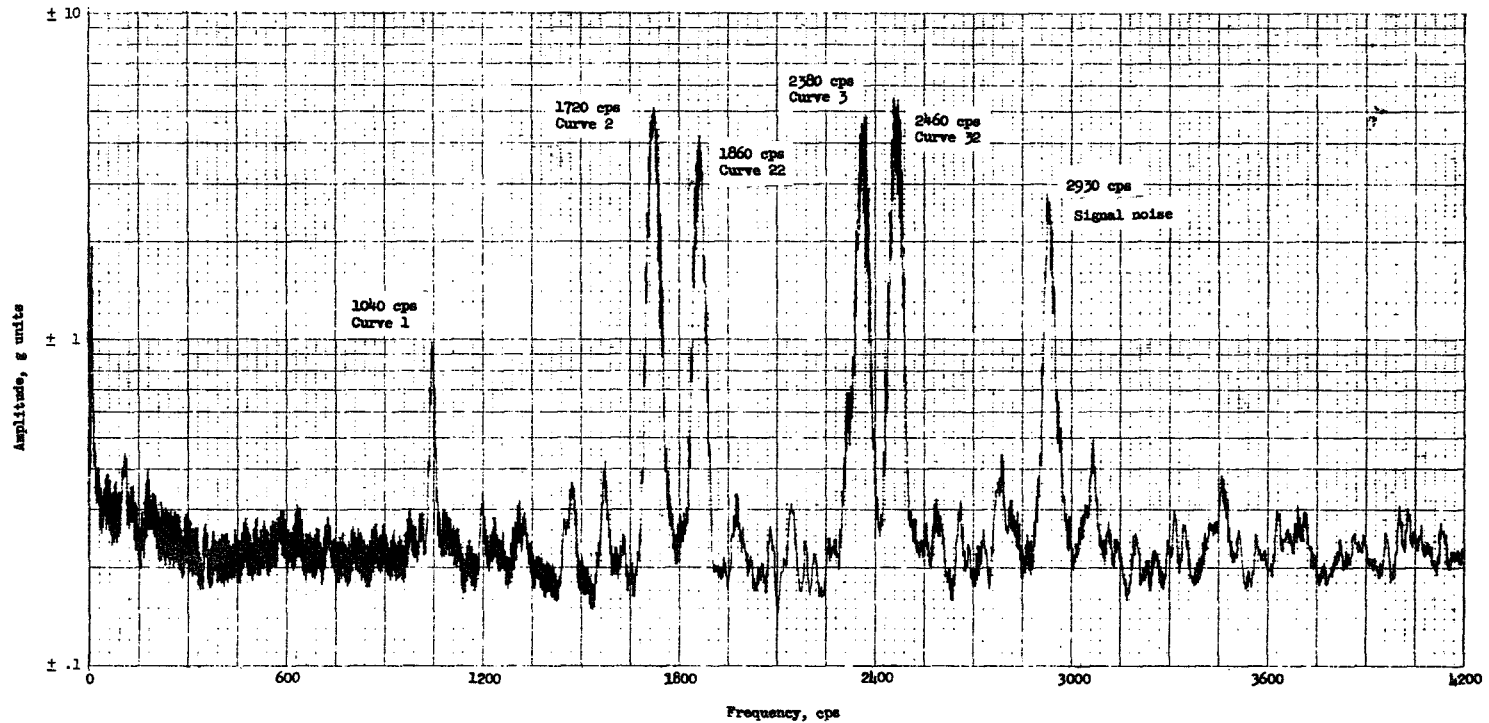
Figure A-8. Typical Wave Analyzer Output Plot Showing the Variation of Amplitude with Frequency of the Guidance Package Transverse Vibration Acceleration from 129.2 to 130.2 seconds (from Ref. A3)

TABLE A-2. DESCRIPTION OF BASE A FM/AM TELEMETER CHANNELS
(from Ref. A3)

Channel frequency, kc	Measurement	Instrument	Range	Overall accuracy		Description of data
				Predicted	Flight	
110.0	Commutation of 8 skin temperatures	Chromel-alumel thermocouples	Ambient to 800° F	±10° F	±10° F	Five thermocouples measure skin temperatures on fin B Two measure bearing housing temperature, and one measures internal temperature of fin strut
119.5	Servo compartment temperature	Resistance thermometer	0° to 350° F	±3° F	±3° F	Measures local servo compartment temperature
*129.5	Fin position indicator, fin A	Variable-inductance coils	±18°	±2 percent	±5 percent up to 21 sec; not reliable beyond 21 sec	Measures the position of the control fin with respect to the model
*139.5	Fin position indicator, fin D	Variable-inductance coils	±18°	±2 percent	±5 percent up to 21 sec; not reliable beyond 21 sec	Measures the position of the control fin with respect to the model
*150.0	Fin position indicator, fin C	Variable-inductance coils	±18°	±2 percent	±5 percent up to 21 sec; not reliable beyond 21 sec	Measures the position of the control fin with respect to the model
*160.5	Fin position indicator, fin B	Variable-inductance coils	±18°	±2 percent	±5 percent up to 21 sec; not reliable beyond 21 sec	Measures the position of the control fin with respect to the model
170.0	First-stage motor headcap pressure	Variable-inductance pressure cell	0 to 485 psia	±2 percent	±2 percent	Supplies chamber pressure time history of Algol motor.
179.5	Normal static acceleration	Variable-inductance accelerometer	±2g	±2 percent	±2 percent	Measures normal acceleration in base A during first-stage burning and coast.
190.5	Transverse static acceleration	Variable-inductance accelerometer	±2g	±2 percent	±2 percent	Measures transverse acceleration in base A during first-stage burning and coast.
199.5	Hydraulic accumulator pressure	Variable-inductance pressure cell	0 to 3,000 psia	±2 percent	±2 percent	Supply continuous monitor of hydraulic accumulator pressure in base A

*Channel deviated from expected normal.

54

TABLE A-3. DESCRIPTION OF TRANSITION D FM/FM TELEMETER CHANNELS
(from Ref. A3)

Channel number	Measurement	Instrument	Range	Special network	Overall accuracy Predicted	Overall accuracy Flight	Description of data
1	Third-stage small-pitch-motor operation	Two valve relay switches; two chamber pressure switches	Switch open or close	Binary coded resistance matrix	±2 percent	±2 percent	Indicates which motor fires; can determine 16 different combinations of switch closures; indicates when voltage is fed to the peroxide valve and when pressure builds up in the motor
*2	Events	Third-stage skin switch; four-command destruct channel no. 7 relay closures, and fourth-stage hold-fire switch closure	Switch open or close; 0 to 32 volts on guidance voltage	Coded resistance circuit	±2 percent	±2 percent	The third-stage skin switch indicates heat-shield ejection; a relay closure of command destruct channel no. 7 indicates the command destruct receivers are captured with radio frequencies from ground transmitter; a ledex relay is used to open the ignition leads to the fourth-stage motor; a contact on this relay was used to indicate on the telemeter when command destruct commanded hold-fire; this channel also continuously monitors the guidance 28-volt power supply.
3	Pitch-program voltage	Voltage for guidance torquer	0 to 5.2 volts	Isolating resistor	±2 percent	±2 percent	Measures voltage being applied to pitch-gyro torquer
4	Second- and third-stage upper-roll-motor operation	Two valve relay switches; and two chamber pressure switches in each stage	Switch open or close	Binary coded resistance matrix in each stage	±2 percent	±2 percent	Indicates which motor fired; can determine 16 different combinations of switch closures; indicates when voltage is fed to the peroxide valve and when pressure builds up in the motor
5	Second- and third-stage lower-roll-motor operation	Two valve relay switches; and two chamber pressure switches in each stage	Switch open or close	Binary coded resistance matrix in each stage	±2 percent	±2 percent	Indicates which motor fired; can determine 16 different combinations of switch closures; indicates when voltage is fed to the peroxide valve and when pressure builds up in the motor
6	Second- and third-stage yaw-motor operation	Two valve relay switches; and two chamber pressure switches in each stage	Switch open or close	Binary coded resistance matrix in each stage	±2 percent	±2 percent	Indicates which motor fired; can determine 16 different combinations of switch closures; indicates when voltage is fed to the peroxide valve and when pressure builds up in the motor
7	Second- and third-stage large-pitch-motor operation	Two valve relay switches; and two chamber pressure switches in each stage	Switch open or close	Binary coded resistance matrix in each stage	±2 percent	±2 percent	Indicates which motor fired; can determine 16 different combinations of switch closures; indicates when voltage is fed to the peroxide valve and when pressure builds up in the motor
8	Second-stage N_2 main-tank pressure	Pressure potentiometer	0 to 3,500 psia	Voltage dropping resistor	±3 percent	±3 percent	Supplies continuous monitor of control-system N_2 pressure
9	Third-stage N_2 main-tank pressure	Pressure potentiometer	0 to 1,500 psia	Voltage dropping resistor	±3 percent	±3 percent	Supplies continuous monitor of control-system N_2 pressure
*10	Second- and third-stage motor headcap pressure	Pressure potentiometer	Second stage - 0 to 600 psia; third stage - 0 to 400 psia	Isolating resistors for feeding both pots to a single channel	±3 percent	±3 percent on third stage; see text for second-stage data	Supplies pressure time history of motor chamber pressure for Castor and Antares motors
*11	Commutation of telemeter 150 volt monitor and 10 compartment temperatures: transition B ambient, transition B N_2, transition C ambient, transition C N_2, four in transition D telemeter compartment, guidance package ambient, guidance gyro block	Thermistors	90° F to 220° F on two guidance temperatures; 30° F to 220° F on remaining temperatures	Voltage dropping resistor and oscillator calibration network	±2° F from 30° to 120° F; ±5° F from 120° F to 220° F; ±2° F from 90° F to 220° F on two guidance temperatures	Same as predicted	Measures temperature during flight in critical areas; monitors 150 volts used to bias binary coded resistance matrices

*Channel deviated from expected normal.

55

TABLE A-3. DESCRIPTION OF TRANSITION D FM/FM TELEMETER CHANNELS
(from Ref. A3) - Concluded

Channel number	Measurement	Instrument	Range	Special network	Overall accuracy		Description of data
					Predicted	Flight	
12	Commutation of 11 skin temperatures	Iron-constantan thermocouples	Ambient to 1,000° F	Oscillator calibration network and d-c amplifier	±20° F	±20° F on eight thermocouples; three thermocouples lost	Obtains skin temperature around transition D section
*13A	Guidance roll-displacement error signal	Guidance roll displacement gyro	±5°	400-cycle phase demodulator	±5 percent to ±8 percent	±5 percent to ±8 percent	Measures the 400-cycle error signal from the guidance roll displacement gyro which is proportional to the vehicle roll displacement in degrees
*13B	Guidance pitch-displacement error signal	Guidance pitch displacement gyro	±5°	400-cycle phase demodulator	±5 percent to ±8 percent	±5 percent to ±8 percent	Measures the 400-cycle error signal from the guidance pitch displacement gyro which is proportional to the vehicle pitch displacement in degrees
*13C	Guidance yaw-displacement error signal	Guidance yaw displacement gyro	±5°	400-cycle phase demodulator	±5 percent to ±8 percent	±5 percent to ±8 percent	Measures the 400-cycle error signal from the guidance yaw displacement gyro which is proportional to the vehicle yaw displacement in degrees
*14A	Guidance roll-rate error signal	Guidance roll rate gyro	±20 deg/sec	400-cycle phase demodulator	±5 percent	±5 percent	Measures the 400-cycle error voltage from the guidance roll rate gyro which is proportional to the vehicle roll rate in deg/sec
*14B	Guidance pitch-rate error signal	Guidance pitch rate gyro	±8 deg/sec	400-cycle phase demodulator	±5 percent	±5 percent	Measures the 400-cycle error voltage from the guidance pitch rate gyro which is proportional to the vehicle pitch rate in deg/sec
*14C	Guidance yaw-rate error signal	Guidance yaw rate gyro	±8 deg/sec	400-cycle phase demodulator	±5 percent	±5 percent	Measures the 400-cycle error voltage from the guidance yaw rate gyro which is proportional to the vehicle yaw rate in deg/sec
15	Guidance 400-cycle supply voltage	Guidance inverter	0 to 15 volts; 0 to 450 cycles	Voltage dropping resistor	Voltage ±2 percent; frequency ±0.01 percent	Voltage ±2 percent; frequency ±0.01 percent	Monitors guidance 400-cycle supply voltage and frequency
*16	Vibration in the transverse direction on the guidance package	Crystal accelerometer	±60g peak	---------------	±5 percent	±10 percent	Measures vibration data in the 10- to 2,000-cycle range
*17	Vibration in the normal direction on the guidance package	Crystal accelerometer	±60g peak	---------------	±5 percent	No data	Measures vibration data in the 10- to 2,000-cycle range
*18	Vibration in the longitudinal direction on the guidance package	Crystal accelerometer	±120g peak	---------------	±5 percent	No data	Measures vibration data in the 10- to 2,000-cycle range

*Channel deviated from expected normal.

56

TABLE A-4. DESCRIPTION OF PAYLOAD FM/AM TELEMETER CHANNELS (from Ref. A3)

Channel frequency, kc	Measurement	Instrument	Range	Special network	Overall accuracy		Description of data
					Predicted	Flight	
119.5	Commutation of six skin temperatures and heat-shield eject switch	Chromel-alumel thermocouples and microswitch	Ambient to 1,400° F	Resistance network for heat-shield eject switch	±20° F	±20° F	Obtains skin temperatures on various points of payload heat shield; indicate when payload heat shield is ejected
*129.5	Longitudinal static acceleration	Variable-inductance accelerometer	-4g to +20g	--------------	±2 percent	±2 percent	Obtains longitudinal acceleration during the firing of each stage; when data are integrated, will obtain velocity of vehicle
*179.5	Yaw rate	Rate gyro	±1 radian/sec	--------------	±2 percent	±2 percent	Measures vehicle rate of displacement in the yaw direction; will supply correlation data for guidance yaw rate data channel 14C transition D FM/FM telemeter
*190.5	Pitch rate	Rate gyro	±1 radian/sec	--------------	±2 percent	±2 percent	Measures vehicle rate of displacement in the pitch direction; will supply correlation data for guidance pitch rate data channel 14B transition D FM/FM telemeter
*199.5	Roll rate	Rate gyro	±1 radian/sec	--------------	±2 percent	±2 percent	Measures the vehicle rate of displacement in the roll direction; will supply correlation data for guidance roll rate data channel 14A transition D FM/FM telemeter

*Channel deviated from expected normal.

TABLE A-5. DESCRIPTION OF PAYLOAD FM/FM TELEMETER CHANNELS (from Ref. A3)

Channel number	Measurement	Instrument	Range	Special network	Overall accuracy Predicted	Overall accuracy Flight	Description of data
*5	Radiation	Geiger-Müller counter	0 to 50 milliroentgens/hr	-------------	See ref. 4	See ref. 4	Measure cosmic radiation rate in the altitude range of the vehicle
6	Fourth-stage motor headcap pressure	Pressure potentiometer	0 to 40 psia	Voltage dropping resistor	±3 percent	No data	Obtains a chamber-pressure time history of the Altair motor
7	Normal static acceleration located forward of the c.g.	Linear accelerometer	±10g	Voltage dropping resistor	±4 percent	±4 percent	Obtains static acceleration in the normal direction; along with channels 8, 9, and 10 will indicate translation and irregular motions of the vehicle axes
8	Transverse static acceleration located forward of the c.g.	Linear accelerometer	±10g	Voltage dropping resistor	±4 percent	±4 percent	Same as channel no 7, except in the transverse direction
9	Normal static acceleration located on or near the c.g.	Linear accelerometer	±5g	Voltage dropping resistor	±4 percent	±4 percent	Same as channel no. 7
10	Transverse static acceleration located on or near the c.g.	Linear accelerometer	±5g	Voltage dropping resistor	±4 percent	±4 percent	Same as channel no. 8
*11	The direction of vehicle with respect to earth's magnetic lines of force, sensor mounted perpendicular to vehicle axis	Schonstedt magnetic aspect sensor	±600 milligauss	-------------	±3 percent	±3 percent	By measuring the local earth's magnetic field, the direction of the vehicle with respect to the magnetic lines of force can be obtained; by knowing earth's local magnetic vector at any point, along with data from the other magnetic aspect sensors and radar data, the attitude of the model can be obtained; at spin-up of the fourth stage this channel shows a sine wave from which the spin rate can be found
*12	Same as channel no. 11 except sensor mounted parallel to vehicle axis	Schonstedt magnetic aspect sensor	±600 milligauss	-------------	±3 percent	No data	Same as channel no. 11, except will not indicate any spin data
*13	Attitude of the fourth stage prior to spin-up	Horizon detector	±180° in pitch direction	-------------	±3 percent	No data	Determines attitude of the fourth stage by detecting the earth's horizon prior to fourth-stage spin-up
*14	Attitude of the fourth stage after spin-up	Naval Research Lab. designed solar aspect system	Vehicle attitude	-------------	±3 percent	No data	Determines attitude of the fourth stage by detecting direction of the earth and sun after spin-up
*15	Commutation of seven telemeter compartment temperatures in the payload	Thermistors	30° F to 220° F	Voltage dropping resistor and oscillator calibration network	±2° F from 30° F to 120° F; ±5° F from 120° F to 220° F	Same as predicted	Measures temperature during flight in critical areas in the payload-telemetry package
*16	Vibration in the transverse direction on the main plate of the payload telemeter	Crystal accelerometer	±100g	-------------	±5 percent	No data	Measures vibration data in the 10- to 2,000-cycle range
*17	Same as channel no. 16 except in the normal direction	Crystal accelerometer	±100g	-------------	±5 percent	No data	Measures vibration data in the 10- to 2,000-cycle range
*18	Same as channel no. 16 except in the longitudinal direction	Crystal accelerometer	±120g	-------------	±5 percent	No data	Measures vibration data in the 10- to 2,000-cycle range

*Channel deviated from expected normal.
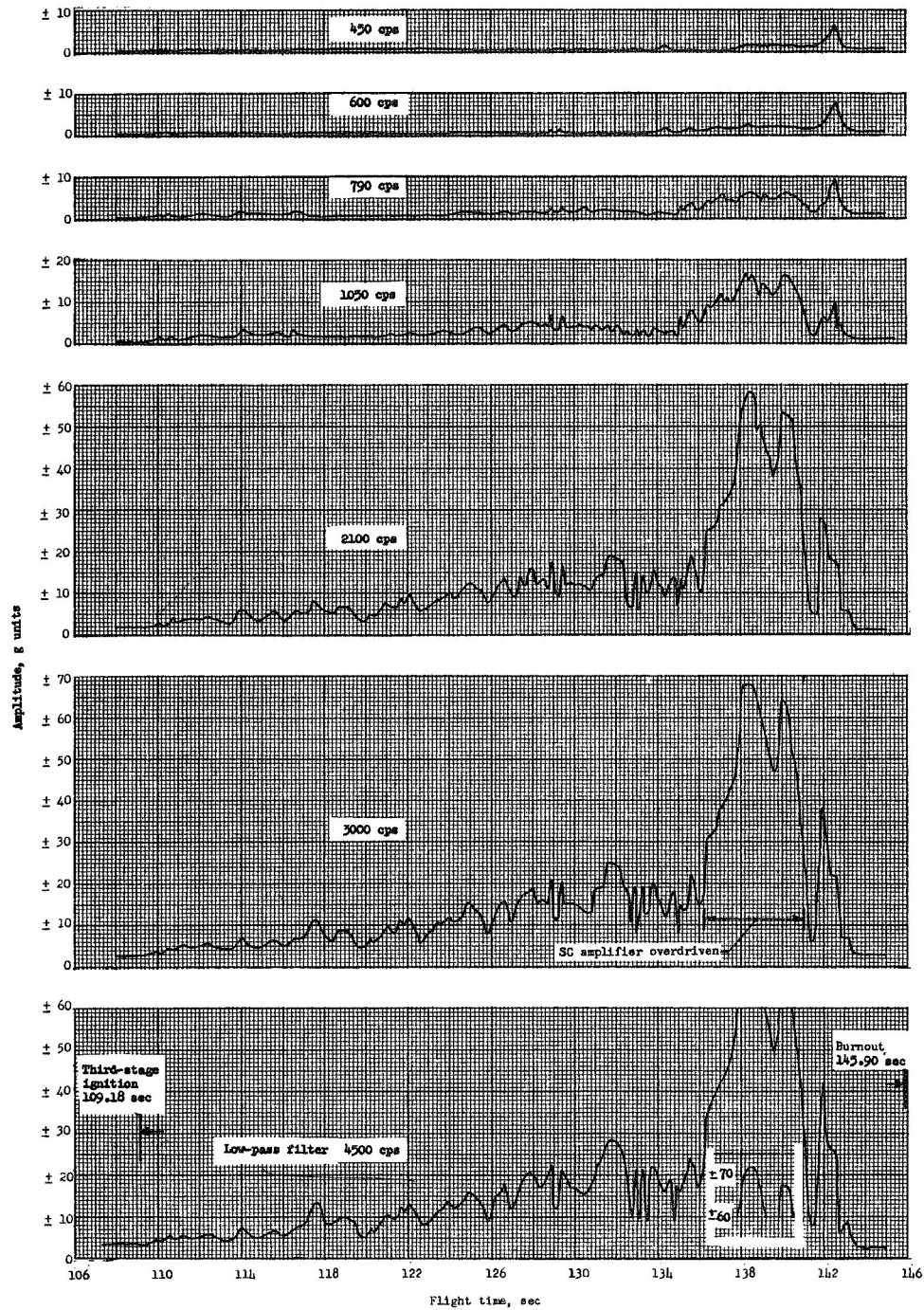
Figure A-9. Time Histories of the Wave Envelopes of the Amplitudes of the Guidance Package Transverse Vibration Accelerations Obtained with Low-Pass Filters (from Ref. A3)

B1. *Papadopoulos, James G., "Dynamic Test Results of SAD-5", MSFC - NASA, MTP-AERO-63-46, June 1963*

Purpose and Scope

The purpose of these vibration tests is to determine the body bending and torsional dynamic behavior of a full scale prototype of the Saturn SA-5 flight vehicle. Since the Saturn is stabilized and controlled by a servo loop, response measurements are needed to properly evaluate the control system.

Test Setup and Procedure

A full scale prototype was vertically suspended in the test tower as indicated in Figure B-1 and excited by shakers mounted at the engine gimbal planes. The vehicle's dynamic response at various applied forcing frequencies was recorded by vibration pickups. The vehicle was tested for both the boost flight with the S-I booster stage and for the S-IV powered flight with the S-I stage removed. Figure B-1 shows the SAD-5 vehicle suspended in the test tower.

Equipment

Approximately 75 accelerometers were mounted on the vehicle's outer surface at 15 stations along the axis and on the fins.

Vehicle vibration amplitudes were recorded as accelerations with 1 g strain gage accelerometers. The accelerometers had a natural frequency of 120 hertz and were critically damped with oil. At lower temperatures (0°F) the response was 95 percent of flat response.

Digitized magnetic tape recording were made by the SEL Data System. This system consisted of two 48-channel multiplexers giving 96 channels of readout. Outputs from each shaker accelerometer and each response accelerometer were recorded on a single SEL data channel. The current, voltage and period of excitation were recorded. The digitized output of each channel was commutatively recorded at a fixed rate of 306 samples/sec.

The digitized accelerometer data tape recorded by the SEL system was reduced using a modified Fourier analysis technique on the IBM 7090 computer.

Readings Obtained

The function $y = A_0 \sin (2\pi ft + \phi) + A_s$ was used with the computer to give useful final readings.

Secondary vibrations and disturbances are automatically filtered out.
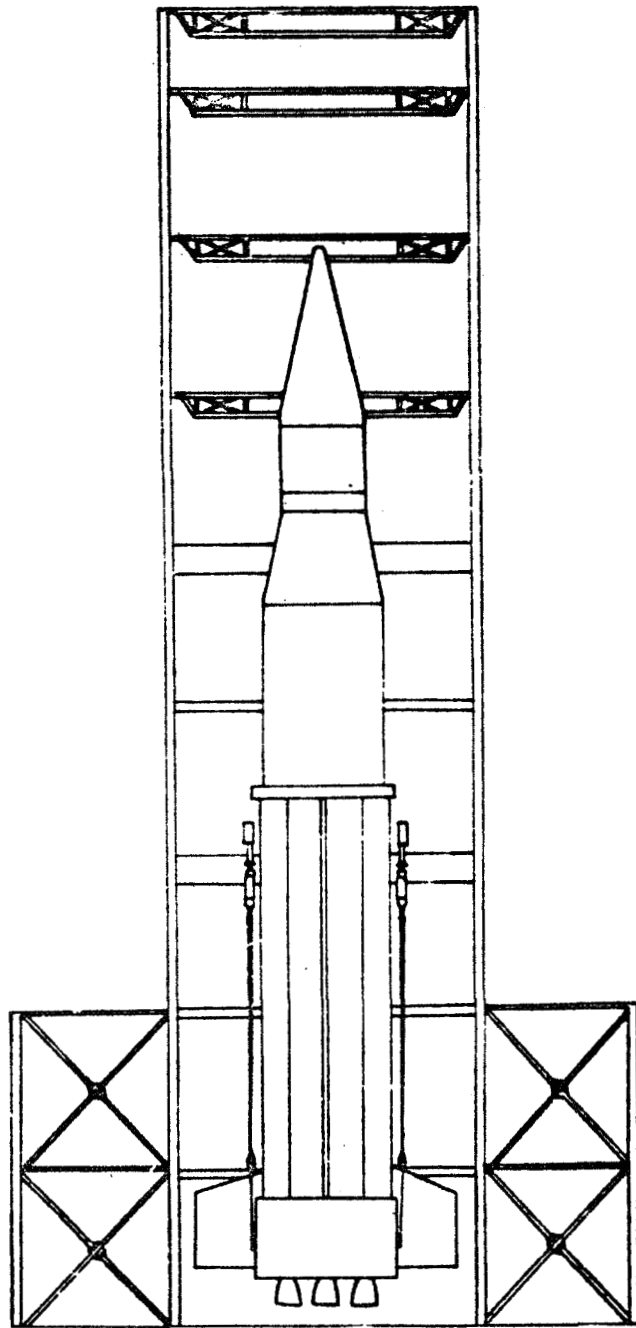
Figure B-1. SAD-5 Vehicle Suspended in Test Tower (from Ref. B1)

Damped ringout amplitudes were determined for each run of free vibration.

Visual aids such as microfilm plots of response as a function of frequency and print plots of the vehicle's mode shapes were utilized.

Vibration Characteristics Noted

The response of the vehicle was automatically digitized and subsequently plotted.

Figure B-2 shows the pitch response at the nose and Figure B-3 shows the pitch response at the instrument unit.

Figure B-4 shows the phase angle of pitch at the instrument unit. Decay curves are not shown. From such curves the damping coefficient ζ is obtained from vibration decay as

$$\zeta = \frac{1}{2\pi n} \ln \left[\frac{X_m}{X(m+n)} \right]$$

where X_m is amplitude of any mth cycle and $X(m+n)$ is amplitude after an additional n cycle of free vibration, and

$$\zeta = \frac{\Delta F}{2 F_n}$$

where ΔF is the width of response curve at 0.707 times the peak altitude, and F_n is the frequency at maximum amplitude.

Also, from phase angle data

$$\zeta = \frac{57.3}{f_n \left(\frac{d\theta}{dt} \right)}$$

where $d\theta/dt$ is the slope of the phase angle as a function of frequency current and F_n and f_n is defined as above.

Comparisons Made

The response amplitudes appear to be only slightly affected by changes in cable suspension but the damping coefficients may be affected to a greater extent.

The response of the nose and the response of the instrument unit indicate a consistency of resonance along the vehicle.

Damping Values Obtained

Damping coefficients at the resonant frequencies determined during the pitch series and the yaw series of tests are shown in Table B-1. A comparison of measured versus computed values of nose gain are shown in Table B-2.

63
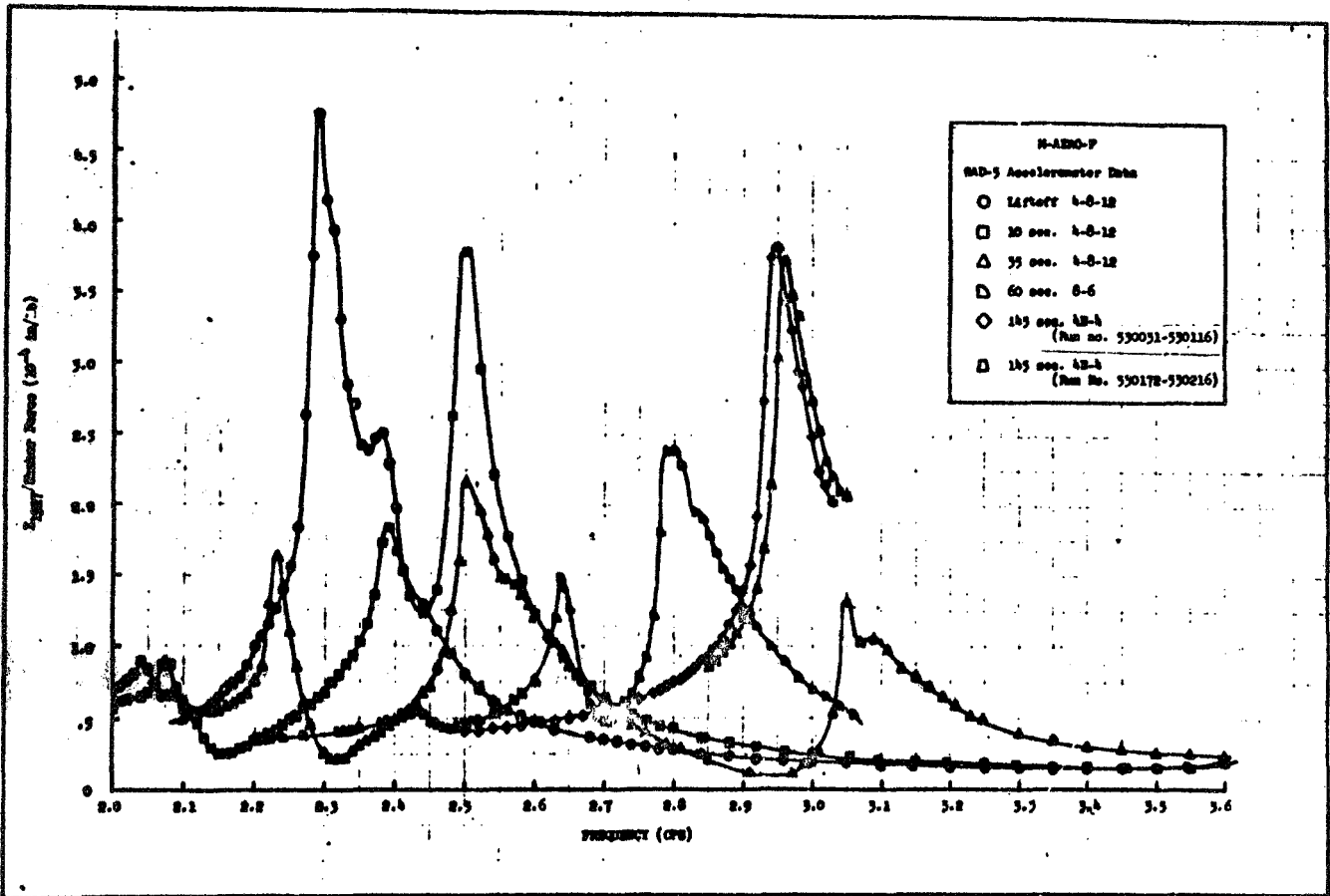
Figure B-2. Pitch Response at Nose for Soft Cable Suspension
(from Ref. B1)
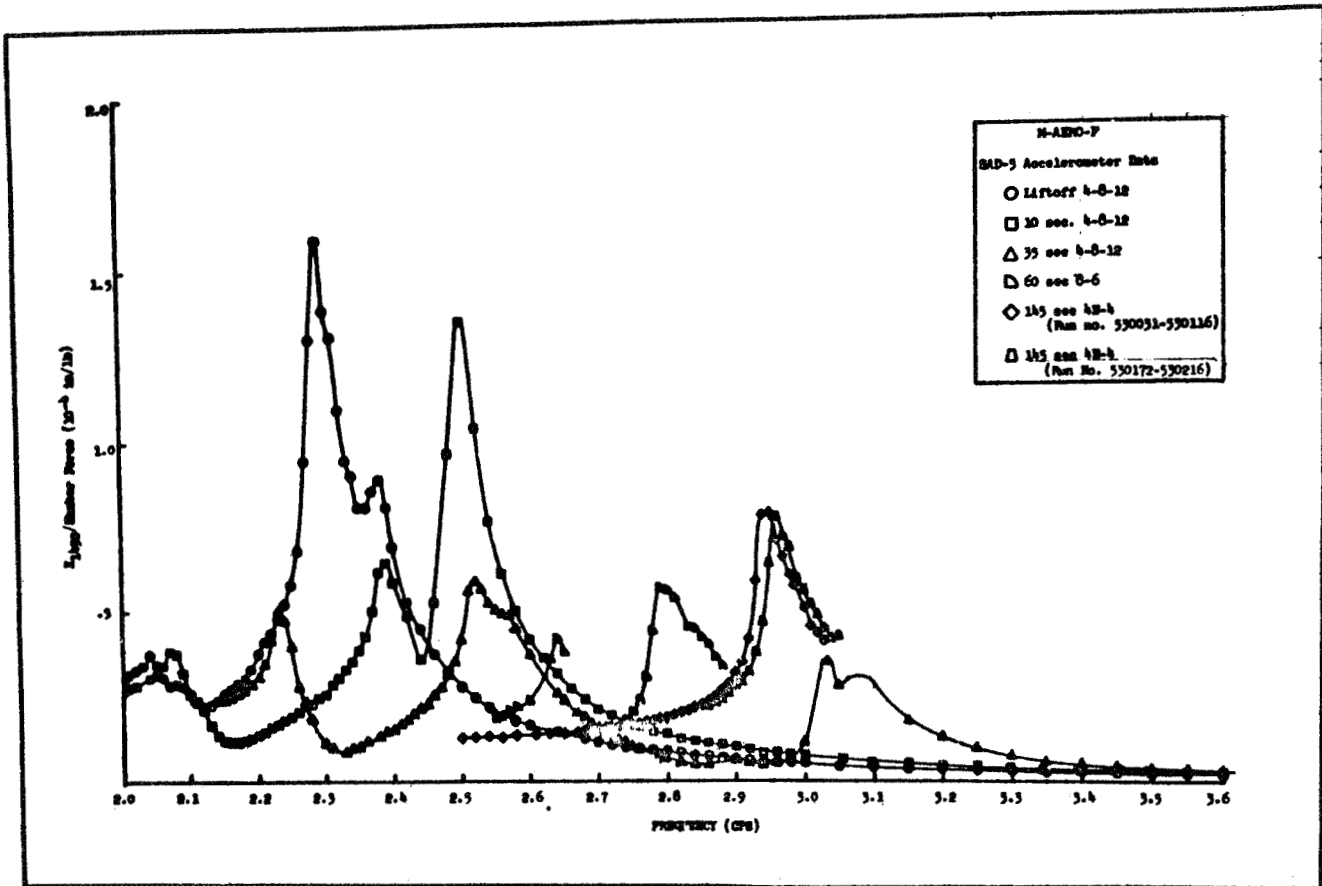
Figure B-3. Pitch Response at Instrument Unit for Soft Cable
Suspension (from Ref. B1)
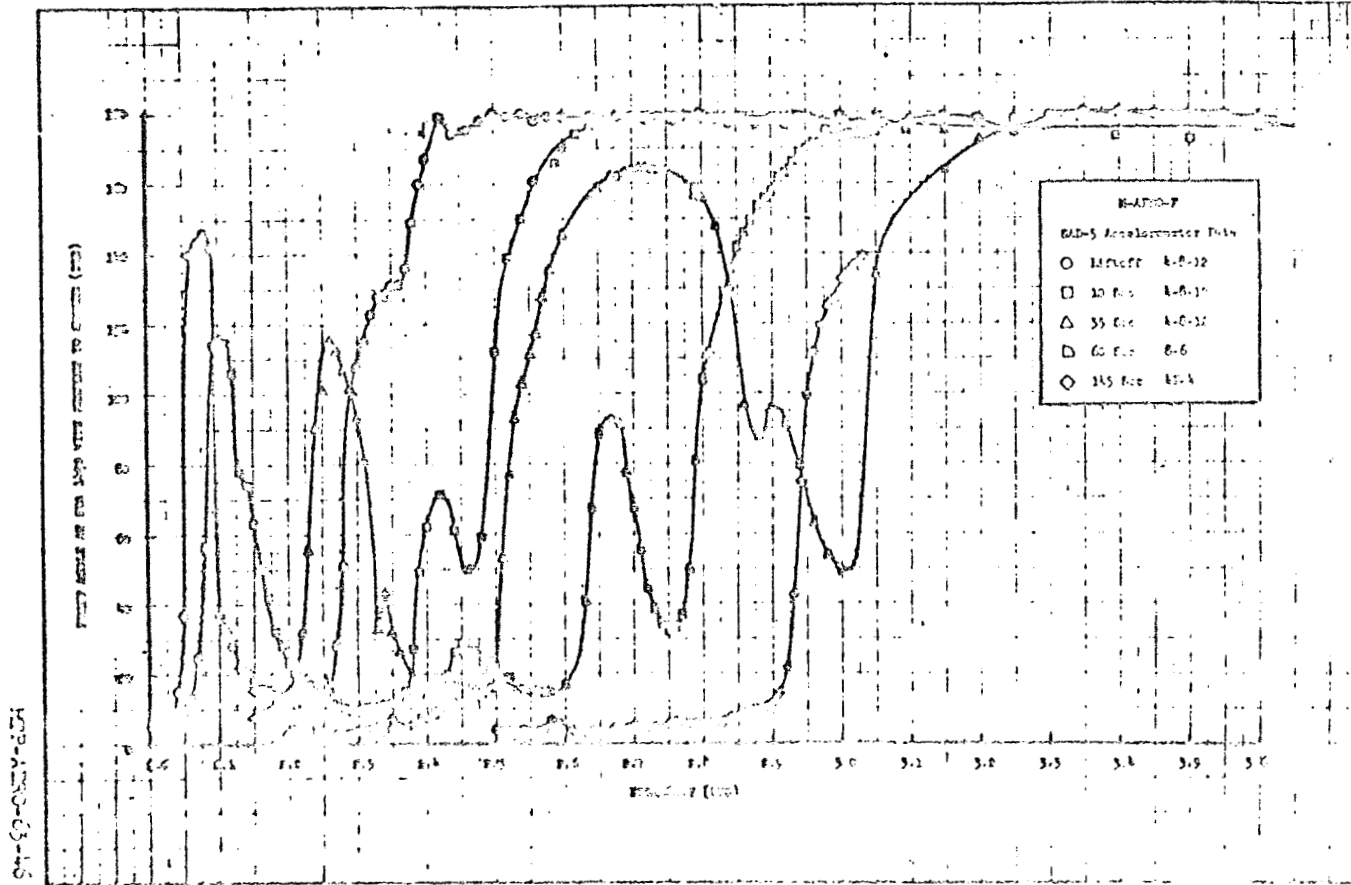
Figure B-4. Phase Angle at Instrument Unit Versus Frequency for Soft Suspension (Pitch) (from Ref. B1)

TABLE B-1. PITCH AND YAW RESONANT FREQUENCIES AND DAMPING COEFFICIENTS
(from Ref. B1)

Condition - Suspension - Mode		Liftoff (Pitch) (4-8-12)	(8-12)	10 Sec (Pitch) (4-8-12)	(8-12)	35 Sec (Pitch) (4-8-12)	(8-6)	(8-12)	60 Sec (Pitch) (8-6)	(8-12)	145 Sec (Pitch) (4K-4)	(4K-12)	Liftoff (Yaw) (4-8-12)	(8-12)
1st Coupled Tank	f (cps)	2.04	2.04	2.08	2.08	2.23	2.23	2.23	2.60	2.66	2.96	2.97	2.06	2.09
	ζ	3.3%	-	1.7%	1.0%	1.0%	.8%	1.1%	1.4%	-	1.3%	1.4%	1.3%	-
1st Bend	f (cps)	2.29	2.30	2.39	2.36	2.5	2.51	2.50	2.79	2.86	-	-	2.32	2.39
	ζ	.9%	1.1%	1.5%	1.8%	1.4%	1.5%	1.6%	1.2%	1.3%	-	-	1.2%	1.0%
2nd Coupled Tank	f (cps)	2.38	2.44	2.50	2.50	3.05	3.05	3.05	3.71	3.73	-	-	-	-
	ζ	-	-	.9%	1.2%	2.0%	1.7%	1.5%	1.6%	1.6%	-	-	-	-
3rd Coupled Tank	f (cps)	3.69	3.70	3.69	3.70	2.85	3.85	3.85	4.45	4.43	-	-	3.70	3.70
	ζ	-	1.0%	-	.9%	1.2%	1.4%	1.5%	2.5%	2.4%	-	-	1.2%	.7%
2nd Bend	f (cps)	4.80	4.80	4.85	4.75	4.75	4.75	4.75	5.03	5.22	8.35	8.40	4.80	4.79
	ζ	1.1%	1.4%	2.7%	3.0%	2.2%	2.5%	2.7%	1.9%	2.6%	2.8%	2.6%	1.5%	1.6%
S-I Engine	f (cps)	6.54	6.54	-	-	-	-	-	7.29	7.46	10.38	10.38	6.18	6.15
	ζ	-	-	-	-	-	-	-	-	2.1%	2.6%	1.9%	-	-
3rd Bend	f (cps)	7.29	7.20	7.63	7.47	8.44	8.46	8.48	9.76	10.17	12.99	12.89	7.15	7.14
	ζ	4.3%	-	-	2.1%	-	-	-	2.1%	-	3.0%	2.5%	-	3.2%
4th Coupled Tank	f (cps)	9.48	-	-	-	10.09	10.16	10.14	10.62	-	-	-	9.39	-
5th Coupled Tank	f (cps)	-	10.67	-	-	-	-	-	12.14	12.29	-	-	-	-
6th Coupled Tank	f (cps)	10.98	10.89	-	-	-	-	-	-	12.67	-	-	-	-

TABLE B-2. NOSE GAIN COMPARISON (MEASURED VS COMPUTED) (from Ref. B1)

File No.	f (cps)	ζ	$\frac{M_B}{kg\text{-}sec^2}$	Y_E	$\frac{\bar{\eta}}{F_s}$ computed (10^{-4} in/lb)	$\frac{\bar{\eta}}{F_s}$ measured (10^{-4} in/lb)
100315	2.04	.033*	1219	.059	0.81	0.86
100332	2.30	.011	3588	.255	1.80	1.52
100413	3.70	.010	7925	.286	0.60	0.42
100441	4.80	.014	1315	.160	0.86	0.98
100226	6.54	.020*	92097	1.25	0.036	0.045
100236	7.20	.030*	4320	.410	0.14	0.144
100272	10.67	.070*	3835	.345	0.26	0.23
100305	10.89	.040*	17308	.500	0.014	0.016

NOTE: $\frac{\bar{\eta}}{F_s}$ computed $= \frac{Y_E}{2M_B \zeta \omega^2}$

$\frac{\bar{\eta}}{F_s}$ measured $= \frac{X_{1967}}{\text{shaker force}}$

*Damping coefficients indicated with asterisk were estimated values based on neighboring measured values shown in Table I.

Y_E is the mode shape displacement at the gimbal station (100 inches) normalized by the nose displacement.

MTP-AERO-63-46

68

Conclusions Drawn

Three modes of bending and six coupled modes for the S-I setup occurred at measured frequencies below 13 hertz.

For the S-IV phase, three other resonant frequencies occurred between 9.94 and 21.72 hertz. Considerable bending was indicated in the instrument section.

There were an adequate number of accelerometers along the center tank in upper stages but four outer tanks were inadequately instrumented.

The procedure utilized in this dynamic test of recording incremental frequency sweep data is necessary for successful analysis of complicated and redundant structures such as the SAD-5.

Conclusions Drawn

The suspension effects are noticeable in the mode shapes and may influence damping coefficients. However, additional refinements to eliminate suspension effects can only be obtained by designing a more sophisticated suspension.

B2. *"Saturn I Dynamic Test", "Ground Vibration Survey SAD 8 and 9", by Dynamic Test Branch, Structures and Mechanics Engineering Department, Chrysler Corporation, HSM-R102, February 23, 1965*

Purpose and Scope

The Saturn I, Block II Dynamic Test Vehicle (SAD 8 and 9) was subjected to a ground vibration survey while suspended in a simulated free-free condition for both booster stage powered flight and S-IV stage powered flight to determine the responses to excitation in pitch, yaw, and torsion (roll) planes for the ignition condition but only in the pitch plane for the 10 seconds and cutoff conditions.

Test Setup and Procedure

The full scale prototype Saturn I Dynamic Test Vehicle was suspended on a system composed of bridge-strand steel cable, helical coiled springs and hydraulic cylinders.

The propellant mass was simulated in the S-I stage and in the S-IV stage LOX tanks with deionized water.

Polystyrene balls with density approximating that of liquid hydrogen were used as ballast in the S-IV stage fuel tank.

Excitation was performed by shakers mounted at the plane of the engine gimbal ring in four planes, e.g., pitch, yaw, roll and longitudinal.

Outputs from accelerometers and gyros were recorded by suitable instrumentation trailers at ground level. One trailer was provided by MSFC-P&VE and the other by MSFC-Astrionics Laboratory. The test was controlled from the P&VE trailer.

Equipment

A listing of all major equipment together with manufacturer, model, capacity and limitations is given in section 3.5 of the report and included here as Table B-3. The equipment is divided into four categories: a) vehicle excitation, b) pickups, c) display, and d) data acquisition.

Readings Obtained

Visual readouts were obtained from display oscilloscopes. Tape recordings were made directly from analog recorders into which the pickups fed directly. Readouts of amplitude, displacement, and phase were automatically processed to give damping factors.

Vibration Characteristics Noted

In the report three factors of vibration characteristics are given and discussed. These are:

1) Resonant frequencies

2) Amplitudes of acceleration and displacement

3) Damping factors.

The resonant frequencies are given for simulated powered flight for the first four bending modes, pitch and yaw modes, the outer tank modes, the coupled modes and torsion modes. Maximum amplitudes at resonance are shown (as illustrated by Figure B-5) for each mode of vibration for each of several types of support and simulated times of flight. Often the individual tanks vibrated differently than the overall vehicle. Supplemental curves show such differences on each major graph.

Damping factors were obtained from vibration decay curves (not shown), resonant response curves (such as Figure B-6) or phase curves (such as Figure B-7). Summaries of damping factors and frequencies are given in Tables B-4 and B-5.

Comparisons Made

Comparisons of frequencies in pitch excitation at lift-off do not indicate any significant change in mode shape for different suspensions. Some frequencies were affected by flight time. Detailed comparisons of values are given to point out differences particularly where components vibrate in a different mode than the vehicle as a whole.

Damping Values Obtained

Damping factors are given in Tables B-4 and B-5.

TABLE B-3. MAJOR EQUIPMENT LIST (from Ref. B2)

The following is a list of major equipment used in the P&VE trailer during the dynamic testing of the simulated SAD-8 and 9 flight vehicle:

a. Vehicle Excitation

    (1) Amplidyne

        Manufacturer: General Electric
        Model: AMF 622F, 4 pole
        Output: 10 KW, 40 AMP, DC, to 15 Hz
        RPM: 1,750

    (2) Power Amplifier

        Manufacturer: Ling
        Model: PP-10/12
        Output: 12 KW, 10 cps to 5 kHz

    (3) Shakers

        Manufacturer: Ling
        Model: A-175
        Force: 1,500 lb peak
        Displacement: 1 in., peak-to-peak
        Model: 219
        Force: 500 lb peak
        Displacement: 1 in., peak-to-peak
        Model: 219 L
        Force: 500 lb peak
        Displacement: 3 in., peak-to-peak

    (4) Oscillator

        Manufacturer: Hewlett-Packard
        Model: 202A
        Frequency: 0.008 to 1,200 Hz

71

b. Pickups

    (1) Accelerometers

        Manufacturer: CEC
        Type: Strain-gage bridge
        Rin: 500 Ω (typical)
        Rout: 340 Ω (typical)
        Excitation: 12 volts maximum
        F.S. Output: 2 mv/v-g (typical)
        Nonlinearity: $\pm 0.25\%$ F.R.
        Natural Frequency: 115 Hz (typical)
        Damping: 0.7 of critical

    (2) Load Cells

        Manufacturer: Baldwin
        Type: Strain-gage bridge, dual element
        Rin: 120 + 0.5
        Rout: 117.5 + 1
        Excitation: 10 volts maximum
        F. S. Output: 2 mv/v
        Max. Nonlinearity: $\pm 0.1\%$ F.S.
        Overload Capacity: 150% of rated

c. Display

    Oscilloscope

        Manufacturer: ANALAB
        Model: 1,100 with high persistance crt and No. 700
            Dual Plug-in
        Zin: 2 meg Ω 500 $\mu\mu$ fd
        Sensitivity: 1 mv to 200 V, F.S.

d.   Data Acquisition

(1)   Digital Recorder

Manufacturer: Systems Engineering Laboratories
Model: 622
Channels: 96 Analog, 4 digital, on 1/2-in. magnetic tape,
          compatable with GE 225 and IBM 7094
Sampling Rate: 32.25 kHz

(2)   Analog Recorder

Manufacturer: CEC
Model: 5-123 Oscillograph
Channels: 36 on 1-ft wide direct print paper

(3)   Analog Amplifiers

Manufacturer: CEC
Model: System D, Class II, 3 kHz carrier
Response: DC to 600 Hz
Channels: 24
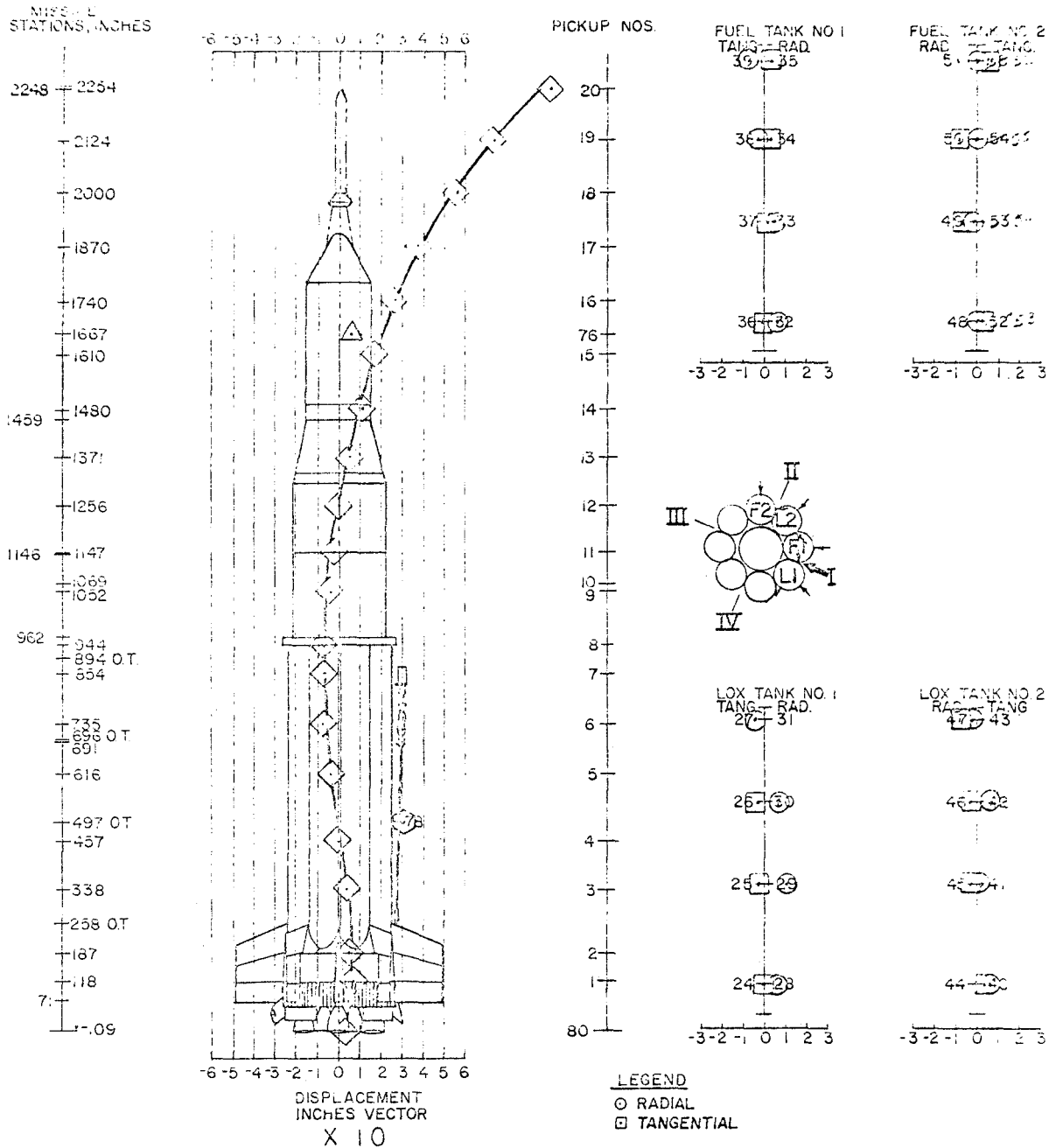
Figure B-5. First Bending Mode (Pitch) for Saturn Vehicle
(from Ref. B2)
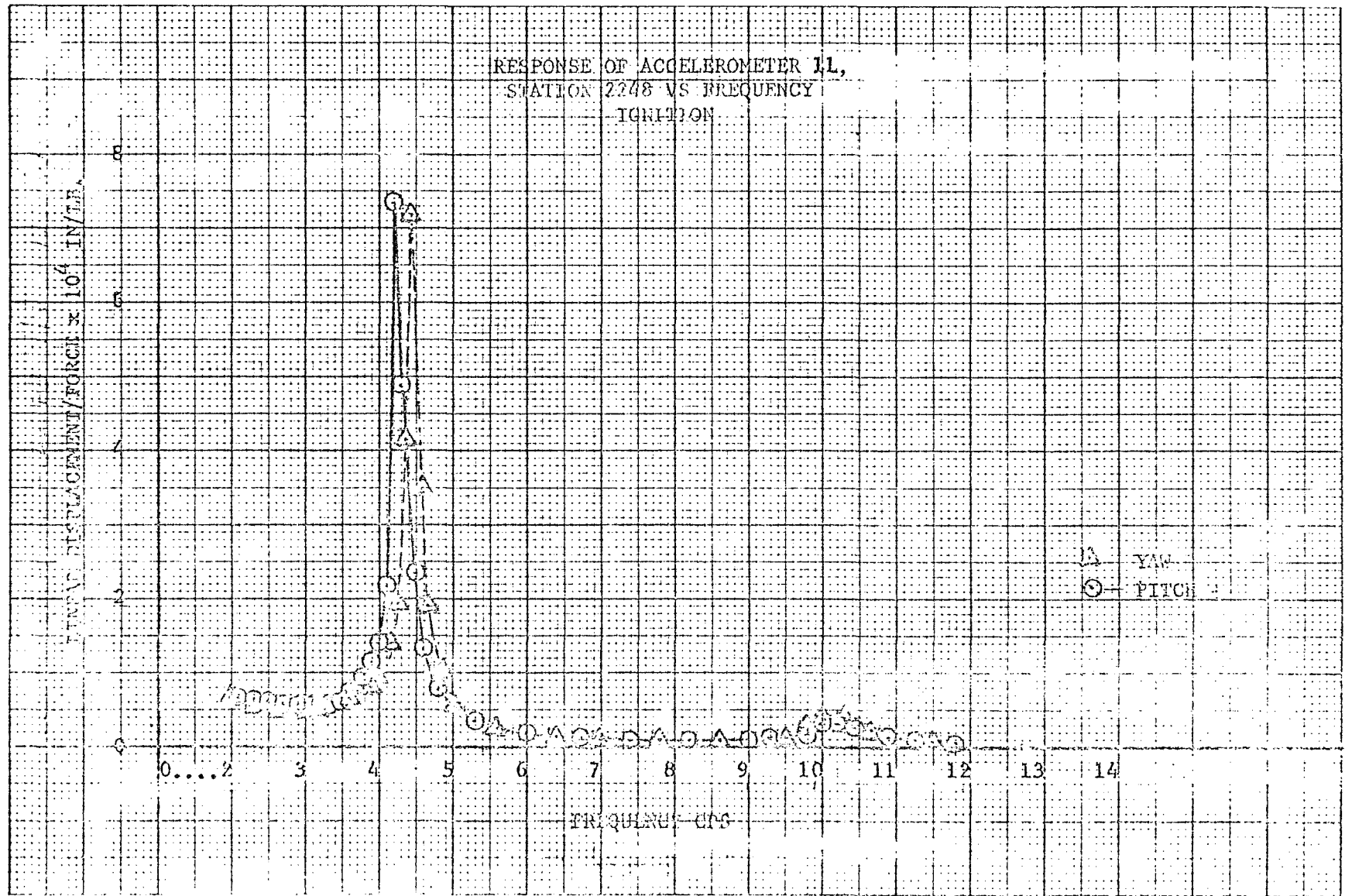
Figure B-6. Response Versus Frequency, Accelerometer 11 (Station 2248) 8-5 Suspension at Ignition (Pitch and Yaw) (from Ref. B2)
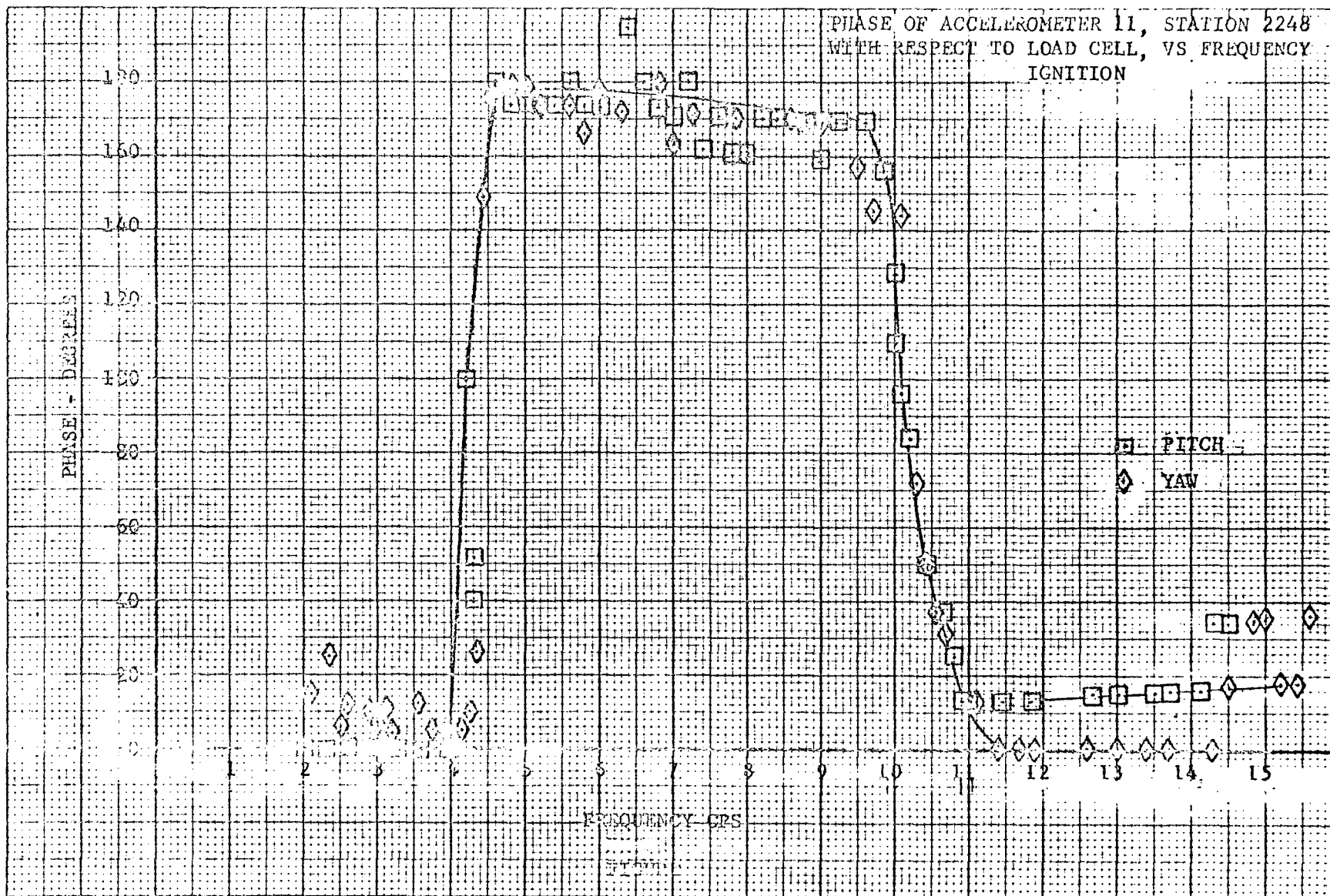
Figure B-7. Phase of Accelerometer 11 (Station 2248) with Respect to Load Cell Versus Frequency, 8-5 Suspension at Ignition (Pitch and Yaw) (from Ref. B2)

TABLE B-4. RESONANT FREQUENCIES AND STRUCTURAL DAMPING FACTORS, PHASE I (from Ref. B2)

Run Number	Mode	Frequency (cps)	Damping (g)
	PITCH, LIFTOFF, 8-8 SUSPENSION		
000573	1st Bending Coupled	1.96	3.30
000576	1st Bending	2.07	0.89
000600	1st Cluster	2.36	2.32
000603	2nd Cluster	3.47	3.38
000605	2nd Bending	3.88	2.83
000607	2nd Bending (Tower Yaw)	3.95	1.62
000611	3rd Coupled	4.27	1.52
000613	3rd Bending	5.39	2.05
000615	4th Bending	5.85	1.00
000620	4th Bending Coupled	7.11	5.47
000621	R_{11}	9.38	1.82
000623	Engine	10.60	-
000625	5th Bending	12.88	2.99
	PITCH, LIFTOFF, 8-12 SUSPENSION		
000122	Fuel Tank (Radial)	1.58	-
000124	1st Bending Coupled	1.95	3.71
000131	1st Bending	2.08	2.05
000135	Cluster	3.47	2.99
000137	2nd Bending	3.96	1.11
000143	3rd Bending	5.39	2.01
000145	2nd Fuel Tanks	5.85	3.30
000147	4th Bending	7.22	4.76
000151	5th Bending	9.37	1.67
000153	Cable	10.28	-
000155	Cable	12.84	1.27

TABLE B-4. RESONANT FREQUENCIES AND STRUCTURAL DAMPING FACTORS,
PHASE I (from Ref. B2) - Continued

Run Number	Mode	Frequency (cps)	Damping (g)
	PITCH, 10 SEC, 8-8 SUSPENSION		
100001	Fuel Tank (Radial)	1.62	-
100003	1st Bending Coupled	1.995	2.50
100005	1st Bending	1.986	2.87
100015	1st Cluster	3.49	1.62
100017	2nd Bending Coupled	3.938	2.05
100021	2nd Bending	3.992	1.16
100026	3rd Bending	5.48	2.19
100030	4th Bending	5.98	4.54
100032	Outer Tanks (2nd)	6.77	2.23
100034	4th Bending Coupled	7.64	4.25
100036	5th Bending and Cable	9.53	1.42
100040	5th Bending and Cable	11.01	2.87
	PITCH, 35 SEC, 8-6 SUSPENSION		
200670	1st Bending Coupled	2.14	-
200672	1st Bending	2.23	4.35
200675	1st Bending Coupled	2.24	5.60
200677	Outer Tanks	3.18	-
200701	Cluster	3.83	2.14
200703	Cluster	3.98	2.83
200705	2nd Bending	4.436	1.00
200707	3rd Bending	5.178	3.11
200711	4th Bending	6.51	0.61
200713	Tower and Engine	8.137	-
200715	Outer Tanks	9.186	3.34
200717	Outer Tanks	10.629	1.21
200721	5th Bending	11.28	3.42
	PITCH, 70 SEC, 8-6 SUSPENSION		
301013	1st Bending	2.354	2.50
301015	Outer Tanks	2.824	2.23
301017	Outer Tanks	3.79	2.58
301022	2nd Bending	4.41	4.09
301024	Cluster	4.81	1.62
301026	3rd Bending	5.37	1.96
301030	4th Bending	7.65	1.96
301034	Tower	10.0	4.82
301036	Cable	10.96	-

78

TABLE B-4. RESONANT FREQUENCIES AND STRUCTURAL DAMPING FACTORS,
PHASE I (from Ref. B2) - Continued

Run Number	Mode	Frequency (cps)	Damping (g)
	PITCH, 82 SEC, 8-6 SUSPENSION		
400001	1st Bending	2.424	2.79
400003	Cluster	3.223	-
400005	2nd Bending Coupled	4.265	-
400011	2nd Bending	4.692	2.50
400013	2nd Bending Coupled	4.814	4.60
400015	Cluster	5.119	4.41
400017	3rd Bending	5.766	0.95
400021	R_8	6.706	1.27
400025	4th Bending	8.489	2.58
400026	Cable	11.10	-
400030	Engine	11.98	5.28
	PITCH, 112 SEC, 8-6 SUSPENSION		
500001	1st Bending	2.396	2.32
500003	2nd Bending	4.703	1.96
500005	Cluster	5.20	5.99
500007	3rd Bending	6.338	5.28
500011	3rd Coupled	6.882	5.39
500014	Engine S-I	8.074	-
500016	R_7	8.968	2.32
500020	S-I Engine (Yaw)	11.467	1.82
	PITCH, 146 SEC, 4-4 SUSPENSION		
600001	1st Bending	2.404	3.07
600003	2nd Bending	4.728	1.62
600006	2nd Bending Coupled	4.848	4.02
600007	3rd Bending	8.371	4.12
600011	3rd Bending Coupled with Outer Tanks	8.483	3.99
600014	4th Bending	12.16	-

TABLE B-4. RESONANT FREQUENCIES AND STRUCTURAL DAMPING FACTORS,
PHASE I (from Ref. B2) - Continued

Run Number	Mode	Frequency (cps)	Damping (g)
YAW, LIFTOFF, 8-8 SUSPENSION			
010040	Fuel Tank (Radial)	1.578	-
010042	1st Bending Coupled	1.966	1.82
010044	1st Bending	2.095	1.67
010047	Outer Tanks	2.338	2.32
010051	2nd Coupled	3.506	1.96
010053	2nd Bending	3.942	0.66
010055	Tower	4.253	2.67
010060	S-IV Engine Mode	4.428	1.27
010061	3rd Bending	5.421	1.77
010063	Tower	5.887	2.10
010065	Outer Tanks	6.398	0.72
010067	4th Bending	7.177	3.81
010071	R_{13}	9.350	1.91
010073	Engine Mode	10.383	2.14
YAW, 10 SEC, 8-8 SUSPENSION			
110002	Fuel Tank (Radial)	1.615	5.25
110005	1st Bending Coupled	2.023	-
110006	1st Bending	2.166	-
110010	Outer Tanks	2.381	-
110012	2nd Bending Coupled	3.536	-
110014	2nd Bending	3.982	-
110016	3rd Bending Coupled	4.530	-
110020	3rd Bending	5.568	-
110022	4th Bending	6.153	-
110026	Tower and Outer Tanks	7.535	-
110030	Engine	10.93	-
YAW, 48 SEC, 8-6 SUSPENSION			
210002	1st Bending	2.269	-
210004	1st Bending Coupled	2.409	-
210007	1st C/W F.T. (Tang.)	3.155	-
210011	Cluster	3.853	-
210013	2nd Bending	4.250	-
210014	3rd Bending	5.204	-

TABLE B-4. RESONANT FREQUENCIES AND STRUCTURAL DAMPING FACTORS,
PHASE I (from Ref. B2) - Continued

Run Number	Mode	Frequency (cps)	Damping (g)
	YAW, 70 SEC, 8-6 SUSPENSION		
311002	1st Bending	2.37	2.28 *
311004	Outer Tanks	2.818	0.89
311006	Tower and Outer Tanks	3.752	-
311011	2nd Bending	4.381	2.45
311013	2nd Bending Coupled	4.442	3.85
311017	Cluster	4.82	2.95
311020	3rd Bending	5.36	2.05
311022	Outer Tanks	7.68	2.05
311024	4th Bending Coupled with Outer Tanks	10.45	8.42
311026	4th Bending Coupled with Cable	11.03	-
	YAW, 112 SEC, 8-4 SUSPENSION		
410001	1st Bending	2.476	-
410004	2nd Bending	4.83	-
410006	Cluster	5.196	-
410012	3rd Bending and Engine	6.152	-
410014	4th Bending and Engine	9.281	-
410020	S-I Engine and 5th Bending	12.853	-
	YAW, 146 SEC, 4E-4 SUSPENSION		
510001	1st Bending	2.486	-
510005	2nd Bending	4.88	-
510010	3rd Bending	8.397	-
510012	3rd Bending	8.527	-
510014	Engine and 4th Bending	10.395	-
510016	Engine and 4th Bending	11.897	-

TABLE B-4. RESONANT FREQUENCIES AND STRUCTURAL DAMPING FACTORS,
PHASE I (from Ref. B2) - Continued

Run Number	Mode	Frequency (cps)	Damping (g)
	LONGITUDINAL, LIFTOFF, 8-8 SUSPENSION		
030001	Bouncing	1.55	-
030005	R_2	4.90	-
030007	R_3	5.78	-
030011	R_4	6.51	1.82
030014	R_5	7.54	2.58
030016	1st Long. Mode	10.17	3.34
030020	Engine and Thrust Structure	13.70	2.05
030022	Fuel Tank	16.41	2.58
030024	R_9	18.64	6.09
030026	R_{10}	20.77	-
030031	R_{11}	24.83	2.28
	LONGITUDINAL, 146 SEC, 4-E4 SUSPENSION		
230001	Bouncing	1.83	1.96
230003	1st Long. Mode	11.41	5.08
230005	Outer Tanks	14.22	5.17
230010	S-IV Engine and Outer Tanks	20.53	5.17
230012	S-IV Bulkhead	25.85	4.41
230014	S-IV Bulkhead and Outer Tanks	28.12	3.56
230016	Outer Tanks	35.87	-
	TORSION, LIFTOFF, 8-8 SUSPENSION		
020003	Outer Tanks Tang.	2.356	2.01
020006	Tower Lateral	3.592	3.38
020007	1st Torsion	3.687	4.32
020012	Tower Lateral	4.036	3.07
020014	Cluster	5.66	2.10
020016	2nd Outer Tanks Tang.	6.594	3.60
020020	R_7	10.04	-
020023	R_8	10.56	-

TABLE B-4.   RESONANT FREQUENCIES AND STRUCTURAL DAMPING FACTORS,
PHASE I (from Ref. B2) - Concluded

Run Number	Mode	Frequency (cps)	Damping (g)
	TORSION, 10 SEC, 8-8 SUSPENSION		
120001	Outer Tanks	2.397	2.67
120006	Tower Lateral	3.629	2.99
120010	1st Torsion	3.895	1.96
120013	Tower Lateral	4.031	3.11
120015	Cluster	5.80	2.01
120017	2nd Outer Tanks Tang.	7.01	1.82
120021	R_7	7.61	2.58
120023	R_8	9.90	-
120025	R_9	11.03	-
	TORSION, 35 SEC, 8-6 SUSPENSION		
220001	Outer Tanks	2.887	1.05
220003	Tower, Yaw	3.838	2.32
220007	1st Torsion	4.601	1.62
220012	Tower Lateral and Engine	4.234	1.41
220013	Cluster	5.923	2.37
220015	Tower Lateral	6.149	2.79
220020	Outer Tanks	10.43	-
220022	2nd Torsion	12.00	3.23
	TORSION, 70 SEC, 8-6 SUSPENSION		
320003	Outer Tanks	2.740	1.42
320004	Tower Lateral and Outer Tanks	3.769	1.57
320006	Tower Lateral	4.688	1.96
320010	1st Torsion	5.35	2.28
320012	Cluster	6.747	6.80
320014	Cluster Coupled with Engine	6.794	6.26
320016	Cluster	7.943	-
320020	2nd Torsion	12.94	2.32
	TORSION, 146 SEC, 4E-4 SUSPENSION		
420001	Outer Tanks	4.934	0.89
420003	1st Torsion	5.646	4.12
420005	Engine and Outer Tanks	8.465	-
420007	Engine and Outer Tanks	10.52	-

TABLE B-5. RESONANT FREQUENCIES AND STRUCTURAL DAMPING FACTORS, PHASE II (from Ref. B2)

Run Number	Mode	Frequency (cps)	Damping (g)
PITCH, IGNITION, 8-5 SUSPENSION			
010036	1st Bending	4.21	2.68
010041	2nd Bending	10.17	6.75
010200	Engine	12.69	-
010202	3rd Bending	19.76	4.02
YAW, IGNITION, 8-5 SUSPENSION			
-	Rocking	0.38	-
020002	1st Bending	4.37	1.67
020004	2nd Bending	10.16	5.21
020137	Engine	11.62	-
020141	Engine	17.34	-
020144	Engine	20.15	2.81
TORSION, IGNITION, 8-5 SUSPENSION			
-	Rocking	0.616	-
030002	Engine	9.95	0.85
030156	2nd Torsion	16.95	3.25
PITCH, 10 SECOND 8-5 SUSPENSION			
110002	1st Bending	9.88	5.25
-	Rocking	0.471	-
110107	Engine	15.79	-
110114	Engine	25.23	3.07
110105	Engine	11.1	3.38
PITCH, CUTOFF, 8-3 SUSPENSION			
-	Rocking	0.808	-
210002	1st Bending	11.76	BTG
210010	1st Bending and Engine	12.52	7.40
210011	2nd Bending and Engine	18.21	-
210016	Engine	20.12	3.31
210017	Thrust Structure	29.70	-

Conclusions Drawn

1) The polystyrene balls used to simulate LH2 contributed appreciably to the vehicular roll moment of inertia.

2) The suspension support ring contributed appreciably to the vehicular roll moment of inertia.

3) The roll moment of inertia of the dynamic test vehicle is 70 percent greater than that of the flight vehicle, due to the effects of the polystyrene balls and the suspension support ring.

4) There is marked coupling between body bending modes and engines at the cutoff pitch condition.

5) Various suspension systems utilized during this test did not have any appreciable effect on the mode shapes and resonant frequencies. Less than one percent change occurred in the resonant frequencies.

6) Phase and response curves cannot be relied on to any great extent for the determination of resonant frequencies due to random type errors.

7) In order to accurately pin-point resonant frequencies, sweeps should be made at 0.01 hertz increments within 0.1 hertz of suspected peak.

B3. *"Saturn I-B Dynamic Test", "Final Report, Total Vehicle Testing of Saturn I-B, Dynamic Test Vehicles, SA200-D in SA202, SA203, SA206 and SA207 Configurations", Chrysler Corporation, HSM-R856, January 31, 1966*

Purpose and Scope

This experimental program was conducted to determine the vibration characteristics of a full scale Saturn I-B prototype SA200-D. The several tests were planned to give free-free conditions for the SA202, the SA203, the SA206 and the SA207 configurations.

Test Setup and Procedure

Each vehicle configuration was suspended on a system of cables, springs, and hydraulic cylinders as shown in Figure B-8. Each was excited electro-dynamically in the lateral (pitch and yaw), longitudinal and torsional modes. Outputs from accelerometers and rate gyros were recorded for each vehicle configuration and for each type of excitation.

The position of each vehicle in relation to the tower was measured by a system of "position plots" at a number of points on the tower.

All measurements of dynamic response were transmitted to appropriate instrumentation trailers at ground level whereas all lift measurements were monitored in the fourth level control room.
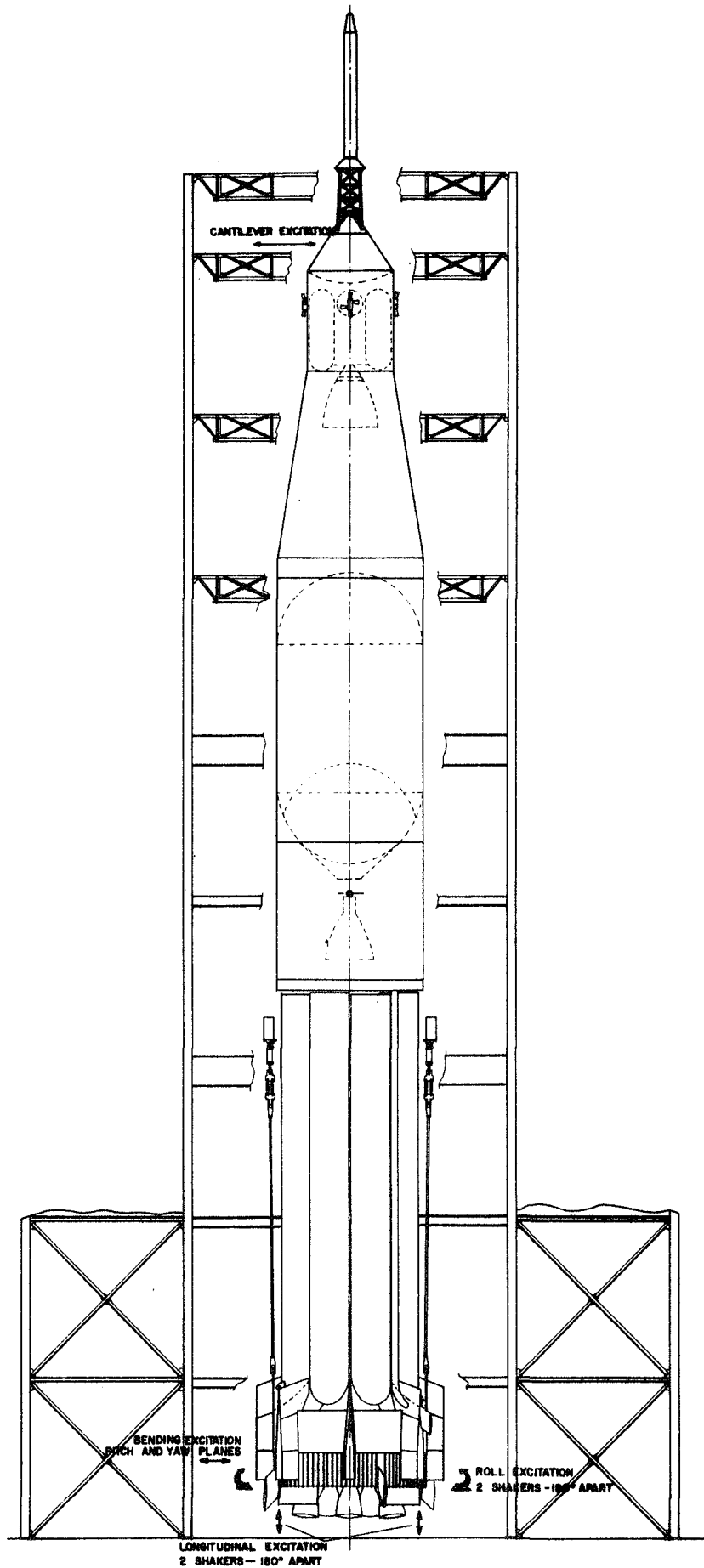
Figure B-8. Saturn Vehicle Suspended in a Free-Free
Condition (from Ref. B3)

Equipment

The dynamic transducers consisted of:

    1) Strain gages.

    2) Inertial spring-mass viscous damped accelerometers.

    3) Rate gyros.

The outputs of the transducers were transmitted to two instrumentation trailers at ground level by way of patch panels conveniently located on the tower.

A tabular listing of the specific types of transducers and recorders is given in the original report.

The shakers were apparently "ling" shakers with variable "g" outputs.

Readings Obtained

Approximately 200 response curves are presented in the original report. The data are presented in four different ways:

    1) Tracing of oscillograph records.

    2) Replicas of charts or plots of displacement and/or acceleration as a function of frequency for each accelerometer in each test.

    3) Summary plots of frequency, amplitude, mode, flight time and location are given in various combinations as shown in Figures B-9, B-10 and B-11.

    4) Summary values of reduced data are given in a series of tables in the report.

Tables B-6 through B-11 are examples of these data.

These raw data were reduced to useful values by computer programs. Some programs have not been officially documented. Among those that have been documented are:

    1) The P&VE computer program established for quick reduction of the dynamic test magnetic tape data immediately after a test run. This enables the test engineers to detect any problems existing in recording reliable readings.

    2) The "Computer Laboratory" computer program gives essentially the same reduction of data tapes as the P&VE computer program and also includes such factors as generalized mass, damping factors, excitation forces and resonant frequencies.

    3) Still other computer programs provide checks on data readings and slightly different dynamic factors.

SA- 206
Run No - 22603?
Frequency (cps) - 4.83
Configuration - 146 Sec. Roll
Suspension - ?-4
Shaker Moment - 22080 N-m
195428 in-lbf

Conversion Factor
1g =   cm
            in

Symbols
○ Center Tank & Upper Stages
□ LOX 1
△ Fuel 1
◁ LOX 2
⬡ Fuel 2
◇ Control Accelerometer
+ Rate Gyro Slope
○ Engine 4 (S-IB) and Engine
(S-IVB)
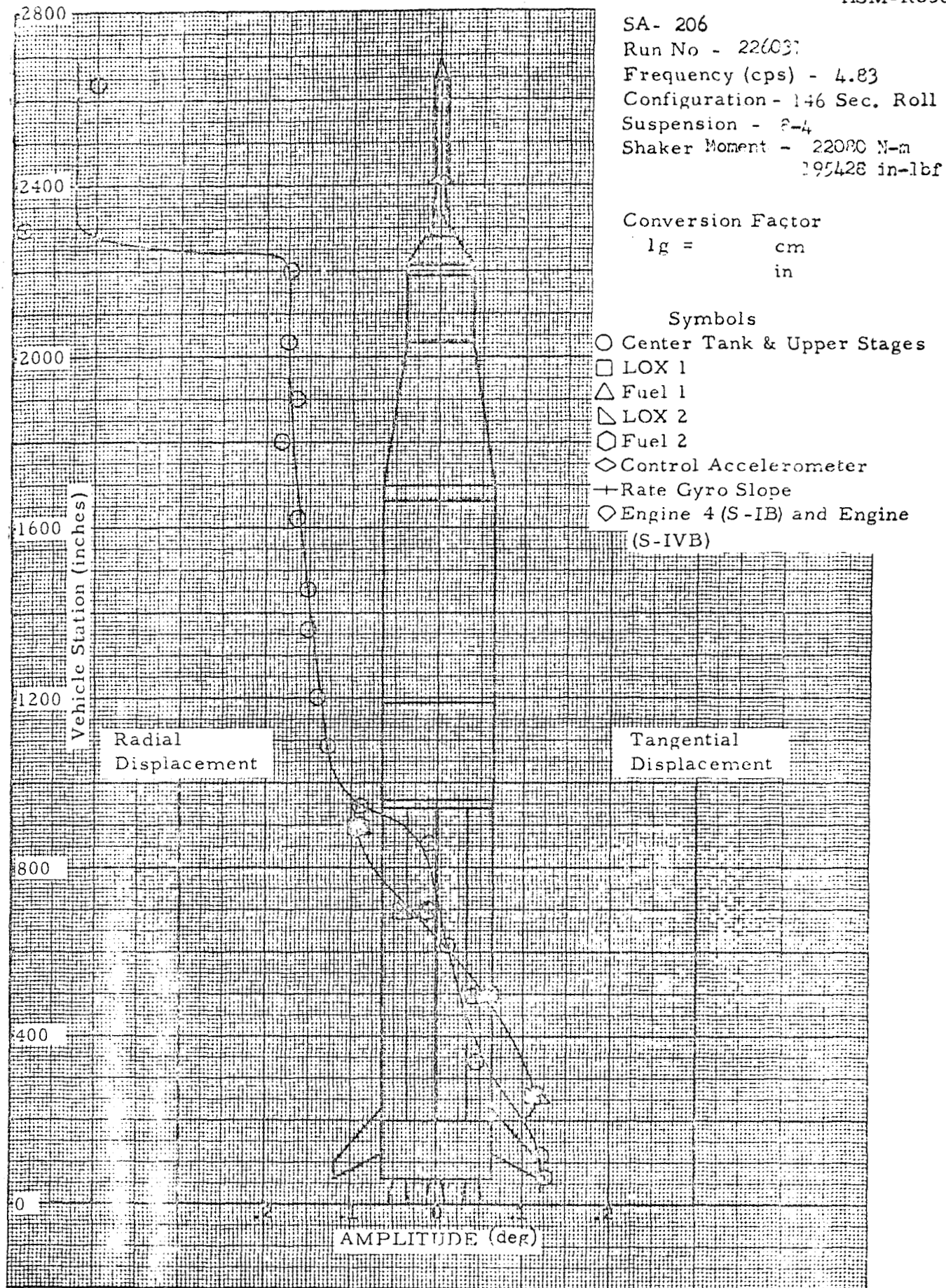
Figure B-9. SA-206, First Torsion Coupled Mode, 146 Seconds Roll (from Ref. B3)
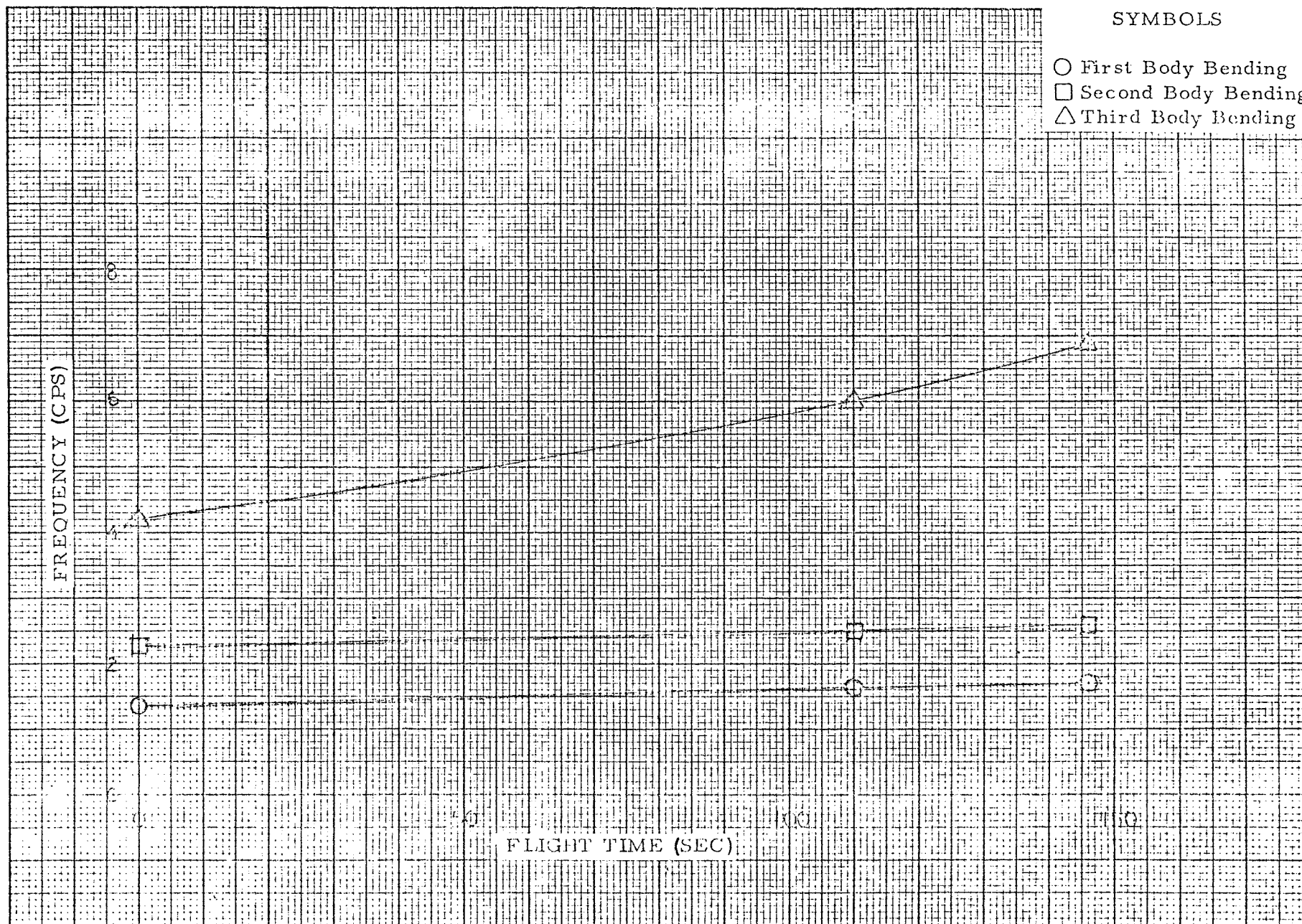
Figure B-10. SA-202 Pitch, Bending Frequency Variation with Simulated Flight Time (from Ref. B3)

HSM-R856
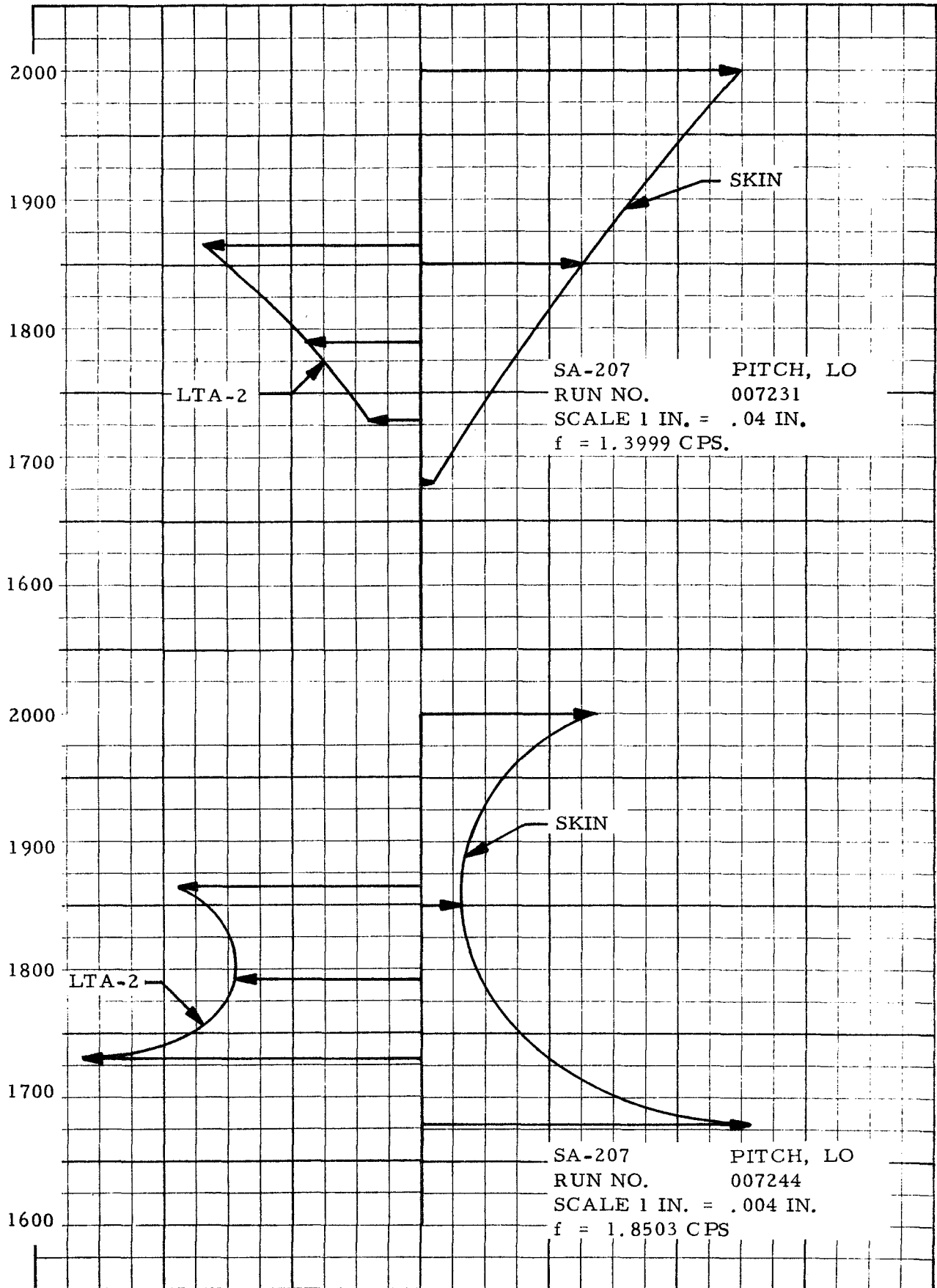
Figure B-11. SA-207, Pitch Lift-Off, Runs No. 007231 and 007244 -- Response of the Accelerometers Located on the LEM and LEM Adapter (from Ref. B3)

90

TABLE B-6. SA-203 MODAL DATA, LIFT-OFF, PITCH, 8-8 SUSPENSION (from Ref. B3)

RUN NUMBER	RESONANT FREQUENCY (cps)	MODE	DAMPING* (ξ %)
000452	1.60	Fuel No. 1 Radial Mode	3.00
000472	2.05	LOX No. 1 Radial Mode	2.26
000477	2.30	First Body Bending Mode	1.07
000311	3.66	LOX Tangential Coupled Mode	1.04
000313	4.32	Engine Coupled Mode	-
000374	5.34	Second Body Bending Mode Coupled With OT	0.75
000413	5.42	Second Body Bending Mode Coupled With OT	0.50
000606	5.72	Second Fuel Radial Mode	-
000615	6.30	Second Bending Mode With Fuel No. 2 Tangential	1.46
000634	7.60	Second LOX Radial Mode	-
000434	8.00	Third Bending Mode Coupled With OT	1.64
000437	8.06	Third Bending and Outer Tank Mode	1.27
000657	9.30	Engine Coupled Mode	-
000331	10.92	Engine Mode	2.54

* ξ Average = 1.55 percent

TABLE B-7. SA-202 MODAL DATA, LIFT-OFF, YAW, 8-8 SUSPENSION (RE-RUN) (from Ref. B3)

RUN NUMBER	RESONANT FREQUENCY (cps)	MODE	DAMPING (ξ %)
602044	1.33	First Bending Mode	1.22
602114	1.65	First Fuel Radial Mode	-
602127	2.10	First LOX Radial Mode	-
602006	2.19	Second Bending Coupled With Outer Tank Tangential	1.02
602010	2.29	Second Bending Mode	1.20
602135	2.40	First Fuel Tangential Mode	-
602011	3.53	First LOX Tangential Mode	1.08
602016	4.14	Third Bending Mode	1.54
602017	4.53	Fourth Bending Mode	-
602024	5.83	Second Fuel Radial Mode	1.12
602252	6.50	Second Fuel Tangential Mode	0.91
602032	7.53	Fourth Bending Coupled With Second Outer Tank	-
602035	8.55	Coupled Tower Mode	1.13
602037	10.06	Engine	-

* ξ Average = 1.15 percent

TABLE B-8. SA-202 MODAL DATA, LIFT-OFF +110 SECONDS, PITCH, 8-4 SUSPENSION (RE-RUN) (from Ref. B3)

RUN NUMBER	RESONANT FREQUENCY (cps)	MODE	DAMPING (ξ %)
712225	1.64	First Bending Mode	1.75
712227	2.51	Second Bending Mode	1.69
712311	2.58	Second Bending Mode With Phase Shift in Outer Tanks	1.17
712235	4.80	First LOX Radial Mode	0.77
712462	6.00	First Fuel Radial Mode	1.89
712506	7.71	Third Bending Coupled With Engine Mode	1.70
712532	9.71	Fourth Bending Coupled With Engine and Tower Mode	1.26
712251	10.66	Engine Mode	-

* ξ Average = 1.46 percent

TABLE B-9. SA-206 MODAL DATA, LIFT-OFF +110 SECONDS, YAW, 8-6 SUSPENSION
(from Ref. B3)

RUN NUMBER	RESONANT FREQUENCY (cps)	MODE	DAMPING* (ξ%)
116000	1.47	First Bending	2.34
116061	2.50	Second Bending Out of Phase	1.20
116156	2.65	Second Bending In Phase	1.37
116101	5.46	First LOX Coupled Radial Mode	1.28
116253	5.80	Third Bending With Outer Tank Coupled	0.86
116114	6.28	Outer Tank and Engine Coupled	-
116305	8.40	Second LOX Radial Coupled	-
116034	10.24	Engine	-

*ξ Average = 1.41 percent

TABLE B-10. SA-206 MODAL DATA, LIFT-OFF +146 SECONDS, PITCH 8-4 SUSPENSION
(from Ref. B3)

RUN NUMBER	RESONANT FREQUENCY (cps)	MODE	DAMPING* (ξ%)
026111	1.45	First Bending	2.38
026010	2.50	Second Bending in Phase	1.06
026143	2.65	Second Bending Out of Phase	2.40
026021	5.83	Third Bending Coupled	0.60
026023	6.94	First Fuel Radial	-
026033	8.75	Engine	-
026034	9.88	Tower Coupled	-

*ξ Average = 1.61 percent

TABLE B-11. SA-206 MODAL DATA, LIFT-OFF +146 SECONDS, PITCH, CANTILEVER
(from Ref. B3)

RUN NUMBER	RESONANT FREQUENCY (cps)	MODE	DAMPING (ξ%)
444402	0.57	First Cantilever	2.02
444406	2.89	Third Cantilever	1.3.
444407	3.05	Third Cantilever Coupled With Outer Tanks	-
444411	6.35	Fourth Cantilever	0.98

*ξ Average = 1.43 percent

Vibration Characteristics Noted

The discussion in the report is centered around the general resonant frequencies and modes of vibration for different excitations. Damping is considered as a percentage of critical damping. Summary tables are given in a following section.

Comparisons Made

Correlations between the behavior during pitch, yaw and roll modes of vibration are discussed. In general the lack of consistency in behavior is the principal factor emphasized in the discussion.

The results from strain gage measurements indicate that the pulsating part of the stresses measured were quite low. Since the strain gages were all mounted on the heavy structural framework holding the command module, this was apparently expected.

Damping Values Obtained

Damping coefficients expressed as a percent of critical damping are given in a series of tables. Tables B-6 through B-11 are examples.

In general, the damping factors ranged from 1/2 to about 4 percent of critical. It was noted that "the outer tank modes exhibited larger damping values...than the uncoupled bending modes".

Conclusions Drawn

Confidence in the accuracy and reliability of the data was severely limited for the following reasons:

1) Attention of the test engineer was not directed toward determining Lunar Excursion Module Test Artical (LTA-2) resonances uncoupled from the vehicle bending modes.

2) Narrow bands of resonance could have been missed. These would greatly modify the results.

3) Lack of instrumentation on the LTA-2 and adjacent skin.

4) No frequencies shown have been taken at a vehicle bending mode. Hence, modes shown may not be representative. There was evidence of considerable LTA-2 resonance.

B4. *Walker, J. H. and R. A. Winje, "An Investigation of Low Frequency Longitudinal Vibration of the Titan II Missile During Stage I Flight", Addendum, TRW Space Technology Laboratory, BSD-TR-65-165, June 1965*

Purpose and Scope

This report should be considered as an addendum to an earlier report, "An Investigation of Low Frequency Longitudinal Vibration of the Titan II Missile During Stage I Flight" by K. J. McKenna, J. H. Walker and R. A. Winje, TRW/STL-Report 6438-6001-RV000, March 26, 1964. This report gives a discussion of the ground test program, a revised analytical model and results of analyses with corrective measures incorporated.

A bibliography of pertinent documentation is also given.

Specific objectives of the tests are:

1) Determination of the interaction between the pump and the suction lines.

2) Determination of the characteristics of the pump under oscillatory conditions.

3) Determination of the thrust chamber reactions to oscillatory flow inputs.

Test Setup and Procedures

Two series of tests were made; one at Aerojet General Corporation, hereafter referred to as Engine Transfer Function Tests (ETFT) and the other at Martin, Denver, referred to as Pump Drive Assembly Tests (PDAT).

The ETFT tests were hot firings whereas the PDAT were conducted with the thrust chamber simulated and the propellants recycled. A schematic arrangement is shown in Figure B-12.

The ETFT consisted of battleship propellant tanks, special oxidizer suction line, flight pumps and a flight thrust chamber. Oscillations in flow and pressure were introduced by means of a horizontal piston and drive assembly.

Pressures throughout the system were measured and recorded.

A total of eight runs of approximately 150 seconds each were made and approximately 60 channels of data were recorded on magnetic tape for each run.

The PDAT were made with essentially the same configuration as the ETFT except that the injector and thrust chamber were simulated with a flow nozzle, orifice plate and cavitating venturi valves. Pulsations were produced as in the ETFT. In addition, provisions were made to pulse the downstream side of the pump.
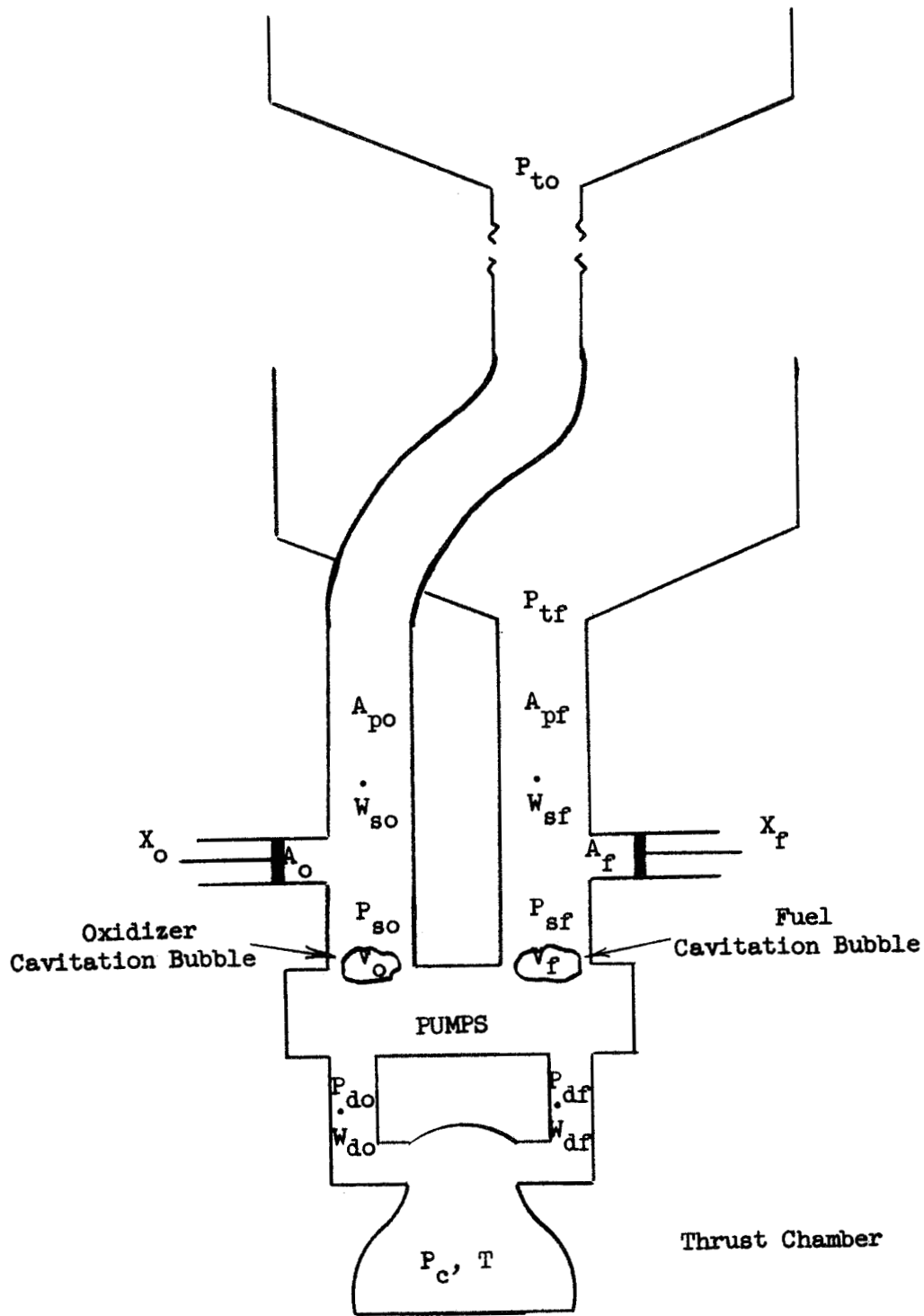
Figure B-12. Ground Test Schematic for Titan III Test (from Ref. B4)

Twenty-two runs were made totaling 2250 seconds of test data which was recorded as for the ETFT.

Equipment

The data resulting from the 60 channels of transducers was recorded on magnetic tape. The records were reduced by analogue techniques. The specific equipment used is not indicated.

Readings Obtained

A sample of the semireduced data obtained from these tests is shown in Figure B-13.

Vibration Characteristics Noted

The tests revealed a characteristic resonant frequency associated with the suction line and pump.

A characteristic resonant frequency was also confirmed for the oxidizer side which was associated with the cavitation index and the compressibility of the fluid in the long line.

Comparisons Made

Comparisons between the fired vibration tests and the mechanical flow tests indicate that all data from the two types of test were in good agreement, i.e., with ±10%.

Comparisons between theory and test indicated either confirmation of, or only slight modification of, the parameters used in the analysis.

Damping Values Obtained

A value of damping (percent) is indicated as 1.0%. This value could have been obtained from curves similar to the curve shown in Figure B-13.

Conclusions Drawn

In general the ground test program was highly successful. The establishment of a fuel line characteristic frequency and its dependence upon the cavitation index as well as the confirmation of the oxidizer characteristic frequency has led to a more thorough understanding of the longitudinal oscillation phenomenon. The fact that much useful information can be obtained from steady state data is in itself a major accomplishment of the test program.
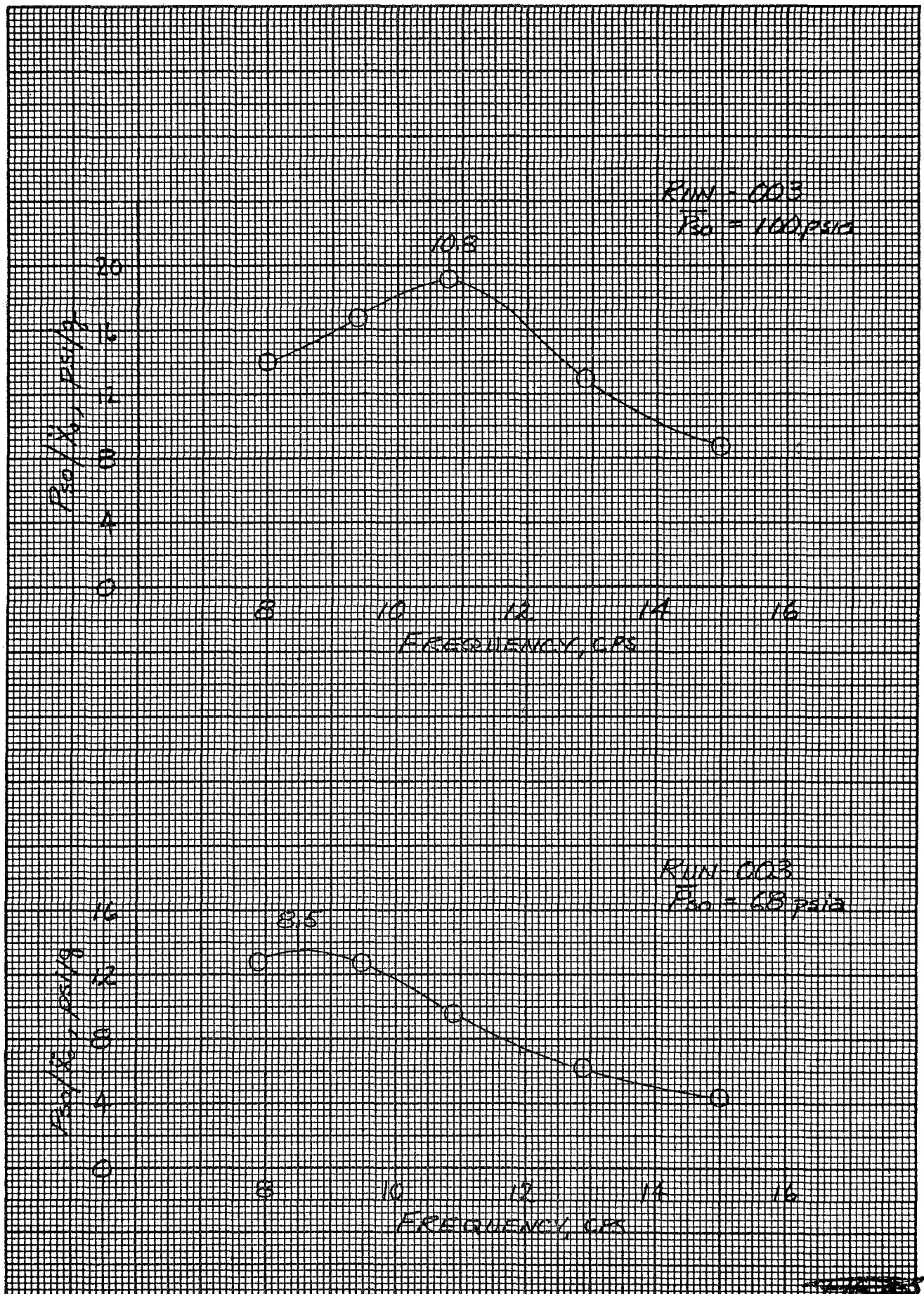
Figure B-13. Relative Amplitude Versus Frequency (Sample of Data Obtained)
(from Ref. B4)

98

B5. *Watson, Charles E. and Kay W. Slayden, "Experimental Vibration Program on a Full Scale Saturn Space Vehicle", George C. Marshall Space Flight Center, NASA-MTP-P&VE-S-62-3, April 26, 1962*

Purpose and Scope

The purpose of the vibration program was to excite the vehicle through a frequency range sufficient to determine the significant free-free lateral, torsional and longitudinal mode shapes, frequencies and associated damping coefficients. Knowledge of these vibration characteristics is needed because of their effects on the vehicle control stabilizing networks.

Five conditions were tested to obtain the variation of bending frequencies during powered flight. These conditions are those at the following times of flight:

T = 0 (lift-off)	T = 63 seconds (Q_{max})
T = 10 seconds	T = 119 seconds (cut-off)
T = 35 seconds	

Test Setup and Procedure

The full scale vehicle was suspended in a simulated free-free condition in a test stand as indicated in Figure B-14.

The suspension system consisted of cables, springs, hydraulic cylinders and turn buckles arranged so as to support the load uniformly. The suspension was varied for different amounts of load (liquid in the tanks) and for different modes of vibration. Deionized water was used in the tanks.

Figure B-15 indicates the various suspensions and shakers used.

Equipment

Instrumentation consisted of velocity pickups mounted at critical locations on the vehicle and roving pickups used to locate nodal points. Strain gage bridge type accelerometers were used. Acceleration outputs were amplified and recorded on direct writing oscillographs.

Four shakers were available for use for lateral and torsional mode shapes. Two or three shakers were used at a time. Two shakers in phase produced longitudinal vibrations.

Resonant frequencies were determined with rate gyros instead of accelerometers because there was no appreciable phase lag below 25 Hz. Outputs from the rate gyros were recorded on an oscillograph.

500 LB SHAKER

500 LB SHAKER

500 LB
SHAKER

150 LB
SHAKER

1500 LB
SHAKER
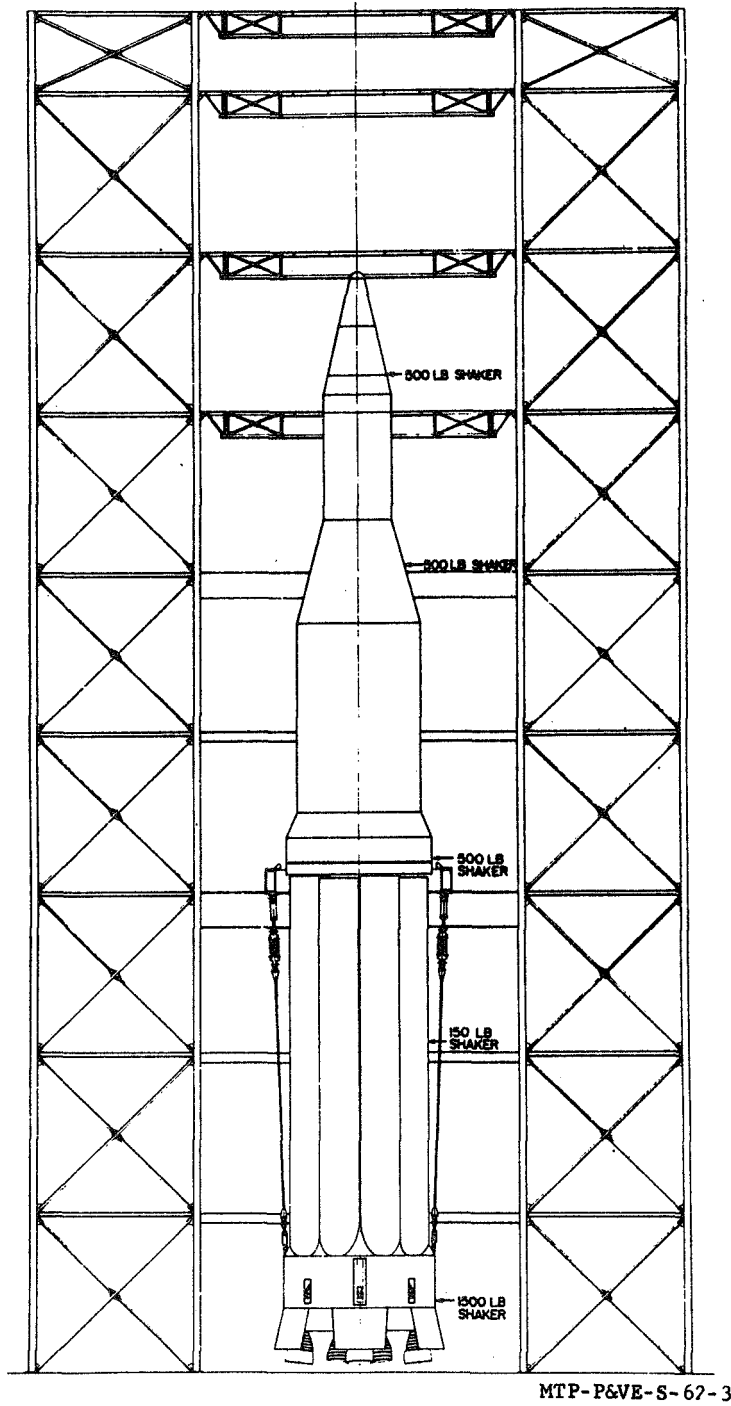
MTP-P&VE-S-62-3

Figure B-14. Drawing of SA-D1 in the Test Tower (from Ref. B5)

100
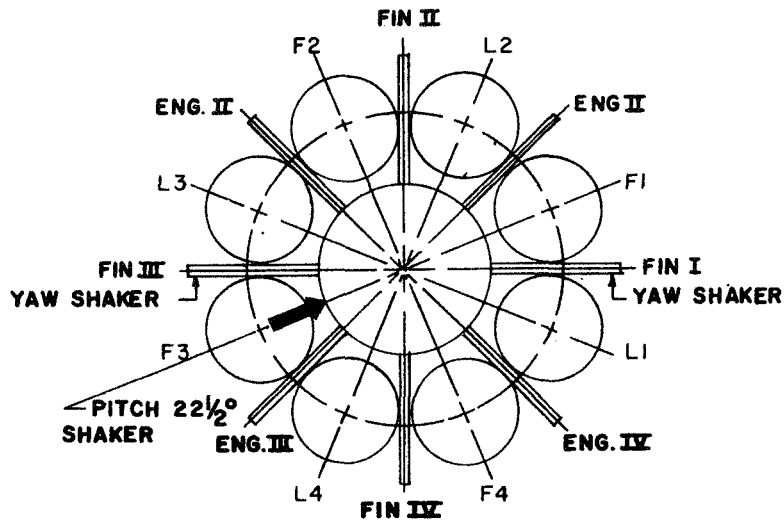
REFERENCE NO | DESCRIPTION | CODE

1. HARD FOR PITCH & YAW, L.O.,10 SECS,& 35 SECS   8(ODD-12S-1C & EVEN-12S-2C)

2. SOFT FOR PITCH, L.O., 10 SECS & 35 SECS   8(ODD-4S-1C & EVEN-12S-2C)

2N. SEE NOTE 1

3. SOFT FOR PITCH, EMPTY & Q MAX   4(EVEN-12S-2C)

3N SEE NOTE 1

4. HARD FOR PITCH, EMPTY & Q MAX   4(ODD-12S-1C)

6. SOFT FOR YAW, L.O., 10 SECS,& 35 SECS $6\left(\begin{array}{l}\text{ODD-12S-1C}\\ \text{2 EVEN ENGINES -12S-2C}\end{array}\right)$

8. SOFT FOR YAW, Q MAX & EMPTY $4\left(4\text{ FINS-12S}\left\{\begin{array}{l}\text{ODD-1C}\\ \text{EVEN-2C}\end{array}\right.\right)$

ODD - OUTRIGGERS I & III, ENGINES I & III

EVEN - OUTRIGGERS II & IV, ENGINES II & IV

S - SPRINGS IN INDIVIDUAL CLUSTER

C - CABLES

NOTE: 1

REFERENCE NUMBERS FOLLOWED BY (N) INDICATE
SUBSTITUTION OF THE NEW LOWER CONNECTING
LINES SHOWN IN FIGURE 5. ALL (N) RUNS
HAVE ONLY 1C OR 1 CABLE.

MTP-P&VE-S-62-3

Figure B-15. Suspension and Shaker Orientation (from Ref. B5)

101

Readings Obtained

Readings of deflection were obtained and plotted in a series of plots of which Figure B-16 is a representative curve.

Typical vehicle response curves are shown in Figures B-17, B-18, B-19 and B-20. These curves show the great variety of patterns obtained. Curves shown in Figure B-20 serve as a means of determining the damping factors for the structure.

Vibration Characteristics Noted

The primary mode shapes are considerably affected by coupling of the outer tanks with the vehicle as a whole. In fact there are no uncoupled first bending modes.

The first cluster mode is distinquished by having only one node on the primary structure. Figure B-17 shows the first mode response at lift-off indicating the close relation or coupling with Lox and fuel tanks.

Second bending modes were clean and strong for the first part of the test. As "flight time" progressed, the second and higher modes became complicated by outer tank resonances.

Cluster and engine modes are accompanied by high values of structural damping.

Cable resonances were annoying when they occurred near vehicle bending resonances.

Comparisons Made

A comparison of SA-DI mode shapes and frequencies with calculated values and with Langley model tests is shown in Figure B-21 and Figure B-22 for the first and second modes of vibration.

Damping Values Obtained

Damping factors were obtained for the vehicle as a whole as indicated by pickups at the forward most location except when a pickup was not working satisfactorily, for which case another pickup was used.

Table B-12 shows damping values obtained for various modes and times of vibration.

Conclusions Drawn

Generally speaking, lateral damping factors decrease with increasing bending mode and cluster frequency.

Torsional modes have a higher damping factor than lateral loads.

Tank slosh frequencies are present in the range of the control system frequency.
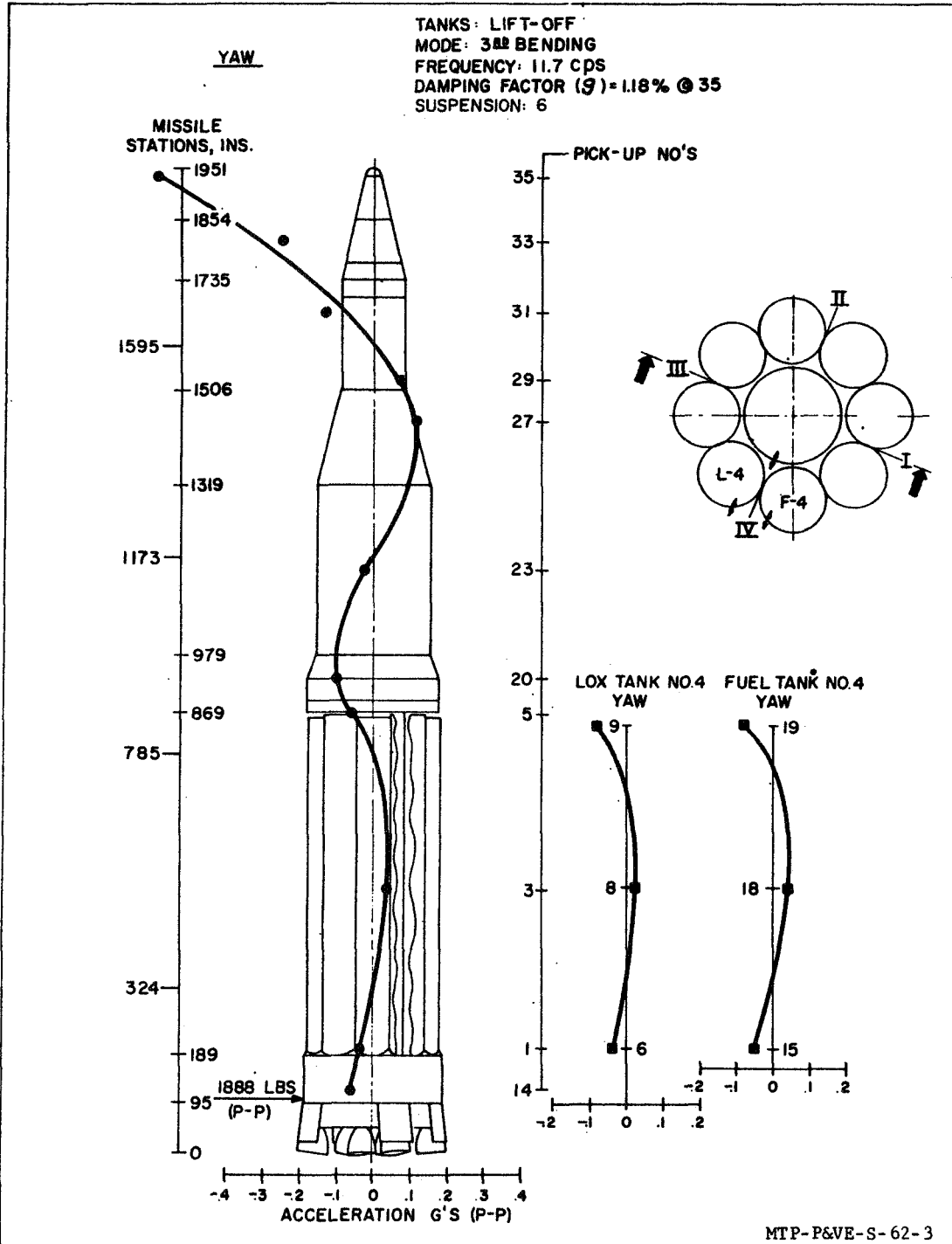
Figure B-16. Lateral Bending Modes (Yaw Plane) (from Ref. B5)
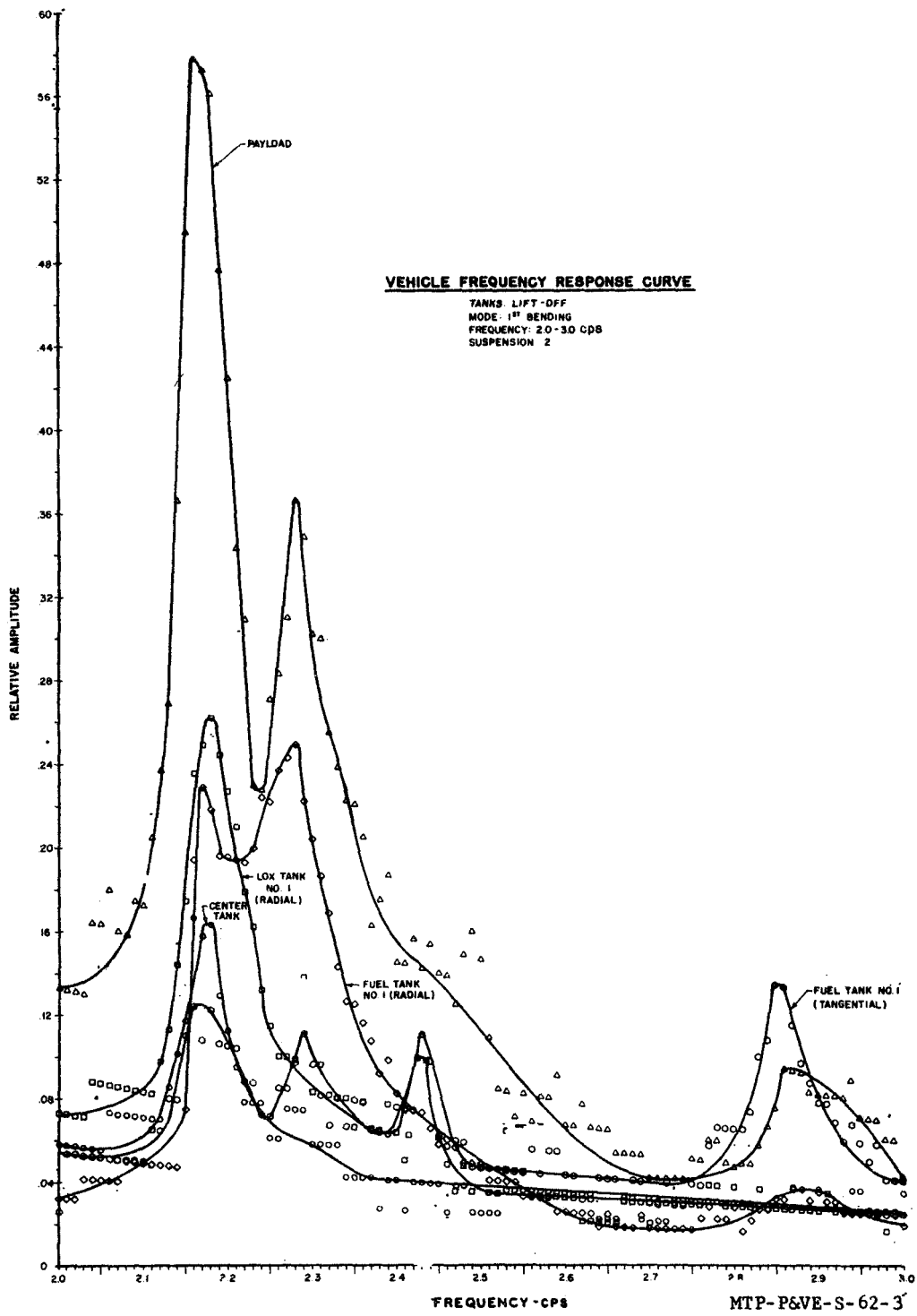
Figure B-17. Vehicle Frequency Response Curves at Lift-Off
(from Ref. B5)

104
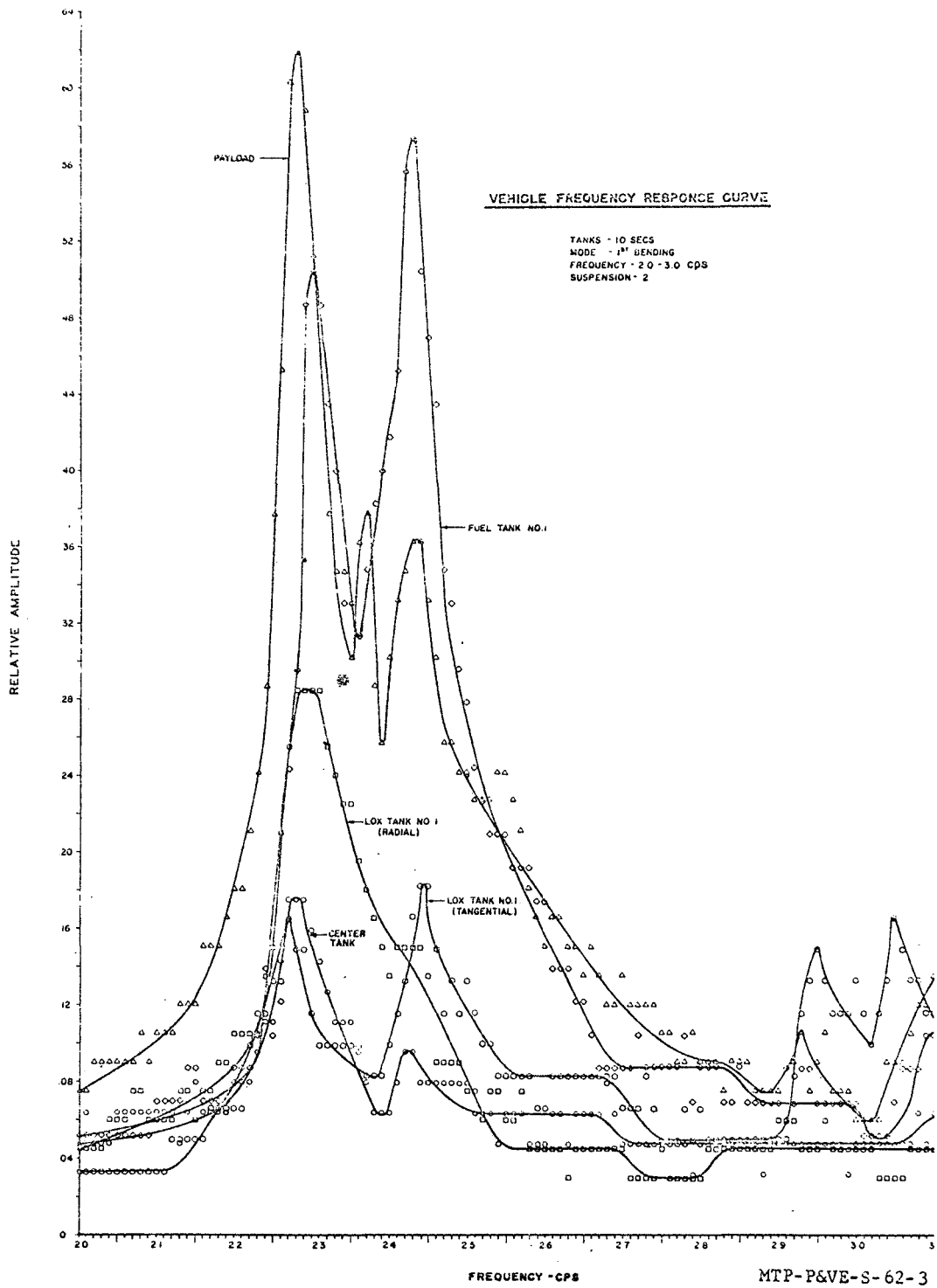
Figure B-18. Vehicle Frequency Response Curves at T = 10 sec (from Ref. B5)

105
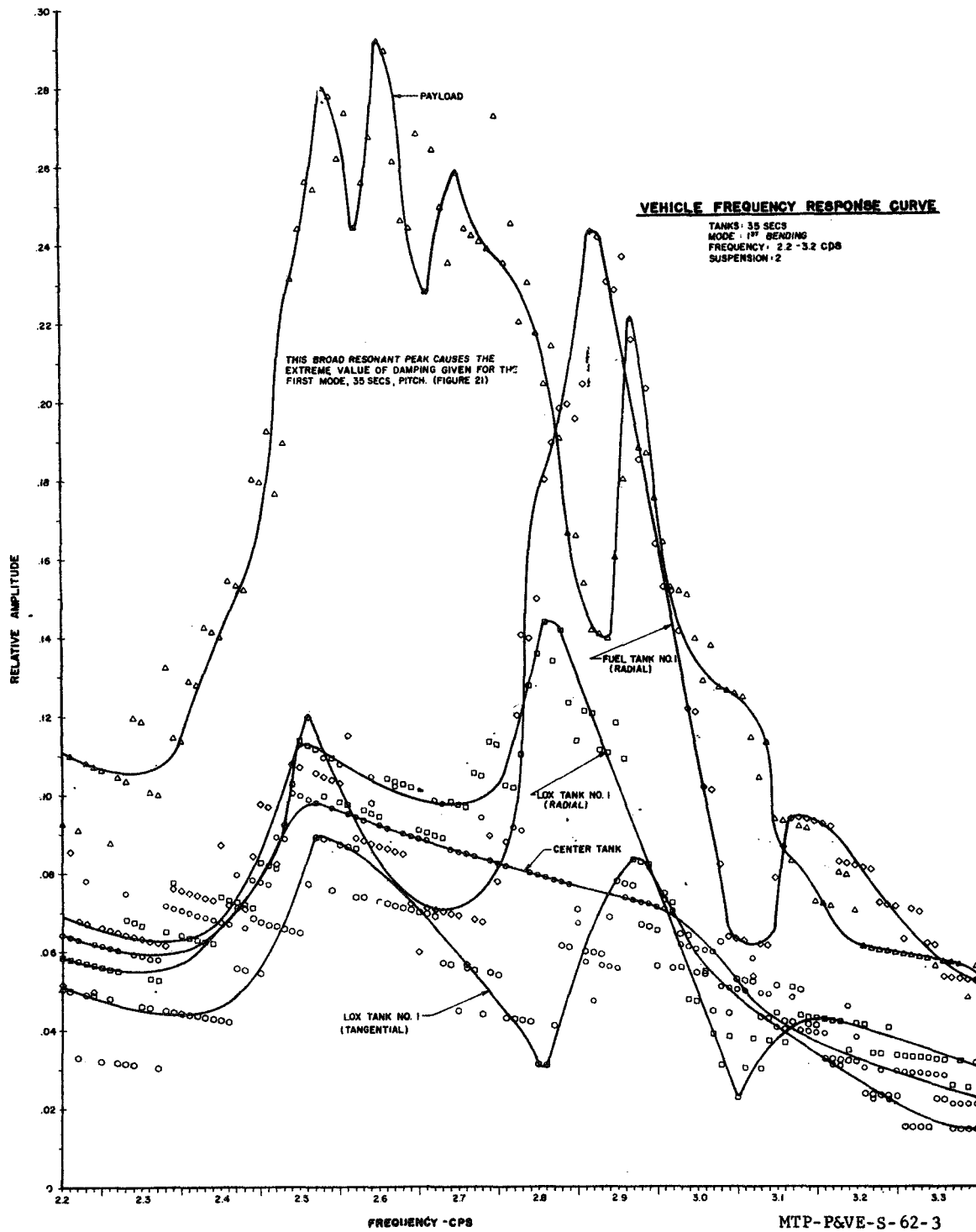
Figure B-19. Vehicle Frequency Response Curves at T = 35 sec
(from Ref. B5)
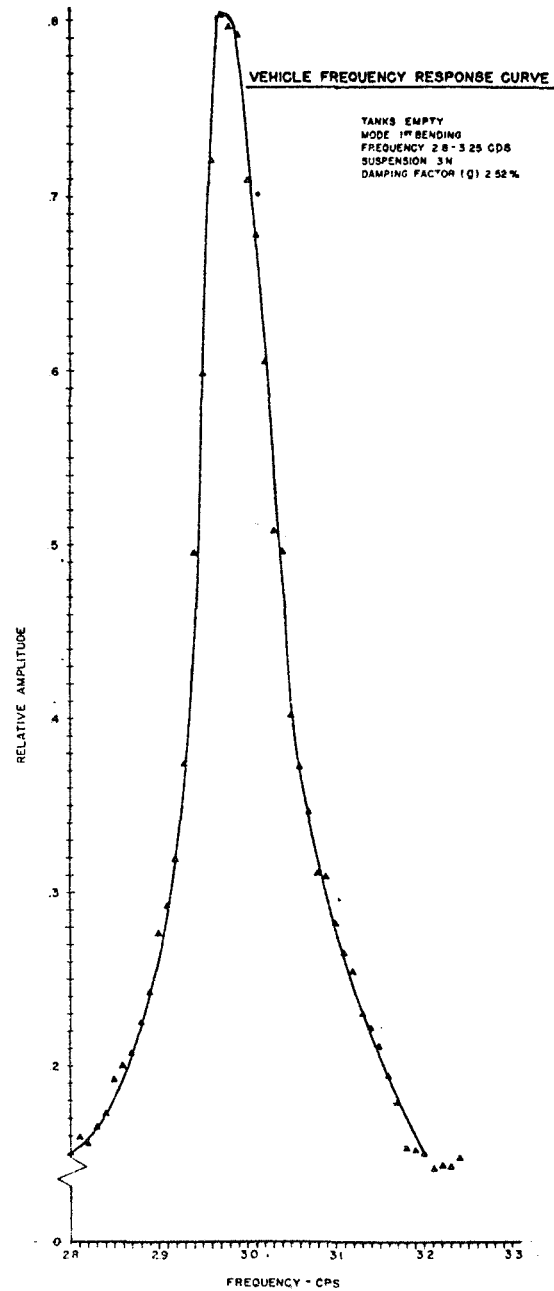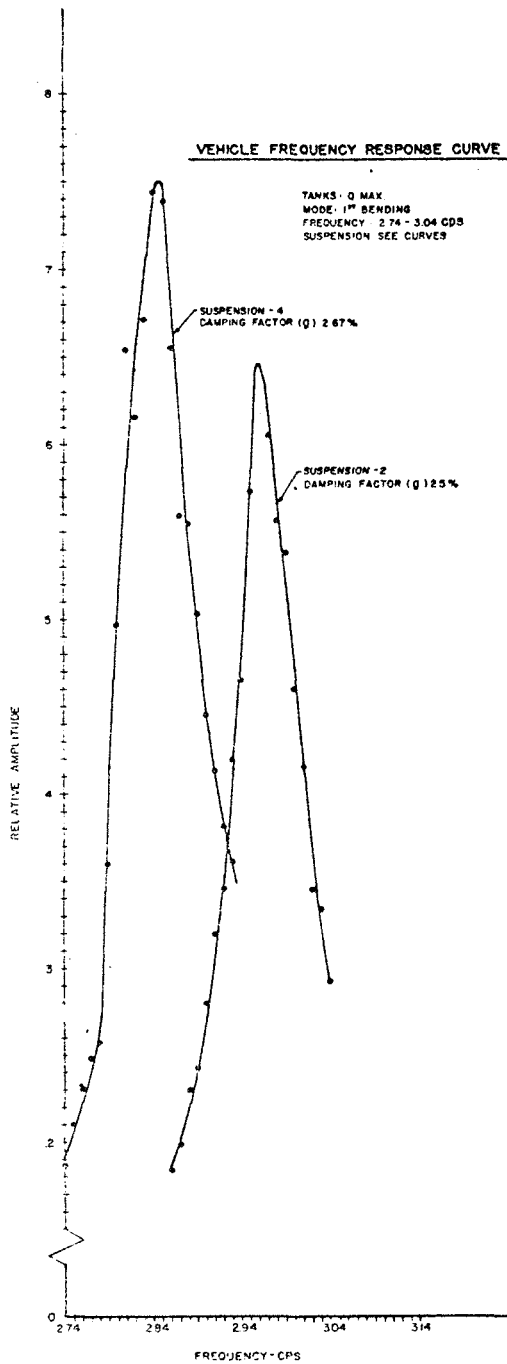
Figure B-20. Vehicle Frequency Response Curves at Q_{max} and Tanks Empty (from Ref. B5)

107
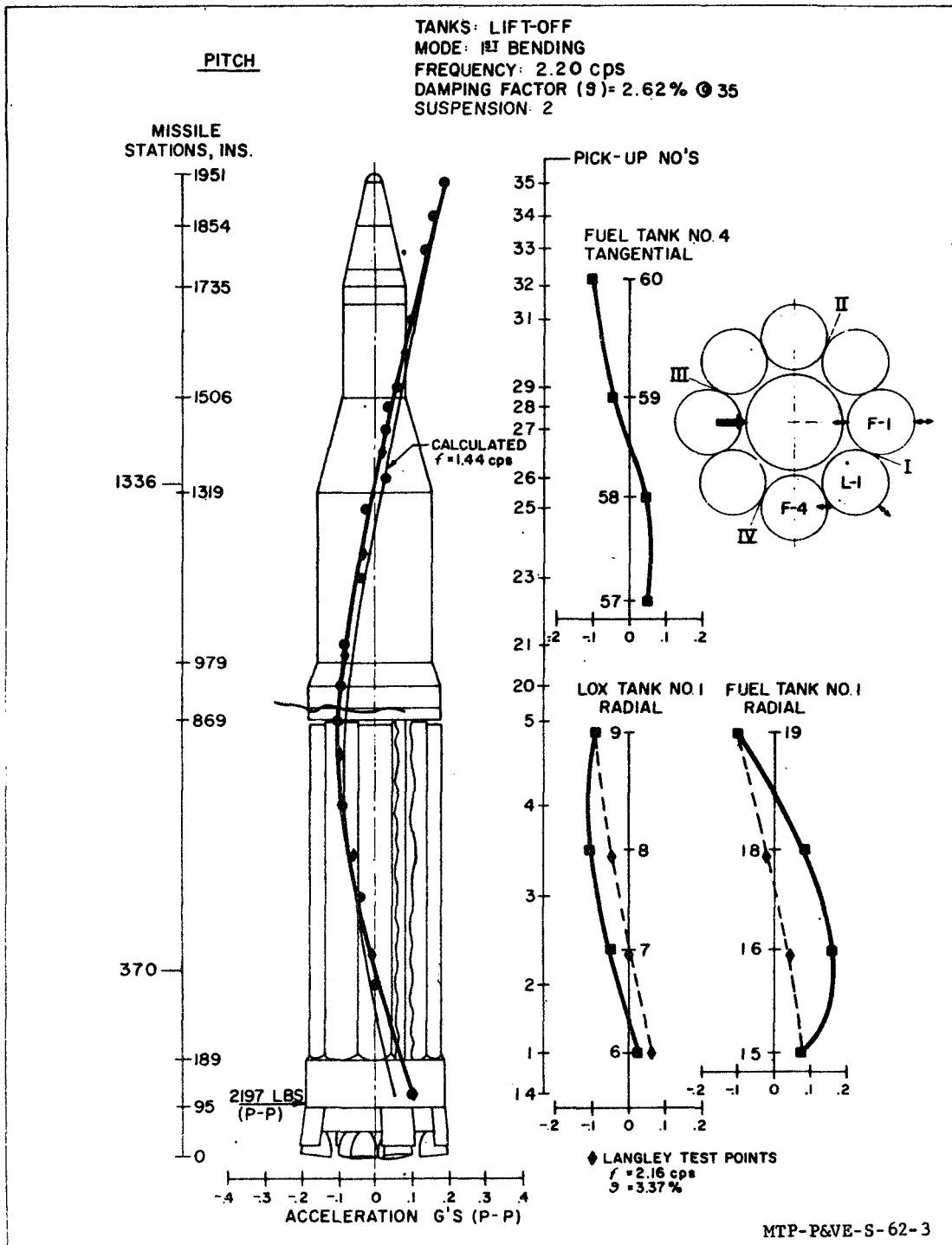
Figure B-21.   Lateral Bending Modes 1st Mode at Lift-Off
(Pitch Plane) (from Ref. B5)

108
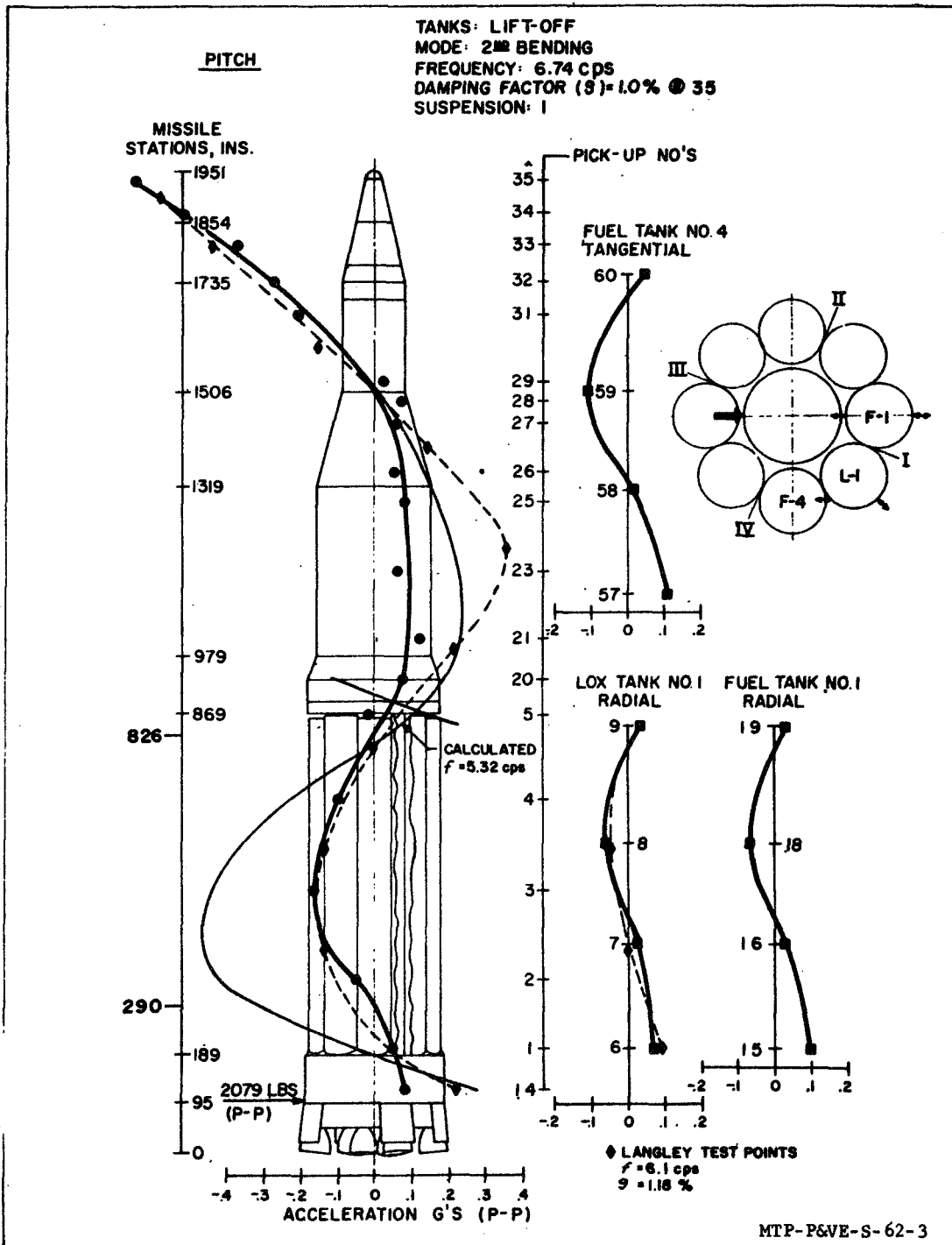
Figure B-22.   Lateral Bending Modes 2nd Mode at Lift-Off
              (Pitch Plane) (from Ref. B5)

109

TABLE B-12. DAMPING VALUES OBTAINED DURING LATERAL AND TORSIONAL EXCITATION
(from Ref. B5)

LATERAL TESTS

$$\% \text{ "g"} = 2 \frac{C}{Cc} \times 100$$

MODE	PITCH					YAW				
	L.O.	10 Sec.	35 Sec.	Q max	Empty	L.O.	10 Sec.	35 Sec.	Q max	Empty
1st	2.62	2.36	11.6[1]	2.27	2.41	4.41	6.15	3.62	2.48	5.0
2nd	1.0	--[2]	1.04	--	1.82	1.07	0.982	0.864	--	3.83
3rd	1.26	1.48	1.75	1.36	--	1.18	1.8	2.7	1.61	--
1st Cluster	2.62	4.99	2.83	2.41	--	2.99	2.0	3.71	4.5	--
2nd Cluster	2.21	2.7	2.09	1.52	--	1.8	2.14	2.5	1.9	--

NOTES:
1. See FIGURE 13. The wide band resonant peak, caused by tank coupling, causes this apparent high damping value.

2. Output is low, making damping values unreliable.

TORSIONAL TESTS

$$\% \text{ "g"} = 2 \frac{C}{Cc} \times 100$$

MODE	L.O.	35 Sec.	Q max	Empty
1st	2.76	1.64	1.58	18.0
Cluster	7.8	8.15	--	--
Engine & Cluster	--[1]	--[2]	--[2]	--

NOTES:
1. Very highly damped; difficult to obtain accurate "g" value.
2. All traces beating giving false "g" value.

110

B6. *"Space Launch Vehicle Full Scale Damping Tests", by General Dynamics Astronautics, A Division of General Dynamics Corporation, G.D.A.-63-0376, Contract AF-04/694/185, June 1963*

Purpose and Scope

The purpose of the full scale Atlas 119D and Atlas 149D Agena tests was to clarify previous tests on models, particularly the vibration damping factors. The tests encompassed several combinations of full and empty Atlas and Agena.

Test Setup and Procedure

The test specimens were the Atlas 119D and Atlas 149D in flight condition, a partially stripped Agena B, and two dummy payloads. The Atlas-Agena configuration was erected on the Pad 2 launcher. All wind screens were closed and the umbilical tower sails extended. Water was substituted for the Agena fuel and methylene chloride for the oxidizer. Additional weights were used to give a proper weight and c.g.

The vehicle was oscillated in its first natural mode of vibration and then disconnected from the excitation mechanism. The rate of decay of vibration was determined as a measure of damping except for wind and fuel slosh.

Equipment

Excitation was accomplished by a hydraulic cylinder with a feedback transducer and servovalve. A special quick releasing system permitted separation of the excitation device from the vehicle.

A Sanborn recorder system with strain gages in both x and y axes was used for both control and recording. The load cell was calibrated using a dead weight system.

Rate gyros and z-position transducer were recorded on a separate Sanborn recorder. Wind velocities and time of day were recorded on a Honeywell Visacorder. Calibration of all equipment was performed under actual conditions as far as feasible.

Readings Obtained

The strain-gages provided measurements of bending moments. The load cell system provided a measure of the axial loads to ±400 pounds total load. The rate gyros measured the bending deflections to within factory specifications of the gyros.

A study of tower deflections from wind showed the deflections measured relative to the tower would be satisfactory so deflection readings are relative to the tower. Relative peak-to-peak vibration decay curves were plotted as in Figure B-23.
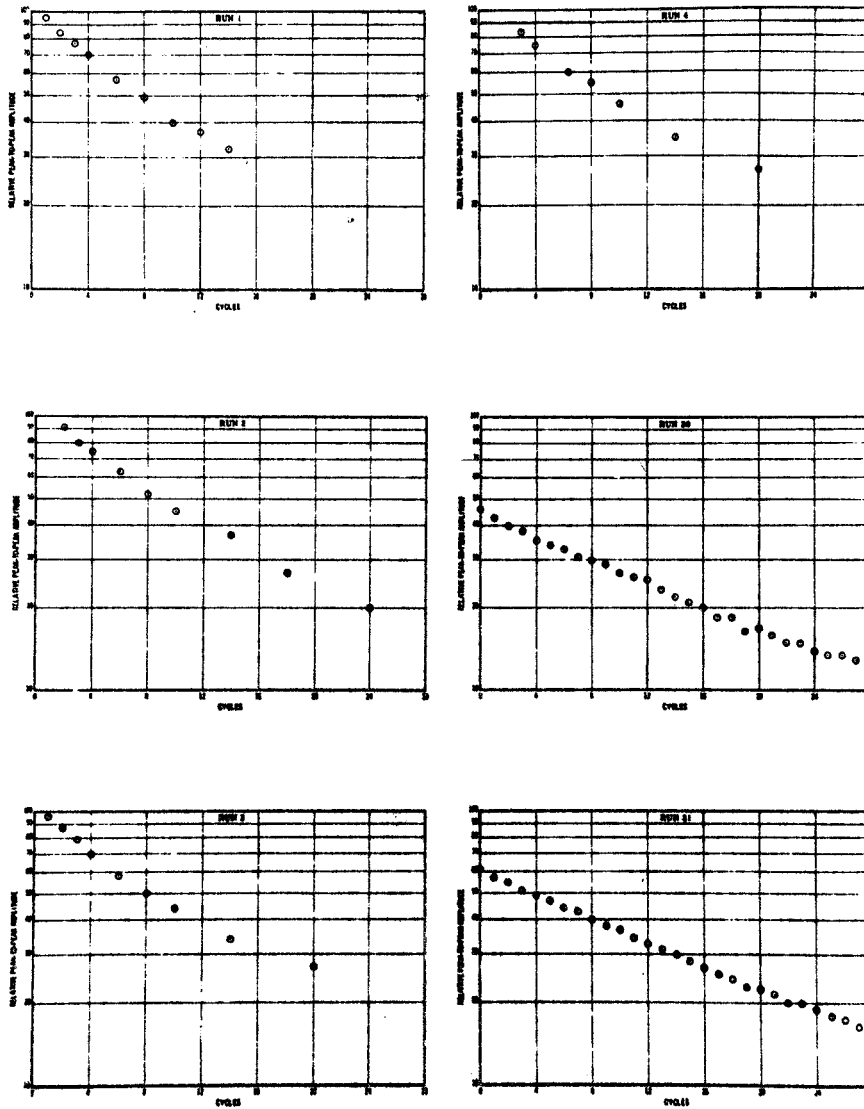
Figure B-23. Typical Plots of Data for Determination of Damping
Factors for Atlas-Agena Assembly (from Ref. B6)

Vibration Characteristics Noted

Motion of fluids inside the tanks caused considerable scatter of measured vibration amplitudes. In some cases beating occurred. Because limiting amplitudes (red line values) were quite stringent, the amplitude buildup was low with low damping values.

Comparisons Made

The relative amplitudes of the models were higher than for the full scale test so that the computed damping factors were correspondingly higher.

Damping Values Obtained

From these tests the only damping factor obtained was the logarithmic decrement. For the amplitudes developed, the decrement values ranged from about 1/2 to 2 percent of critical. The higher values pertain to higher amplitudes.

Conclusions Drawn

It is recommended that the use of a constant force exciter be considered. Thus, damping factors under beat conditions might be found.

Much more study is needed to determine vibration behavior in all tanking conditions.

B7. *Abrams, S. S. and R. F. Teuber, "Thor Delta Vibration Test", Environmental Quarterly, Douglas Aircraft Company, Inc., September 1963*

Purpose and Scope

The purpose of these tests was to help locate areas of structural discontinuity and to find structural influence coefficients. These factors will contribute to vibration analysis and make computations more reliable. The results of the tests were correlated with computed configurations and modified analytical factors and methods developed for predicting control stability and body bending modes.

Test Setup and Procedure

The 80 foot long Douglas Delta space vehicle was suspended elastically in a horizontal position from cables. The structure was vibrated with a shaped impulse controlled by a rate gyro which is in turn fed to the engine gimbals. Thus, a dynamic structural response is set up.

Equipment

The vehicle was instrumented with rate gyros, HIG (Hydraulic Input Generator), electronic feed back pots and impulse shaping networks. The outputs of the gyros and control systems were observed and recorded.

Readings Obtained

The control system information was recorded for three points on the vehicle. These records were analyzed to give values for vibration in modes of vibration, such as shown in Figure B-24.

Vibration Characteristics Noted

During initial activation of the control system, an instability developed at the second bending mode. Correction of the support bracket for the rate gyro eliminated the pitch plane instability.

Comparisons Made

The relative deflections for the measured modes were compared with preliminary computations. The computations were revised and again compared. Figure B-24 shows comparisons of computed deflections as a function of measured deflections.

Damping Values Obtained

No mention of damping is made in the article.

Conclusions Drawn

If tests had not been made, the faulty action of the rate gyro would not have been noted and proper correction made.

The test also gave bending mode data that led to a more accurate bending model that led to a more accurate bending model that will be valuable in future analyses.

B8. *Alley, V. L., Jr. and S. A. Leadbetter, "Prediction and Measurement of Natural Vibrations of Multistage Launch Vehicles", AIAA J. 1, No. 2, April 1962*

Purpose and Scope

To provide a comparison of measured vibration frequencies with prior calculated values. It was also the purpose to determine what measurable effects structural or skin joints have on the vibrational characteristics of the vehicle as a whole.

The test vehicle was made of the following rockets: first stage, Lance; second stage, Lance; third stage, Recruit; fourth stage, T55.

THIRD BODY BENDING MODE

3RD MODE FREQUENCY

PRELIM. COMP. MODE 26.1 cps
TEST MODE 19.3 cps
FINAL COMP. MODE 23.0 cps

SECOND BODY BENDING MODE

2ND MODE FREQUENCY

PRELIM. COMP. MODE 17.9 cps
TEST MODE 14.5 cps
FINAL COMP. MODE 14.7 cps

FIRST BODY BENDING MODE

1ST MODE FREQUENCY

PRELIM. COMP. MODE 4.9 cps
TEST MODE 4.5 cps
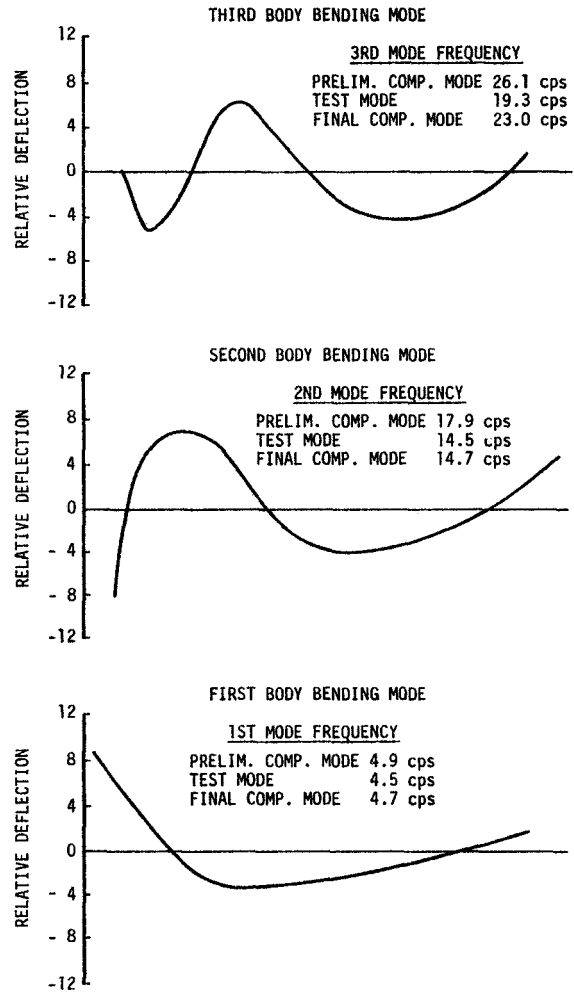FINAL COMP. MODE 4.7 cps

Figure B-24. Measured and Computed Modal Shapes for
Thor Delta (Ground Test) (from Ref. B7)

115

Test Setup and Procedure

The vehicle shown in Figure B-25 was supported in a vertical attitude by cables so as to represent free flight in one plane. An upper support composed of two spring loaded cables attached near the upper nodal point of the vehicle stabilized the vehicle in the vertical attitude. The vehicle was excited by an electromagnetic shaker connected to the vehicle 10 1/2 inches from the bottom.

The first three modes of vibration were determined and then repeated for the vehicle turned 90 degrees about the longitudinal axis of symmetry.

Measurements were made to determine joint tightness, natural frequencies at each mode of vibration, and amplitude of oscillation for several positions along the vehicle.

Equipment

Eight strain-gage accelerometers were located along the length of the vehicle. The outputs from the accelerometers were fed through amplifiers to oscillograph recorders.

The accelerometer nearest the exciter was used as a control instrument to define the amplitude of oscillation.

Readings Obtained

Readings of frequencies, amplitudes at points along the length of the vehicle, and decay of amplitude when the shaker was disconnected were recorded but were not shown in the article.

Vibration Characteristics Noted

By means of a matrix notation, the equations of motion for discrete mass representation of the vehicle parts elastically constrained were developed. The analytical results given in this report were obtained by considering 31 discrete masses.

The first three natural modes and the natural frequency of each were calculated. The relative amplitudes were also determined as shown in Figure B-26.

The effects of joint looseness (free rotation) were recognized as nonlinear but equivalent effects were obtained by assuming the joint factor K to be proportional to the inverse of the third power of the diameter.

The test results indicated that the natural frequency was dependent to a degree upon the amplitude. For small amplitudes (approximately 0.02 inches) the frequency was not significantly dependent upon the joint loosenesses obtained in the tests reported in the report. For large amplitudes (0.30 inches) the frequency appeared to be decreased and more dependent on joint looseness. Figures B-27 and B-28 show the trends.

116
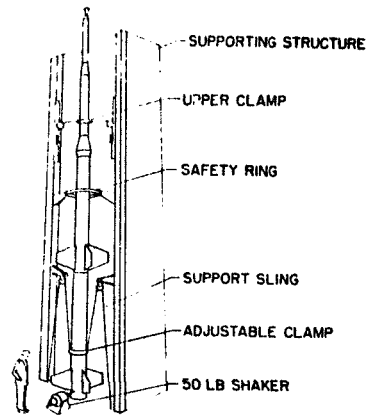
Figure B-25. Principal Features of Test Apparatus
(from Ref. B8)
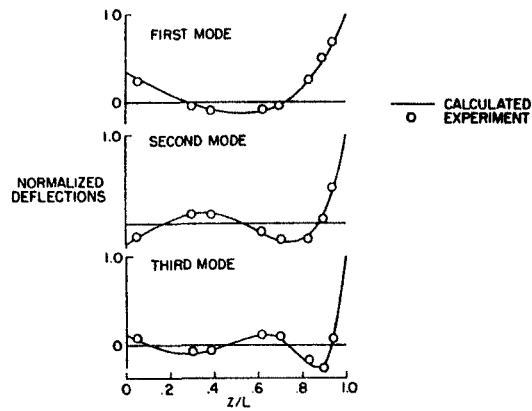
Figure B-26. Comparison of Experimental and Calculated Natural
Mode Shapes (from Ref. B8)

Comparisons Made

Figure B-26 shows a comparison between calculated and measured natural mode shapes. Other test conditions gave similar agreement as indicated in the table of Figure B-29. The greatest discrepancies occurred for the third mode.

The authors suggest that the observed variations in measured values of the natural frequencies are due to nonlinearities and the limitations of response for the recording unit.

Damping Values Obtained

The damping factor, g, was determined for the outputs during decay of oscillations. It was found to be on the order of 0.04, 0.05 and 0.06 for the first, second and third modes, respectively.

Conclusions Drawn

Among other conclusions drawn are the following:

1) The mode shapes of the first three modes were accurately predicted by the analytical procedure presented.

2) With loose interstage connections, the frequency dependency upon amplitude is typical of the nonlinear behavior associated with systems having free play.

3) The structure, although designed to be geometrically symmetrical about the longitudinal axis, showed a small but consistent difference in the vibration characteristics of the first three modes between two planes 90 degrees with respect to each other (see Figure B-29).

This unsymmetrical behavior indicates that the inherent influences of tolerances and fabrication effects might produce unpredictable variations in frequencies of several percent in theoretically similar vehicles.
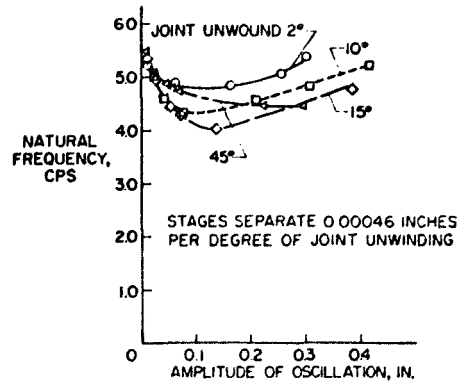
Figure B-27. Variation of Natural Frequency of First Mode with
Joint Looseness and Amplitude of Oscillation
(from Ref. B8)
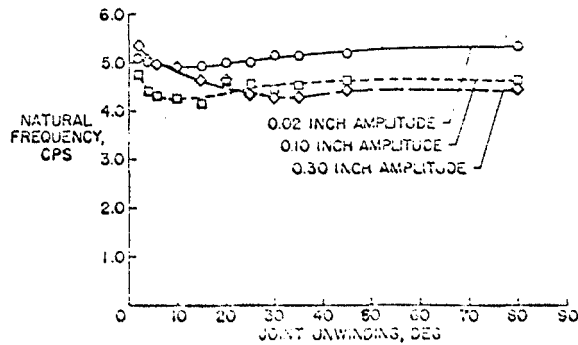
Figure B-28. Variation of Natural Frequency of First Mode with
Joint Looseness and Amplitude of Oscillation
(from Ref. B8

MODE	CALCULATED FREQUENCIES	TEST 1	TEST 2	TEST 3
		EXPERIMENTAL FREQUENCIES		
1	5.46	5.41	5.45	5.36
2	11.45	10.54	10.62	10.33
3	19.82	17.22	16.24	15.68

(ALL FREQUENCIES GIVEN IN CYCLES PER SECOND)
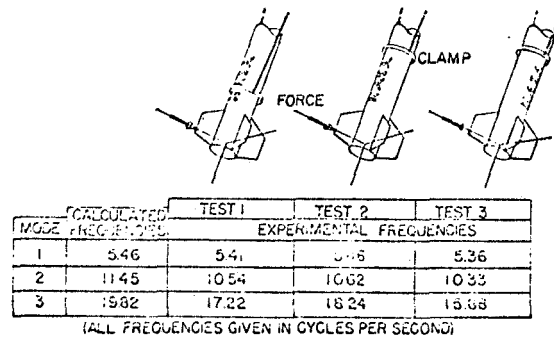
Figure B-29. Comparison of Experimental and Calculated Natural
Frequencies for Three Test Conditions for Lance
Recruit Assembly (from Ref. B8)

119/120

APPENDIX C - SCALE MODEL GROUND TEST
SUMMARY DATA SHEETS

C1. *Jaszlics, Ivan J. and George Moroson, "Dynamic Testing of a 20% Scale Model of the Titan III", Paper in AIAA Symposium on Structural Dynamics, September, 1965*

Purpose and Scope

The purpose of the test was to experimentally verify the analytical method used for vibration analysis of the Titan III.

Test Setup and Procedure

The model was constructed to simulate, to scale, the thicknesses of various parts, longitudinal members, and welded and riveted joints. The model was resiliently supported to give a free-free vibration in three dimensions. It was loaded at discrete points to simulate fuel and payloads. It was excited to give various modes of vibration in one or more dimensions. Several configurations and loadings of the model were tested.

Readings of vibration response were taken at numerous points in the planes of pitch, roll, yaw and longitudinal as well as coupled modes when they existed.

Equipment

Eight electrodynamic shakers were used to excite the model into various modes of vibration.

An extensive system of both fixed and roving vibration pickup transducers was used. The types of transducers or recorders are not given.

Readings Obtained

Readings of amplitude and frequency were made for several modes of vibration, namely, pitch, roll, yaw, longitudinal and coupled modes of two or more of these modes. The measured frequencies were apparently within ±6 percent of the calculated values for the different modes computed as indicated in Figure C-1.

Vibration Characteristics Noted

The mode shapes of the vehicle as a unit were in good agreement with the results of analytical studies.

It was experimentally confirmed that as fuel burned out with time after firing, the frequency of the transverse modes of vibration increased.

The model tests gave a much more complete coverage of vibration behavior than the analytical studies as indicated by Figure C-2.

121
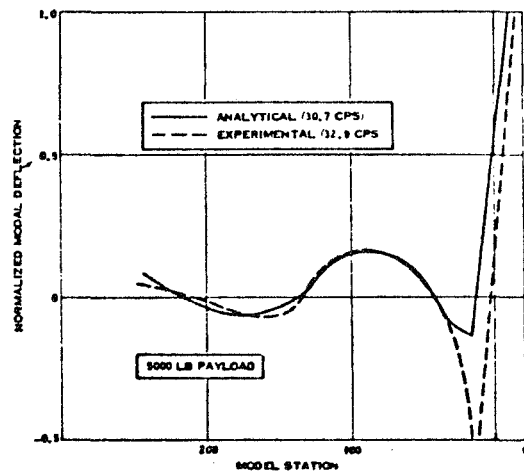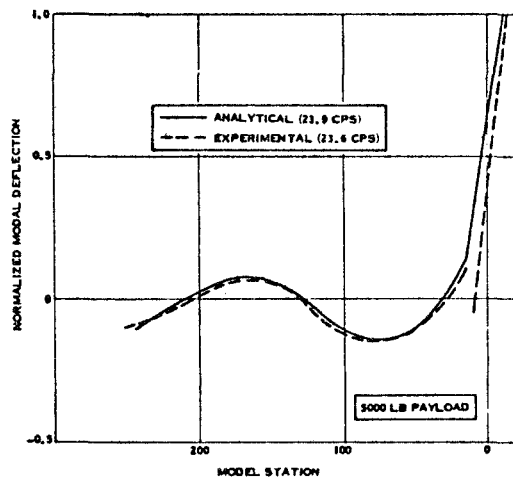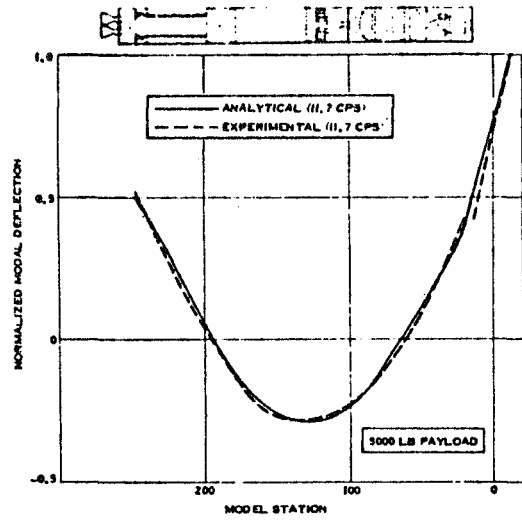
Figure C-1. Measured and Computed Lateral Mode Shapes for Titan III
in Vibration (from Ref. C1)

Comparisons Made

The analytical modes and the model modes agreed very well with the limited results obtained from flight tests.

It was pointed out that damping, particularly for transverse vibration, obtained from the model would probably not be applicable to that for the prototype because of deviations in details such as the lack of insulation in the model.

Damping Values Obtained

Damping values for vibration of the model for both longitudinal and transverse or lateral vibration are given in Figure C-3. The measured damping for lateral vibration is definitely less than the measured values for longitudinal modes. However, there was no discussion as to how these values were obtained.

Conclusions

The author points out three advantages of model testing, namely

1) Model testing permits a vibration survey before the full scale vehicle is built.

2) A number of test conditions with several fuel and payloads can be tested.

3) It is easier to establish a free-free vibration for the model than for a full scale ground test.

The authors conclude that the modes and frequencies of the vibration of the model are in good agreement with the full scale ground test and flight test.

They also conclude that to provide adequate high fidelity, scaling the model should be somewhere on the order of 25-40 feet and this appears more important than the scale factor.

C2. *Mixson, John S., John J. Catherin and Ali Arman, "Investigation of the Lateral Vibration Characteristics of a 1/5 Scale Model of Saturn SA-1", Langley Research Center, NASA TN-D-1593, January 1963*

Purpose and Scope

The purpose of this investigation was to determine the vibration characteristics of a 1/5 scale replica of a Saturn vehicle. The results of this test provide data which are compared with full scale tests to establish the validity of model tests.

Future comparisons of the data obtained from these tests with data obtained from full scale tests will allow more detailed conclusions to be drawn.

Tests were made on the first stage, the upper stages and the total vehicle.

123
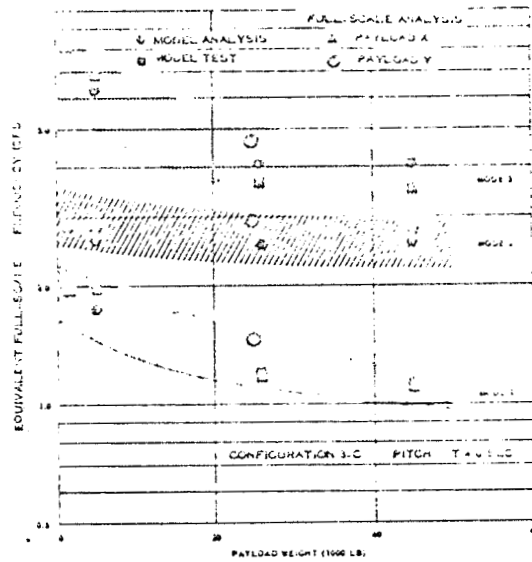
Figure C-2. Comparison of Full-Scale Analyses and Model Frequency
Data (from Ref. C1)
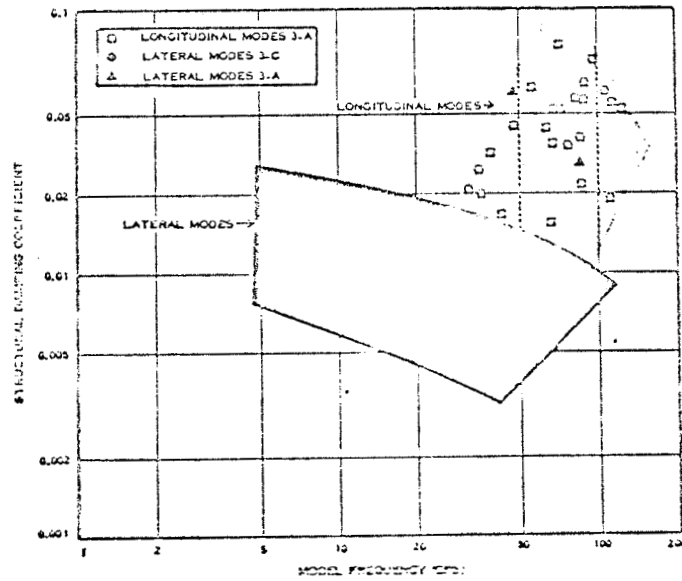
Figure C-3. Summary of Modal Damping Data - Titan III, 1/5
Scale Model (from Ref. C1)

124

Test Setup and Procedure

Figure C-4 shows the general configuration, dimensions and nomenclature of the 1/5 scale model of Saturn SA-1. It was suspended in a simulated free-free condition in the vibration test tower. Water was used in place of the fuel and lox.

The weight, center of gravity, and stiffness were all determined prior to test.

The model was suspended on a two-cable system. The weight was transferred through outtriggers by a yoke attached to two vertical cables supported on rollers at the top of the tower. Turnbuckles were provided for adjustments to account for shift of c.g.

Some of the frequencies were materially affected by the adjustments. Before starting the test, the booster and third stage tanks were pressurized and the pressures maintained throughout the tests.

The system was excited by electromagnetic shakers. For most tests a single shaker was used but two shakers, one at Station 24 and one at Station 345 were used with different amounts of "out of phase" shaking.

Deflections and frequencies were obtained from accelerometers strategically located on the skin of the model.

For each weight configuration the first step of the test was a frequency sweep with a constant shaker force.

Equipment

In addition to the fixed accelerometers, a portable pickup was used. Accelerometer output was fed through carrier amplifiers and recorded on an oscillograph. Strain gages were placed around the periphery of the midsection.

Readings Obtained

The frequency sweep graphs served as a basis of determining maximum model response under subsequent sustained vibration at peak frequencies. Readings to serve for damping decrements were obtained by instantaneously cutting the input to the shaker. Plots of decaying amplitude were made on semilogarithmic paper. Tables C-1 and C-2 show typical tabulated results.

Vibration Characteristics Noted

Response frequencies of vibrations ranged from about 5 Hz to about 90 Hz for these tests. For the tanks about half full (considered representative of all water levels) there were eight major response peaks whereas only three calculated natural frequencies occurred in this band. Figure C-5 is a typical response curve during a sweep test. The first bending mode showed remarkable agreement between

125

Model station, in.

388.6 ──────

Payload nose cone

347.0 ──────
344.6 ──────

Third-stage water ballast tank, 24-inch diameter

301.2 ──────
290.3 ──────

Third-stage adapter structure

271.9 ──────
263.8 ──────

Second-stage outer shell, 44-inch diameter

Second-stage water ballast tank, 22-inch diameter

206.6 ──────
195.9 ──────

Second-stage adapter structure

177.9 ──────

Spider beam

Booster tanks, 52 inches overall diameter

37.9 ──────
21.0 ──────

Corrugated barrel and outrigger structure

Engines

0 ──────

Figure C-4. General Configuration, Dimensions, and Nomenclature of 1/5-Scale Model of Saturn SA-1 (from Ref. C2)

126
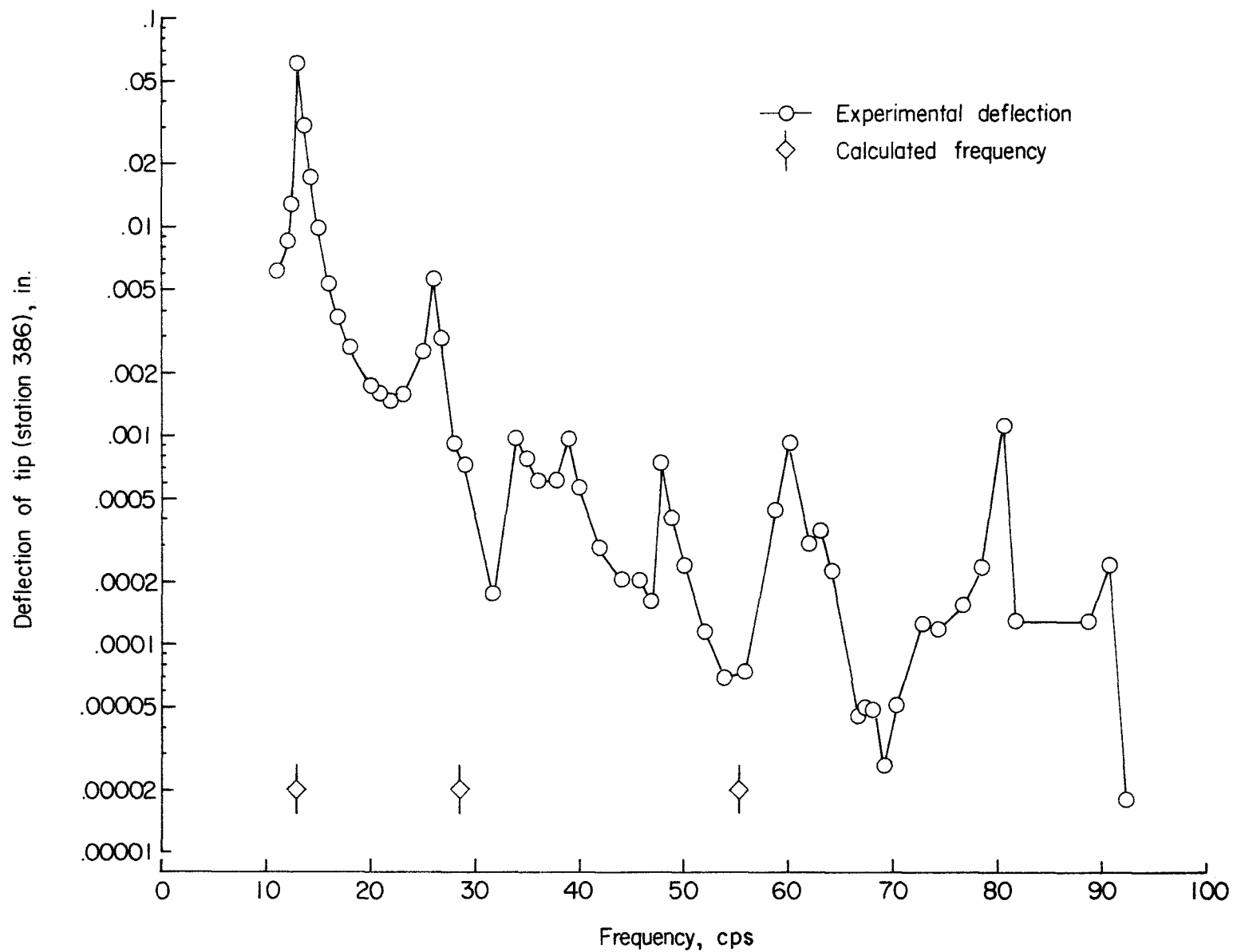
Figure C-5. Variation of Tip Deflection (Station 386) with Shaker Frequency. Booster Tanks 48 Percent Full; Force, 22.5 Vector lb when Frequency < 65 cps and 13.5 Vector lb when Frequency > 65 cps (from Ref. C2)

TABLE C-1. NORMALIZED SECOND CLUSTER MODE SHAPE FOR BOOSTER 75 PERCENT FULL
(from Ref. C2)

[Frequency, 27.6 cps; amplitude, 0.40G peak-to-peak at station 386]

Force input:
  Shaker 1 at station 24, 15 vector lb

Damping at station 386:
  When $x_0(G) = 0.34$, $g = 0.022$
  When $x_0(G) = 0.175$, $g = 0.016$

(a) Main structure[a]

Station	Deflection	Station	Deflection
386	1.00	235	-0.07
385	.84	225	-.09
375	.85	215	-.12
365	.73	207	-.40
355	.62	205	-.16
346	.52	194	-.38
341	.46	184	-.34
335	.45	180	-.18
325	.33	178	-.09
315	.20	164	-.15
306	.11	144	.19
304	.08	113	.67
295	-.03	84	.73
285	-.06	54	.39
275	-.07	35	-.07
265	-.12	29	-.17
255	-.04	24	-.32
245	-.04		

[a]Main structure includes third stage, second-stage outer shell, booster center lox tank, and barrel.

128

TABLE C-2. NORMALIZED SECOND BENDING MODE SHAPE FOR BOOSTER 75 PERCENT FULL (from Ref. C2)

[Frequency, 36.9 cps; amplitude, 0.36G peak-to-peak at station 386]

Force input:
Shaker 1 at station 24, 15 vector lb

Damping at station 207:
When $x_0(G) = 0.09$, g = 0.039
When $x_0(G) = 0.026$, g = 0.019

(a) Main structure[a]

Station	Deflection	Station	Deflection	Station	Deflection
386	1.00	282	0	184	0.20
385	1.27	275	.13	180	.25
375	.97	265	.13	176	.53
365	.88	255	.34	164	.41
355	.71	245	.44	144	.55
346	.59	235	.41	113	.61
341	.47	225	.44	84	.29
335	.53	215	.59	54	-.22
325	.34	207	-.32	35	-.52
315	.20	205	.51	29	-.52
306	.26	194	.16	24	-.47

[a]Main structure includes third stage, second-stage outer shell, booster center lox tank, and barrel.

(b) Booster outer tanks

Station	Normalized deflection for tank -							
	1	2	3	4	5	6	7	8
38	-0.62	-0.57	-0.55	-0.22	-0.49	-0.66	-0.85	-0.73
58	-.46	-.44	-.51	-.14	-.53	-.52	-.73	-.53
78	-----	-.16	-1.09	-----	-2.01	-----	-.27	-.26
98	.29	.31	.79	.20	2.53	.37	.62	.35
118	.53	.59	1.13	.25	1.82	.64	1.08	.73
138	.71	.63	1.19	.25	-----	.70	1.04	.70
158	.63	.60	.90	.15	.77	.56	1.01	.58
173	.55	.55	.61	.16	.58	.48	.72	.50
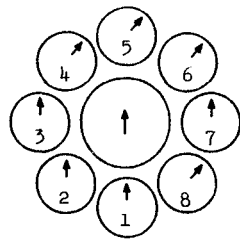
Booster cross section - station 120
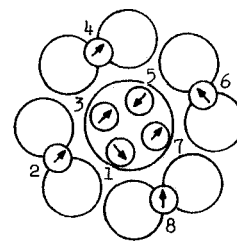
Engine motion - station 0

(c) Engines

Station	Normalized deflection for engine -							
	1	2	3	4	5	6	7	8
0	-3.41	1.27	2.91	1.27	-1.59	2.47	3.01	4.66
10	-1.46	-.35	2.34	2.09	-.89	2.23	2.49	5.54
20	-.55	-.23	.36	-.44	-.40	.26	.42	-.83

129

measured and computed deflections as is shown in Figure C-6. Other configurations showed a more complicated behavior as shown in Figure C-7. No typical decay curves are shown.

Comparisons Made

Comparisons were made between calculated and measured frequencies. Whereas there were three calculated natural frequencies within the test range of 5 to 90 Hz, a total of eight response peaks were measured.

The calculated deflections for the first bending mode of vibration agreed remarkably well with measured values.

Other calculated values could not be compared with measured results.

Damping Values Obtained

Table C-3 shows a summary of resonant frequencies and damping factor "g" for various modes and water levels in the tanks.

Conclusions Drawn

1) The number of resonant frequencies obtained on the model is significantly greater than the number calculated.

2) The mode shapes associated with the additional frequencies have shown significant independent behavior of the tanks in the clustered booster.

3) In calculation frequencies and modes of vibration, each tank must be considered independently.

C3. *Mixon, John S. and John J. Catherine, "Experimental Lateral Vibration Characteristics if a 1/5 Scale Model of Saturn SA-1 with an Eight Cable Suspension System", Langley Research Center, NASA TN-D-2214, November 1964*

Purpose and Scope

The scope of these tests was to determine the transverse vibration characteristics of the model suspended in a simulated "free-free" condition and to compare these characteristics for various modifications of the support mechanisms. The purpose was to determine the feasibility of using dynamically scaled models to obtain vibration data for use in the design of complex launch vehicle structures and control systems.

Test Setup and Procedure

The model was mounted in a vertical position on an eight cable and spring suspension system. The arrangement was so organized that two or more of the cables could be used without involving the unused ones. Link suspension was also used.

130
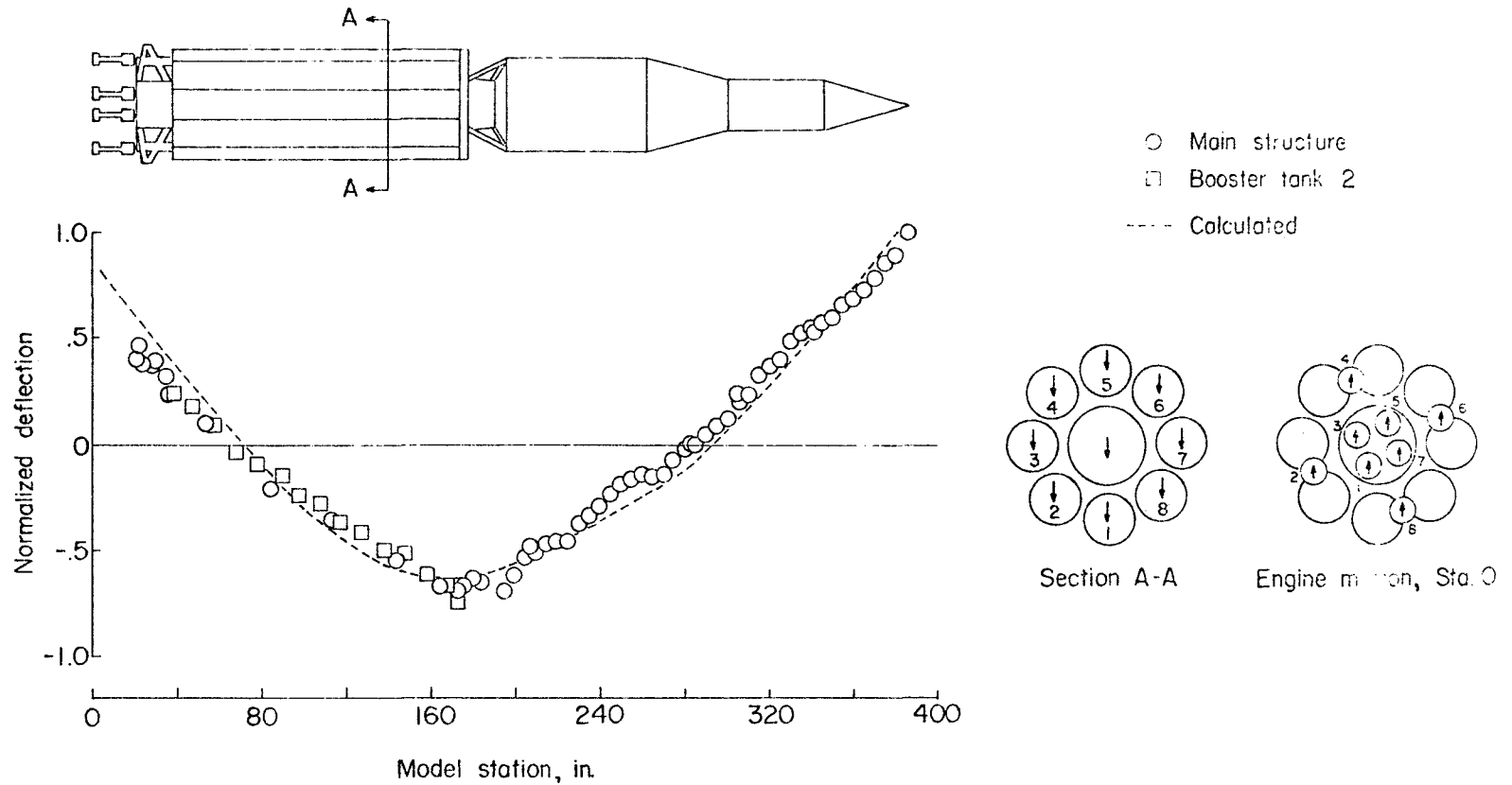
Figure C-6.   First Bending Mode of 1/5-Scale Saturn.   Booster Tanks 48 Percent
Full; Frequency, 13.0 cps; Damping at Station 386:   when $x_0(G)$ = 0.43,
g = 0.032 and when $x_0(G)$ = 0.178, g = 0.17 (from Ref. C2)
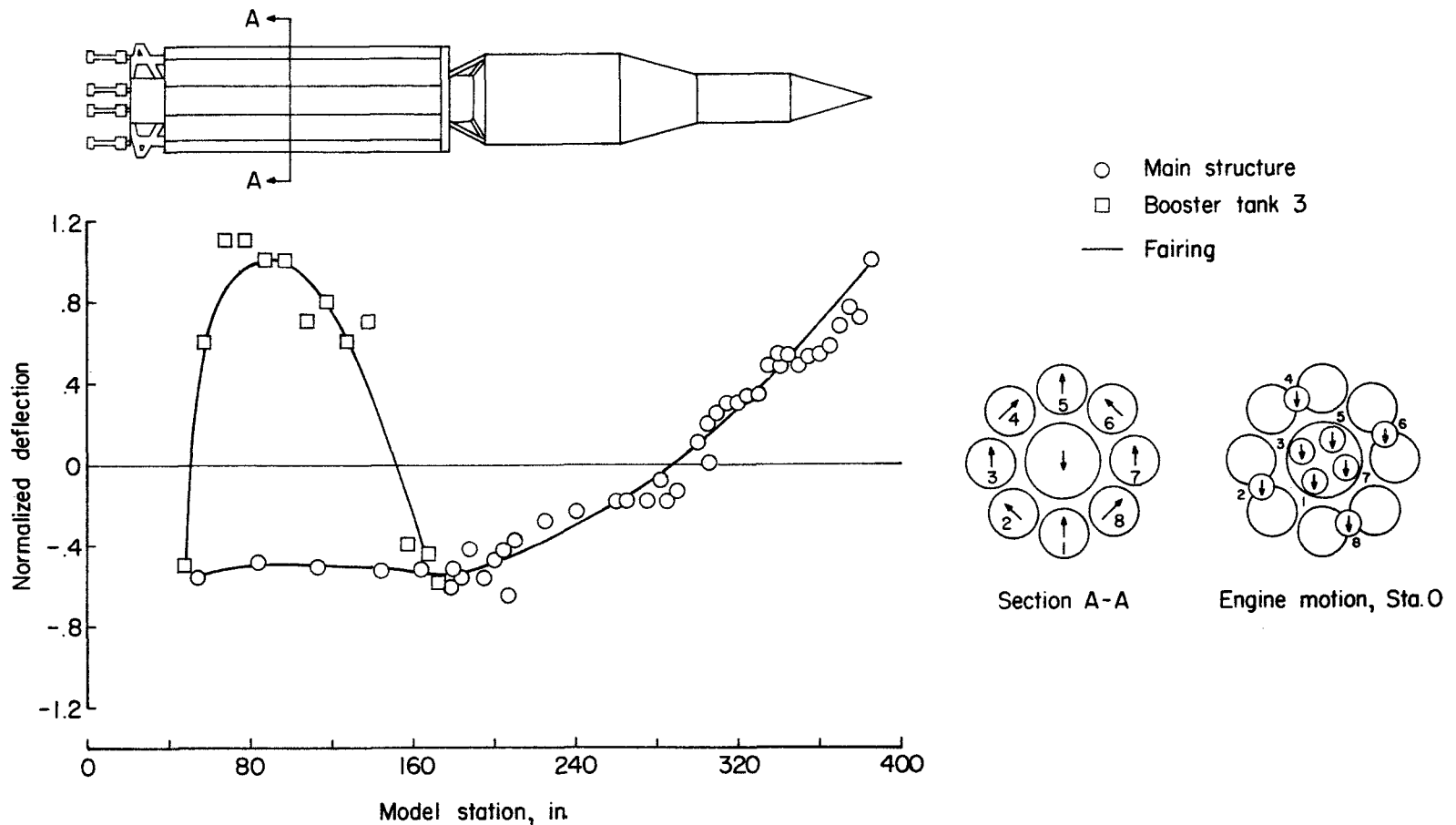
Figure C-7. First Cluster Mode of 1/5-Scale Saturn. Booster Tanks 48 Percent Full; Frequency, 26.0 cps; Damping at Station 164: when $x_0(G) = 0.078$, $g = 0.23$ and when $x_0(G) = 0.032$, $g = 0.011$ (from Ref. C2)

TABLE C-3. SUMMARY OF RESONANT FREQUENCIES AND ASSOCIATED DAMPING
FOR 1/5-SCALE MODEL (from Ref. C2)

Mode	0 percent full (burnout)		25 percent full		48 percent full (maximum dynamic pressure)		75 percent full		100 percent full (lift-off)	
	Frequency, cps	Damping, g	Frequency, cps	Damping, g	Frequency, cps	Damping, g	Frequency, cps	Damping, g	Frequency, cps	Damping, g
Outer fuel tank	----	----------------	----	-----	----	----------------	----	-------------	9.1	----------------
First bending	13.4	0.030 and 0.017	13.6	0.052	13.0	0.032 and 0.017	12.1	0.020	10.5	0.033 and 0.025
First cluster	----	----------------	----	-----	26.0	.023 and .011	20.8	.025 and .015	18.4	.017
Second cluster	----	----------------	----	-----	33.9	----------------	27.6	.022 and .016	24.0	.014
Second bending	44.7	.046 and .032	44.6	-----	38.9	----------------	36.9	.039 and .019	30.6	.010
Third bending	----	----------------	----	-----	47.8	.017	----	-------------	----	----------------
Fourth bending	----	----------------	----	-----	60.0	.011 and .007	----	-------------	----	----------------

The model was excited to vibrate in either one or a combination of natural modes by means of a vibrator attached at a strategic point. The frequency of excitation was gradually increased until resonant response was obtained. Readings of acceleration, stress, and displacement were recorded for various inputs. Figure C-8 shows schematically the location of the shaker and accelerometers.

Equipment

An electromagnetic shaker having a capacity of 50 vector pounds of force was used to vibrate the model.

Vibration deflections, frequencies and damping of the model were determined from unbonded strain-gage accelerometers having natural frequencies ranging from 90 to 300 Hz and a damping factor of about 2/3 critical damping.

Fixed accelerometers were mounted at several points and movable accelerometers with vacuum attachmets at other points. The accelerometer outputs were recorded on an oscillograph. Additional strain gages were used to determine the static longitudinal load.

Readings Obtained

Readings of accelerations, displacements of station 62 and at station 385 as indicated in Figure C-8 were recorded and compared. Values were recorded for various liquid levels in the booster tanks as well as for various support details.

Vibration Characteristics Noted

Table C-3 shows the general frequencies and damping capacities derived from the above readings. The variations of damping coefficient

$$g = \frac{1}{n\pi} \ln \frac{x_0}{x_n}$$

with the support details for various modes of vibration are given in Table C-4. The variations of frequency with the liquid level in the booster are shown in Figure C-9.

It was noted that the damping coefficient, g, was higher for large amplitudes and lower for small amplitudes.

Comparisons Made

It was noted that more modes of vibration were obtained with the three cable suspension than for the two cable suspension. No comparisons are made with flight tests.

134
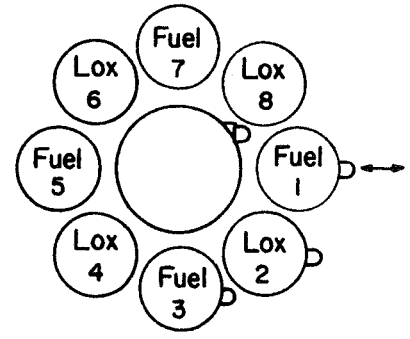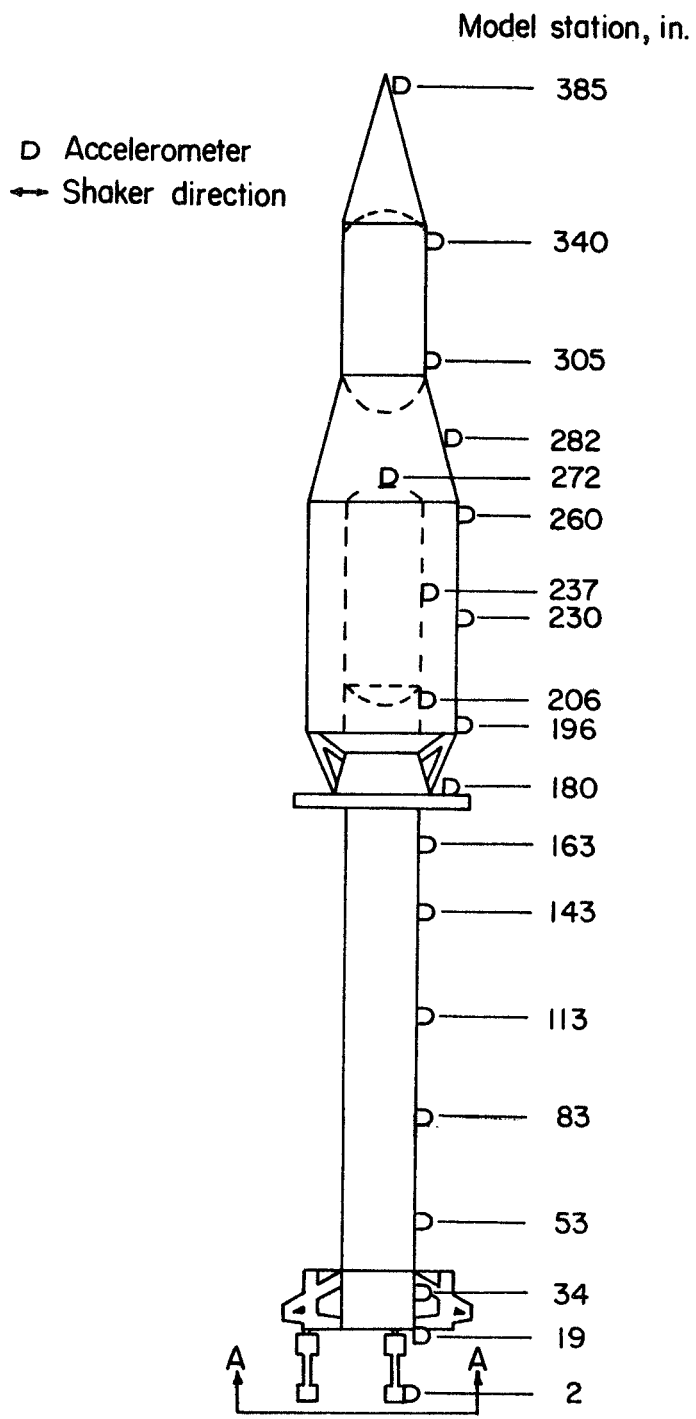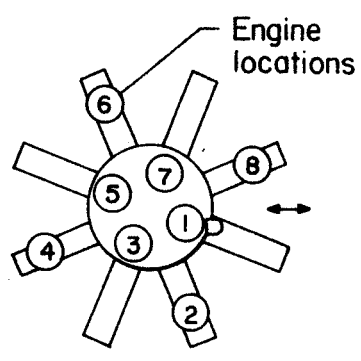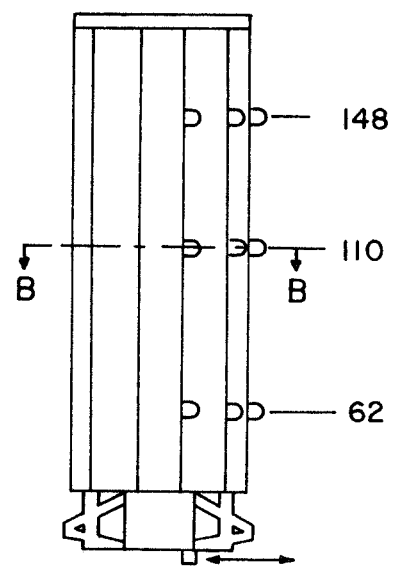
Figure C-8. Location of Accelerometers on 1/5-Scale Saturn Model for Tests with the Eight-Cable Suspension (from Ref. C3)

Figure C-9. Variation of Resonant Frequencies of the 1/5-Scale Saturn Model with Booster Water Level (from Ref. C3)

TABLE C-4. SUMMARY OF FREQUENCIES AND DAMPING OF THE 1/5-SCALE SATURN MODEL WITH THE EIGHT-CABLE SUSPENSION SYSTEM (from Ref. C3)

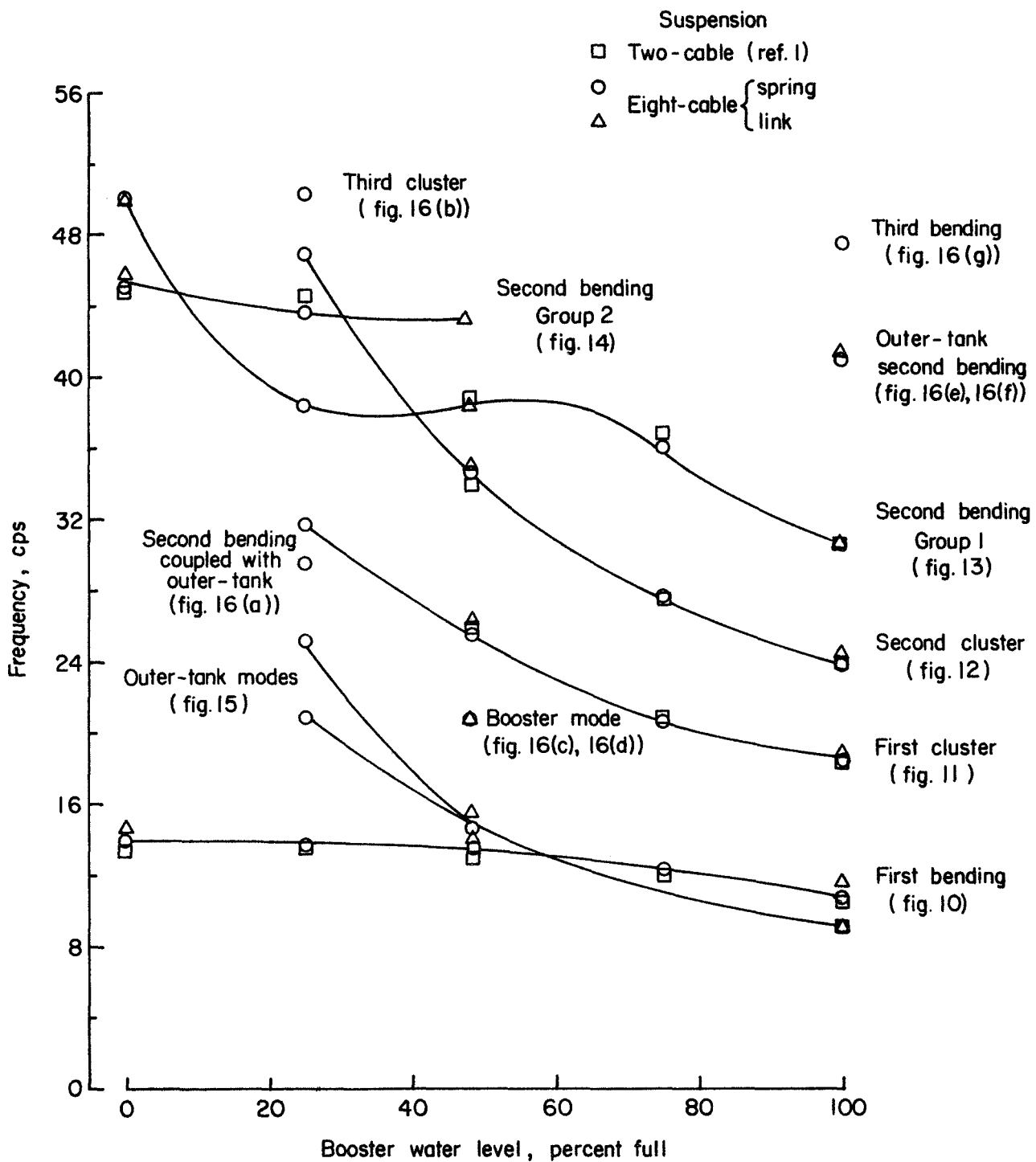| Mode	Booster, empty				Booster, 25 percent full		Booster, 48, percent full				Booster, 75 percent full		Booster, 100 percent full			
	Frequency, cps		Damping, g		Frequency, cps	Damping, g	Frequency, cps		Damping, g		Frequency, cps	Damping, g	Frequency, cps		Damping, g	
	Spring	Link	Spring	Link	Spring suspension		Spring	Link	Spring	Link	Spring suspension		Spring	Link	Spring	Link
Fuel tank no. 1	----	----	------------	------	25.2	0.006	----	----	-------------	-------------	----	--------------	9.1	9.1	------	0.01
First bending	14.0	14.7	*0.032, 0.015	0.03	13.8	*.029, .016	13.6	14.1	*0.030, 0.013	*0.033, 0.012	12.3	*0.037, 0.015	10.7	11.7	0.030	.01
First bending and outer tank	----	----	-------------	-----	21.0	------------	14.7	15.5	--------------	--------------	----	--------------	----	----	------	-----
Booster	----	----	-------------	------	----	------------	20.8	20.8	--------------	--------------	----	--------------	----	----	------	-----
First cluster	----	----	-------------	------	31.8	------------	25.5	26.3	--------------	*.030, .013	20.8	--------------	18.7	18.9	------	-----
Second cluster	----	----	-------------	------	47.0	.013	34.7	35.0	--------------	--------------	27.7	.012	23.9	24.6	.015	.018
Second bending	45.1	45.8	*.026, .011	.024	38.5	------------	----	38.5	--------------	--------------	36.2	.017	30.8	30.8	------	-----
Second bending	50.1	50.0	-------------	------	43.7	------------	----	43.4	--------------	--------------	----	--------------	----	----	------	-----
Second bending and outer tank	----	----	-------------	------	29.6	.029	----	----	--------------	--------------	----	--------------	----	----	------	-----
Outer tank second bending	----	----	-------------	------	----	------------	----	----	--------------	--------------	----	--------------	41.1	41.5	------	-----
Third bending	----	----	-------------	------	----	------------	----	----	--------------	--------------	----	--------------	47.5	----	------	-----
Third cluster	----	----	-------------	------	50.4	------------	----	----	---------------	--------------	----	--------------	----	----	------	-----

*The large value of g was measured for large values of decaying amplitude; the small value of g was measured for smaller amplitudes.

137

Damping Values Obtained

In general the measured damping coefficient, g, ranged from about 0.01 to about 0.05. The value of g tended to increase as the amplitude of vibration increased. Tables C-4 and C-5 give detailed values.

Conclusions Drawn

The lowest natural frequencies occurred with the two cable-spring support system.

Higher frequency modes of vibration were not affected by the support system used.

The model showed about the same damping coefficients with both two cable and eight cable supports.

Higher amplitudes of vibration gave higher damping factors.

C4. *Mixon, John S. and John J. Catherine, "Comparison of Experimental Vibration Characteristics Obtained from a 1/5 Scale Model and from a Full-Scale Saturn SA-1", Langley Research Center, NASA TN-D-2215, November 1964*

Purpose and Scope

The purpose of this report is to present comparisons of the bending vibration characteristics of the 1/5 scale Saturn model with those of the full-scale Saturn SA-1 vehicle. The data on which the comparisons are based are presented in separate reports on the 1/5 scale model and on the full scale vehicle.

A brief description is given of the full scale Saturn vehicle, the 1/5 scale model and the scaling concepts employed in the design and test of the model.

Test Setup and Procedure

Test setup and procedure are given in the separate report, NASA TN-D-2214. Figures showing the full scale vehicle ready for test and a schematic of the 1/5 scale model are shown in other reports.

Equipment

No equipment has been used in addition to that used in the ground tests of the 1/5 scale model and the full scale vehicle.

Readings Obtained

The readings used were those of the test of the model and of the full scale vehicle plus data from another study. These other data were obtained from an unpublished report of D. G. Douglas of the Marshall Space Flight Center on the linearity of the response of the full-scale Saturn vehicle.

138

TABLE C-5. COMPARISON OF DAMPING OF 1/5-SCALE SATURN MODEL WITH TWO-CABLE
AND EIGHT-CABLE SUSPENSIONS (from Ref. C3)

$$\left[\text{Values given are for } g = \left(\frac{1}{n\pi}\right)\log_e \frac{x_o}{x_n}\right]$$

page-left margin

139

		Booster, empty (burnout)	Booster, 25 percent full	Booster, 48 percent full (maximum Q)	Booster, 75 percent full	Booster, 100 percent full (liftoff)
First bending mode						
Two-cable Eight-cable:	Spring Link	*0.030, 0.017 *.032, .015 .030	0.050 *.029, .016 -------------	*0.032, 0.017 *.030, .013 *.033, .012	0.020 *.037, .015 -------------	*0.033, 0.025 .030 .01
First cluster mode						
Two-cable Eight-cable:	Spring Link	------------- ------------- -------------	------------- ------------- -------------	*0.023, 0.011 ------------- *.030, .013	*0.025, 0.015 .021 -------------	0.017 ------------- -------------
Second cluster mode						
Two-cable Eight-cable:	Spring Link	------------- ------------- -------------	------------- 0.013 -------------	------------- ------------- -------------	*0.022, 0.016 .012 -------------	0.014 .015 .018
Second bending mode						
Two-cable Eight-cable:	Spring Link	*0.046, 0.032 *.028, .011 .024	------------- ------------- -------------	------------- ------------- -------------	*0.039, 0.019 .017 -------------	------------- ------------- -------------

*The large value of g was measured for large values of decaying amplitude; the small value of g was measured for smaller amplitudes.

Vibration Characteristics Noted

The vibration of the 1/5 scale model vehicle exhibited nonlinear characteristics somewhat more pronounced than did the full scale Saturn vehicle as indicated for comparable frequencies in b and c of Figure C-10.

In a number of instances the model exhibited sharply defined differences in detailed vibration from the full scale vehicle. Illustrative of this is Figure C-11.

Comparisons Made

1) The model and full-scale first bending mode frequency parameters are in good agreement.

2) For most modes the damping of the model is of the same order of magnitude as the damping of the full scale Saturn.

3) The mode shapes of the model in the first bending, first first cluster and second cluster are in agreement with the full scale mode shapes. Sharp differences in details of the second bending mode shapes are believed to be caused by structural differences.

4) Both model and full scale vehicles exhibited a nonlinearity of the first bending mode response.

Damping Values Obtained

Table C-6 gives comparisons of the logarithmic damping decay factor, g, for the model and full scale vehicles for various types of supports.

As mentioned earlier, the damping factors, g, were of the same order of magnitude for the model and for the full scale vehicle.

Conclusions Drawn

It was generally concluded that the model tests gave vibration results in general agreement with the results of the full scale tests.
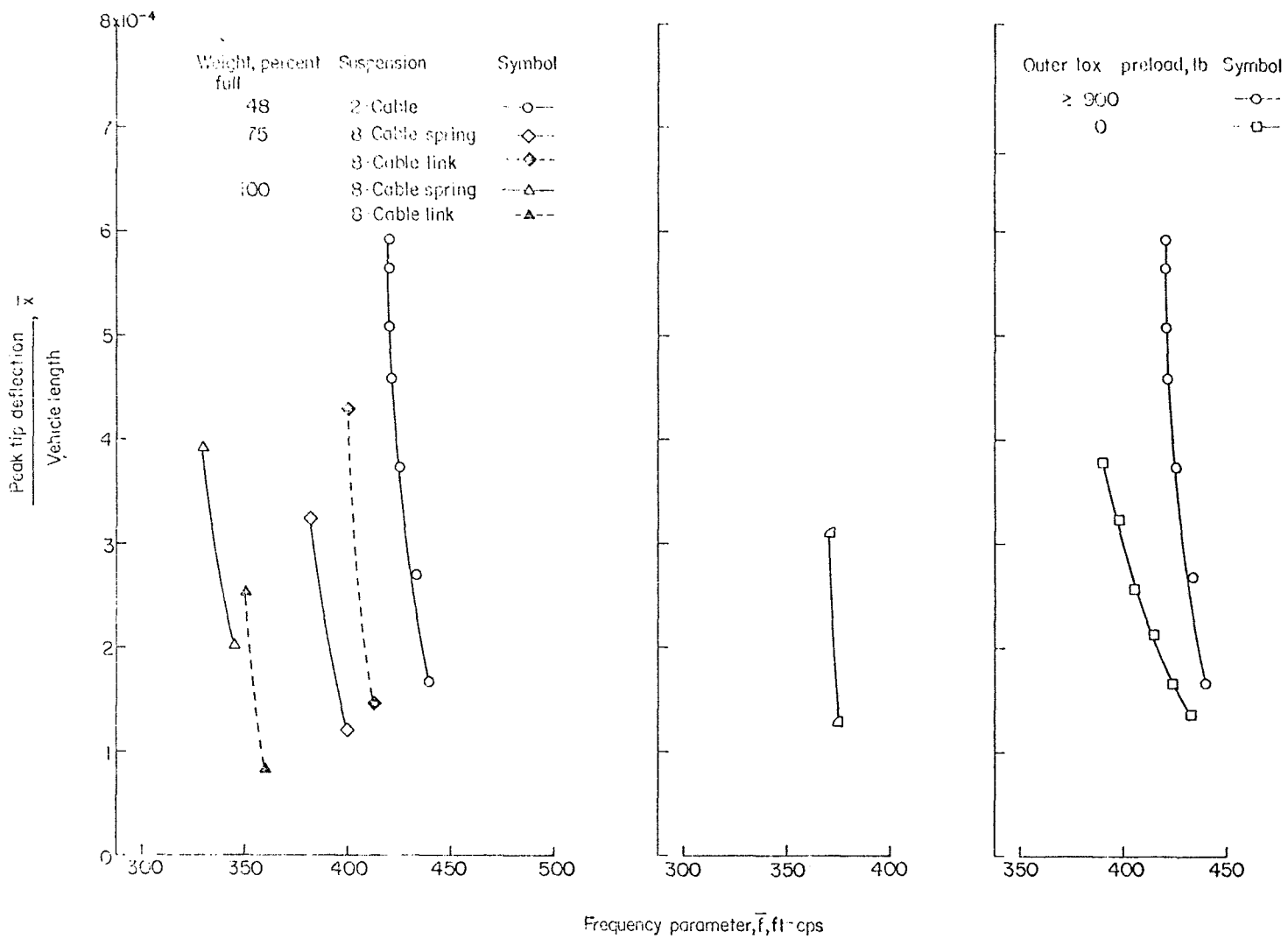
140

8×10^{-4}

Weight, percent full	Suspension	Symbol
48	2-Cable	—o—
75	8-Cable spring	—◇—
	8-Cable link	··◆··
100	8-Cable spring	—△—
	8-Cable link	-▲--

Outer lox preload, lb   Symbol

≥ 900   —o—

0   —◻—

Peak tip deflection / Vehicle length, x

Frequency parameter, $\bar{f}$, ft·cps

(a) Effect of suspension and weight variations. 1/5-scale model; outer lox preload ≈ 900 lb.

(b) Full-scale vibration test vehicle. Block II(SAD-5). Lift-off weight.

(c) Effect of outer lox tank preload. 1/5-scale model; two-cable suspension; weight at maximum dynamic pressure.

Figure C-10.   Variation of Resonant Frequency of Saturn First Bending Mode with Vibration Amplitude (from Ref. C4)
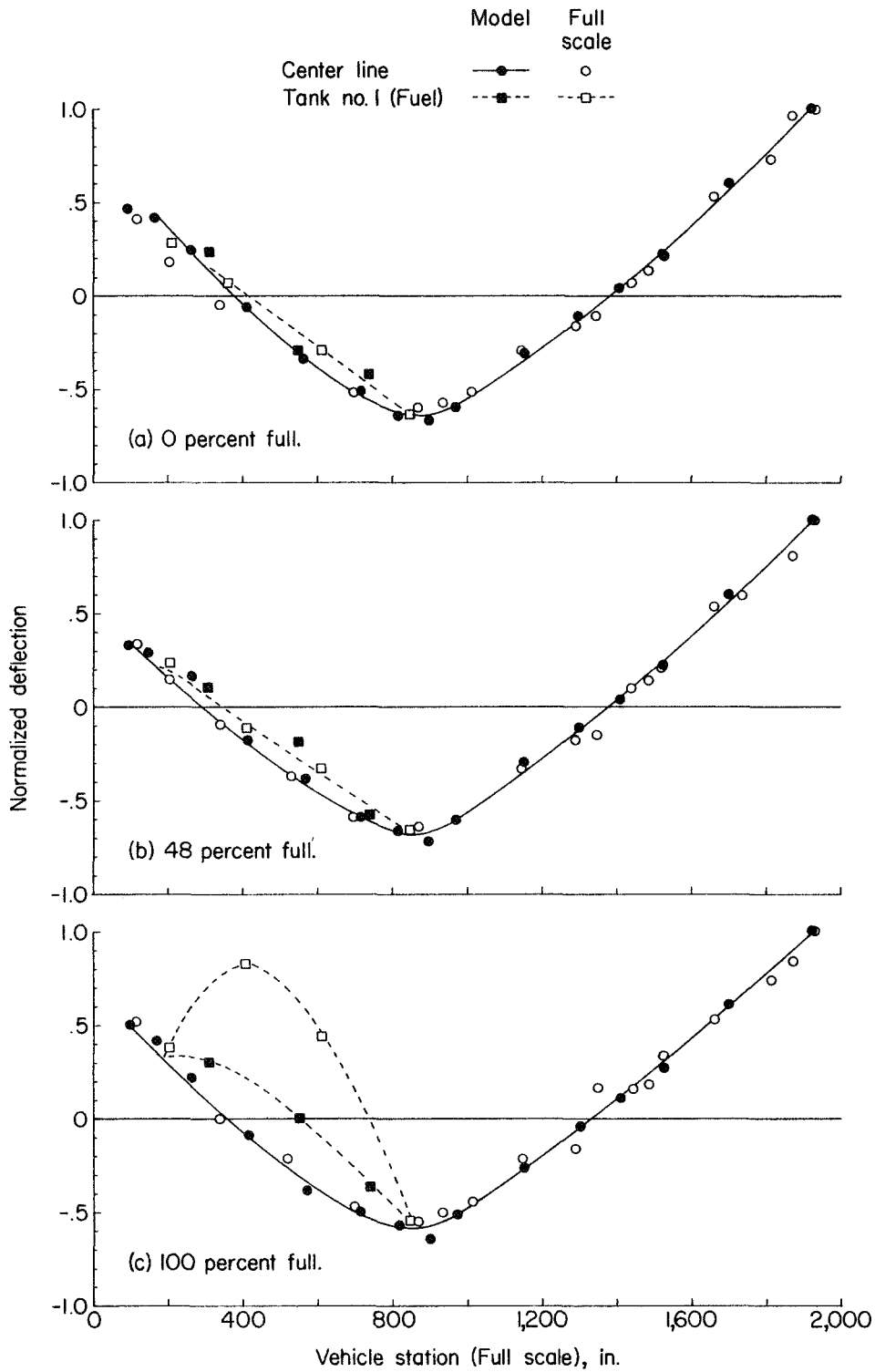
Figure C-11. Comparison of Model with Full-Scale First Bending Modes of Saturn (from Ref. C4)

142

TABLE C-6.   COMPARISON OF DAMPING FACTORS OBTAINED FROM FULL-SCALE
AND 1/5-SCALE MODEL OF SATURN SA-1 (from Ref. C4)

$$\left(g = \frac{1}{2\pi n} \log_e \frac{x_n}{x_0} \right)$$

Configuration	Damping Factors for -						
	Booster Tank Empty (Burnout)		48 Percent Full (Maximum Dynamic Pressure)		75 Percent Full (35 sec)	100 Percent Full (Lift-Off)	
	Soft Suspension	Stiff Suspension	Soft Suspension	Stiff Suspension	Soft Suspension	Soft Suspension	Stiff Suspension
First Bending Mode							
Full-Scale Saturn	0.024	--	0.023		0.116	0.026	--
1/5-Scale Model - 2 Cable	0.030, 0.017		0.032, 0.017		0.020	0.033, 0.025	
1/5-Scale Model - 8 Cable	0.032, 0.015	0.03	0.030, 0.013	0.033, 0.012	0.037, 0.015	0.030	0.01
First Cluster Mode							
Full-Scale Saturn	--	--	0.024		0.028	0.026	--
1/5-Scale Model - 2 Cable	--		0.023, 0.011		0.025, 0.015	0.017	
1/5-Scale Model - 8 Cable	--	--	--	0.030, 0.013	--	--	--
Second Cluster Mode							
Full-Scale Saturn	--	--	--	--	0.021	0.022	--
1/5-Scale Model - 2 Cable	--		--		0.022, 0.016	0.014	
1/5-Scale Model - 8 Cable	--	--	--	--	0.012	0.015	0.018
Second Bending Mode							
Full-Scale Saturn	0.018	--	--	--	0.010	0.010	--
1/5-Scale Model - 2 Cable	0.046, 0.032	--	--	--	0.039, 0.019	0.010	
1/5-Scale Model - 8 Cable	--	--	--	--	0.017	--	--